QATAR UNIVERSITY

Graduate Studies

College of Pharmacy

THE CELLULAR INTERPLAY BETWEEN Na^+/H^+ EXCHANGER ISOFORM I AND OSTEOPONTIN IN CARDIAC HYPERTROPHY

A Thesis in
College of Pharmacy
By
Iman Ahmed Abdelaziz

Submitted in Partial Fulfillment
of the Requirements
for the Degree of
Master of Science in Pharmacy

June 2013

The thesis of Iman Abdelaziz was reviewed and approved by the following:

We, the committee members listed below accept and approve the Thesis/Dissertation of the student named above. To the best of this committee's knowledge, the Thesis/Dissertation conforms the requirements of Qatar University, and we endorse this Thesis/Dissertation for examination.

Name _____

Signature _____ Date_____

Name _____

Signature _____ Date_____

Name _____

Signature _____ Date_____

Name _____

Signature _____ Date_____

Name _____

Signature _____ Date_____

Name _____

Signature _____ Date_____

Abstract

The Na^+/H^+ exchanger-1 (NHE1) is a ubiquitously expressed housekeeping glycoprotein that functions to regulate intracellular pH. Enhanced expression/activity of NHE1 has been implicated in cardiac hypertrophy (CH). Recently, transgenic mice expressing active-NHE1 demonstrated a>1500-fold increase in osteopontin (OPN) gene expression. OPN, a component of the extracellular matrix, has also been implicated in CH. In our study, upregulation of NHE1 in cardiomyocytes resulted in a significant increase in OPN protein expression (342.7%±69.22%). To determine whether OPN contributes to the hypertrophic effects of NHE1 during CH, cardiomyocytes were infected with active NHE1 in the presence and absence of OPN, or a silencing RNA (siRNA). CH was assessed by measuring cell area, protein content and atrial natriuretic peptide (ANP) mRNA. Overexpression of NHE1 and OPN in cardiomyocytes significantly increased cell area (158.4±3.59% of control); this was significantly reduced in the presence of siRNA-OPN (68.5±0.24% vs. 190.9±8.66% NHE1-infected). Protein content and ANP mRNA expression were also significantly increased in NHE1-infected cardiomyocytes, however they were significantly abrogated in the presence of OPN-siRNA (87.8±12.58% vs. 136.8±11% NHE1-infected) and (64.6±19.9% vs. 247.7±30.81% NHE1-infected). OPN appeared to contribute to NHE1-induced CH independent of extracellular-signal-regulated kinases, p90-ribosomal-S6 kinase and protein kinase B (Akt). Interestingly, NHE1 expression and activity in cardiomyocytes infected with NHE1 and OPN were significantly enhanced (636.5±128.75% of control) and (163.1±19.49% vs. 114.7±9.48% NHE1-infected). This was significantly abolished in the presence of

siRNA-OPN (20.2 fold decrease±0.12 of control) and (68.5±0.24% vs. 586.5±103.54% NHE1-infected). Moreover, cleavage of OPN was enhanced in cardiomyocytes infected with both NHE1 and OPN, which was significantly reduced in the presence of siRNA OPN. Our study is the first to demonstrate a two-way cross talk between NHE1 and OPN in CH *in vitro*. Our findings demonstrate that NHE1 upregulates OPN in cardiomyocytes, which in turn regulates NHE1 expression/activity and contributes to the NHE1-induced hypertrophic response. Our study highlights OPN as a potential therapeutic target to reverse NHE1-induced CH and activity, one which maybe more beneficial than directly inhibiting NHE1.

Table of Contents

List of Tables

Table **Page**

List of Figures

Abbreviations

Akt, Protein kinase B/Akt

α1-AR, α1 adrenergic receptor

Ang II, Angiotensin II

ANP, Atrial natriuretic peptide

ARVM, Adult rat ventricular cardiomyocytes

ATP, Adenosine 5'-triphosphate

$\alpha_v\beta_5$, Integrin

BNP, β-natriuretic peptide

BCECF-AM, 2'-7'-bis(2-carboxyethyl)-5(6)-carboxyfluorescein acetoxymethyl ester

Ca^{2+}_i, Intracellular Ca^{2+}

CAII, Carbonic anhydrase II

CaM, Calmodulin

CaMK II, Ca^{2+}/Calmodulin-dependent protein kinase II

CD44, Hyaluronic acid receptor 44

CH, Cardiac hypertrophy

DMEM, Dulbecco's Modified Eagle's Medium ERK Extracellular signal-related kinase

ERK, Phosphorylated extracellular signal-regulated kinase

ERM, Ezrin, radixin and moesin

ET-1, Endothelin-1

FBS, Fetal bovine serum

GAPDH, Glyceraldehyde 3-phosphate dehydrogenase

GFP, Green fluorescent protein

GPCR, G protein coupled receptors

GSK-3β, Glycogen synthase kinase-3β

HA, Hemagglutinin

I/R, Ischemia/reperfusion

JNK, c-Jun N-terminal kinase

MAPK, Mitogen activated protein kinase

MI, Myocardial infarction

MOI, Multiplicity of infection

Na^+_i, Intracellular Na^+

NCX, Na^+/Ca^{2+} exchanger

NHE1, Na^+/H^+ exchanger 1

NRVM, Neonatal rat ventricular cardiomyocyte

OPN, Osteopontin

PE, Phenylephrine

PFU, Plaque formation units

pH_i, Intracellular pH

RSK, p^{90} ribosomal S6 kinase

SEM, Standard error of the mean

siRNA, silencing RNA

VSMCs, Vascular smooth muscle cells

Acknowledgments

I would like to thank my supervisor and mentor, Dr. Fatima Mraiche for the support and guidance she provided with while I worked to complete my Master's thesis project in her lab at Qatar University. Dr. Fatima is extremely dedicated to science and research, and I highly appreciate how she trained me to the highest of standards while never showing any signs of impatience.

I would like to acknowledge the members of my Graduate Student Supervisory Committee; Dr. Ali Eid, Dr. Asad Zeidan, Dr. Mohamed Izham, Dr. Shankar Munusamy, Dr. Sherief Khalifa and Committee chair; Dr. Feras Alali, for their valuable advice and critical analysis which led to the successful completion of my thesis project. To all my professors who have taught me over the past two years; your endless encouragement and support have made this a pleasurable learning experience.

I am also grateful for the support of Dr. Fatima's Pharmacology lab members; Mrs. Maiy Youssef, Ms. Soumaya Bouchoucha and Dr. Mohamed Mlih who provided me with assistance and intellectual guidance along the way. A special thank you goes to Ms. Taqdees Mahroof, for being my first companion in the program and in the lab. I would like to thank Dr. Gary Lopaschuk and Dr. Larry Fliegel of the University of Alberta, for opening up their labs to me and allowing me to learn various new techniques.

I would also like to acknowledge all the efforts and support of Qatar University and the College of Pharmacy. I would like to thank them for the funding I received as a graduate Teaching Assistant and for funding my travels, allowing me to attend conferences regionally and internationally. I would also like to thank Dr.

Ayman El-Kadi for all his support and Dr. Peter Jewesson; for always believing in me.

Last but not least, I would like to thank my parents for their unconditional love and support and to my brothers and sisters; for each one of you, a full thank you. Finally, to my wonderful friends and support system; thank you for always being there for me.

Dedication

To my loving family:

Eng. Ahmed Abdelaziz

Mrs. Najwa Khairalla

Mahmoud, Fatma, Wael, Reem and

Hana

Chapter 1: Introduction

1.1 Cardiovascular Diseases

1.1.1 Epidemiology

Despite the advances in the treatment of cardiovascular diseases (CVDs), they remain one of the leading causes of death worldwide. The World Health Organization estimates that by 2030, more than 23 million people will die annually from cardiovascular diseases, with the largest increase occurring in the Middle East (1). Over the past three decades, the national burden of disease in the population of Qatar has shifted dramatically. A recent study has shown that ischemic heart disease is a primary cause of death in Qatar (2). As a result, it has become an absolute necessity to aim global research efforts at better understanding the underlying causes of CVDs.

1.1.2 Cardiovascular Diseases

CVDs, which include coronary heart disease, arrhythmia, myocardial infarction (MI), stroke and cardiomyopathy ultimately lead to heart failure if left unresolved (3). During the course of heart failure, the heart undergoes numerous abnormalities, which predispose the heart to cardiac remodeling. Cardiac remodeling can occur as a result of pressure overload (hypertension), volume overload (valvular regurgitation), inflammatory disease (myocarditis), dilated cardiomyopathy (DCM) and post-MI and ischemia reperfusion (I/R) injury (4). CH is a common type of cardiac remodeling and is characterized by enlargement of the heart and cardiomyocytes and can lead to heart failure (4).

1.1.3 Cardiac Hypertrophy

Hypertrophy of the heart is thought to be a compensatory (physiological) response for the preservation of cardiac function, specifically during strenuous exercise and pregnancy (5). Pathological CH, which occurs as a result of pressure overload, volume overload or loss of contractile mass post-MI injury (6), is initially a compensatory mechanism. Unresolved hypertrophy can lead to impairment of the left ventricle (LV), which can predispose to heart failure (7). Both physiological and pathological CH involve the synthesis of new contractile proteins and assembly of sarcomeres that ultimately leads to increased contractile force per cell and preserved function of the heart (7). Unlike physiological hypertrophy, pathological CH is associated with fibroblast activation, increase in collagen deposition and fibrosis leading to enhanced necrosis and apoptosis (5). Pathological CH has been classified into two major classes, *concentric* and *eccentric* hypertrophy (8). Concentric CH is associated with an increase in wall thickness and minimal alterations in the ventricular cavity size, while the eccentric phenotype is accompanied by a more apparent increase in both cavity volume and progressive dilation (8). CH in the concentric form is reflected by hypertrophic cardiomyopathy, meanwhile DCM typifies the eccentric phenotype (9). Both concentric or eccentric hypertrophy ultimately lead to enhanced synthesis of hypertrophic markers including α and β myosin heavy chain isoforms (α and β MHC), α skeletal actin as well as reinduction of the fetal gene program and elevated expression of the atrial and β-natriuretic peptides (ANP and BNP) (10).

Various signaling pathways have been identified as regulators of the hypertrophic response. Such pathways include the calcineurin Nuclear Factor

Activated T-cells (CaN/NFAT), mitogen activated protein kinases (MAPKs) pathways, the activation of cardiac specific membrane proteins, integral components of the extracellular matrix (ECM) as well as natriuretic peptides (10-12). Intracellular Ca^{2+} (Ca^{2+}_i) has been demonstrated to play a critical role in the pathogenesis of CH (6). One means by which Ca^{2+}_I induces CH is through activation of CaN which in turn causes enhanced translocation of NFAT and activation of GATA transcription factors (13, 14). Many studies have identified the Na^+/H^+ exchanger isoform I (NHE1) as a critical factor involved in the induction of CH both *in vitro* and *in vivo* (14-18). In addition, matricellular proteins of the ECM, such as osteopontin (OPN), have also been shown to play a role in mediating cardiac remodeling and CH (19, 20). Interestingly, upregulation of both NHE1 and OPN has been observed in several models of CH *in vivo* (21-24). A better understanding of the hypertrophic signals initiated at the cell membrane leading to hypertrophic gene expression is critical for designing new strategies for the prevention or treatment of CH.

1.2 Na^+/H^+ Exchangers

1.2.1 Subfamilies of NHE

One family that is known to regulate intracellular pH (pH_i) are the Na^+/H^+ exchangers (NHE) that function to transport one intracellular H^+ in exchange for one extracellular Na^+ thereby returning pH_i to its native less acidic state (25). There are currently 10 known isoforms of NHE that can be found either bound to the cell membrane or within the cell (26). The first clone of the NHE exchanger was isolated, sequenced and expressed in 1989 by Sardet et al. (25). Similar to NHE1 are NHE2 to NHE5, which are membrane bound proteins distributed primarily along the membrane

of kidney, intestines and through out cerebral tissue (27). NHE2 and NHE3 can be found located along the brush border membrane of intestinal epithelial cells (28). On the other hand, NHE4 has been found to be expressed more abundantly in the inner renal medullary renal tubules, uterus, skeletal muscle as well as the stomach (25). The last isoform of the membrane bound exchangers, NHE5, was found to be highly expressed in the brain and non-epithelial tissue including that of the spleen, testis and skeletal muscle tissue (28). It has also been postulated that NHE5 may modulate synaptic transmission through local regulation of pH at the synapse (29), suggesting an important role for the exchanger in synaptic transmission.

The physiological importance of NHE6-9 has been studied more extensively in the cytosol. NHE6 to NHE9 are considered intracellular proteins that are more inclined to regulate organelle pH within the cell (27). NHE6 is expressed in the recycling endosomes of cells (30). Isoforms 7 and 8 appear to be quite similar in that they are both located at different positions with in the Golgi apparatus (27). NHE9 is more predominantly found in the late recycling endosomes and was more recently discovered (30). The most recent isoform of the NHEs to be identified, NHE10, is localized to osteoclasts where it functions to maintain bone marrow-derived osteoclast differentiation and survival (31). The gene of the NHE family of exchangers has been conserved since their discovery by Sardet et al. (28) The structures of all isoforms of the NHE family has not been completely resolved, however, based on homology modeling using the known structure of the E. coli Na^+/H^+ antiporter, NhaA, the general perception is that features of the NhaA and mammalian NHEs are conserved (25). In our study, we will be focusing on NHE1, the only cardiac specific isoform of NHEs.

1.2.2 Cardiac-Specific NHE1

NHE1, a ubiquitously expressed housekeeping glycoprotein, is the only isoform of NHEs to be expressed in the heart (32). NHE1 resides mainly on the cell membrane, more specifically, in the intercalated discs located at the bipolar ends of both atrial and ventricular cardiomyocytes (33). NHE1 has also been found to be enriched in the lamellipodia of fibroblasts (34) NHE1 is composed of 815 amino acids, of which 500 amino acids make up the hydrophobic membrane N-terminal and 315 form the hydrophilic cytoplasmic C-terminal and (25). The N-terminal contains 12 α-helices of transmembrane (TM) segments that cooperate to optimize the function of the exchanger (efflux of one H^+ in exchange for influx of Na^+ with a stoichiometry of 1:1) (33). The N-terminal is also considered the binding site for NHE1 inhibitors. The importance of the N-terminal has been highlighted in studies in which mutation of specific amino acids sequences pertaining to different TM segments, such as segments IV, VII and IX, led to the resistance of NHE1 to inhibitors and even abolished its function (30). The C-terminal is responsible for the regulation of NHE1 activity through phosphorylation and interaction with other regulatory proteins (25). A detailed description of the structure of NHE1 is very important in order to shed light on its role and regulation in both healthy and diseased hearts.

1.2.2.1 Physiological Role of NHE1

NHE1 is expressed by cardiomyocytes at basal levels under normal conditions (16). As the pH_i is lowered, NHE1 becomes readily active, therefore protecting the cell from intracellular acidosis by maintaining a stoichiometric exchange of H^+ to Na^+ ions (30). The role of NHE1 as a housekeeping protein of physiological importance

has been outlined in numerous reviews (28, 30, 35). The following section highlights some of the key roles of NHE1 in different physiological processes.

NHE1 has been implicated in the regulation of *cell volume* and *differentiation* (25, 30, 36). Xiuju et al. recently demonstrated that NHE1 protein expression facilitated cardiomyocyte embryonic stem cell differentiation (37) In their study, treatment of embryonic CGR8 stem cells with EMD87850, an NHE1 inhibitor, inhibited differentiation of the CGR8 stem cells into cardiomyocytes. NHE1 can also protect cells against shrinkage as it acts as a portal for the influx of Na^+ (28). NHE1 has also been considered a component of regulatory cell volume increase (RVI) in response to hypertonic stimulation as well as apoptotic volume decrease (AVD) (28, 38). Taken together, these findings suggest that NHE1 is a key regulator of numerous cellular regulatory processes including regulating cell differentiation and volume.

NHE1 has also been known to regulate apoptosis and influence *cell survival* (25, 39). Interestingly, NHE1 activation in response to cisplatin-induced apoptotic stress in kidney proximal tubule cell line, LLC-PK1, counteracted apoptosis through the activation of prosurvival kinase, Akt (40). This is consistent with another study in which tubular epithelial cell apoptosis was associated with decreased NHE1 expression and increased indices of apoptosis in a neonatal rat model of ureteral obstruction (41, 42). On the contrary, Karki et al. demonstrated that enhanced NHE1 protein expression in isolated primary cardiomyocytes promoted apoptosis following hypoxia/reoxygenation (43). Although NHE1 clearly plays an important role in the regulation of apoptosis, the role of NHE1 to either promote cell death or survival will depend on the nature of the cells.

NHE1 has recently been shown to act as a plasma membrane *anchoring*

protein through interactions with the Ezrin/Radixin/Moesin (ERM) proteins (28). In fact, two ERM binding motifs have been identified along amino acids 553-564 of the NHE1's C-terminal (44). The ERM proteins are binding proteins that function to create cytoskeletal cross-links, which are critical elements of cell structure (44). Fibroblasts expressing a mutant NHE1 that lacks ERM appear mislocalized (45). These findings suggest that activation of NHE1 following interaction with the ERM proteins appears to play a major role in maintaining cytoskeletal structure.

NHE1 appears to be a very important housekeeping protein, implicated in various physiological processes such as differentiation, apoptosis as well as maintaining the cytoskeletal structure (25, 37). Owing to the diverse physiological roles of NHE1, it has been studied in a variety of physiological and pathological events.

1.2.2.2 NHE1 Inhibitors

Several NHE1 inhibitors have been developed that target NHE1 selectivity and potency. The first generation of NHE1 inhibitors included amiloride derivatives, which included pyrazine ring containing EIPA (5-(N-ethyl-N-isopropyl) amiloride) and 5-(N, N-Dimethyl) amiloride hydrochloride (DMA) (46). In an effort to enhance NHE1 inhibitor selectivity and potency, a second generation of NHE1 inhibitors were developed (46). This class included EMD87850 (N-(2-methyl-4,5-bis(methylsulfonyl)-benzoyl)-guanidine hydrochloride), cariporide (HOE-642), eniporide (EMD85131) and BIIB513, a more potent selective NHE1 inhibitor (47). This class of inhibitors was more selective towards NHE1 and NHE2; with BIIB513 being 8 times more potent than cariporide, and their selectivity towards NHE3 and

NHE5 was to a much lesser extent (48, 49). Almost a decade and a half after the initial screening of the amiloride derivatives, zoniporide, a highly selective and potent human NHE1 inhibitor was discovered by Guzman-Perez et al. (50). The exceptionally high aqueous solubility of zoniporide was attributed to the presence of a cyclopropyl and a 5-quinolinyl substituent on the central pyrazole ring (50). Sabiporide and its derivative, N-(4-(1-acetyl-piperidin-4-yl)-3-trifluoromethyl-benzoyl)-guanidine, were recently found to have cardioprotective effects against ischemic damage in a model of I/R injury in rat hearts (51). To date the amiloride and benzoylguanidine containing (EMD and HOE type) NHE1 inhibitors appear to be the most ideal tools for inhibition of NHE1 for both *in vitro* and *in vivo* studies (52, 53). Moreover, the use of sabiporide and zoniporide for the treatment of acute MI in animals have recently showed rather promising results (51).

1.2.2.3 Regulation of NHE1 activity

Recent studies have indicated that enhanced activity of NHE1, rather than protein expression, is more deleterious in cancer and cardiovascular diseases (17, 18, 21, 54-56). The C-terminal tail of NHE1 has been shown to comprise a number of distinct subdomains responsible for regulating NHE1 activity (Figure 1.1) (25). Intracellular acidosis and cell shrinkage are the main stimuli for NHE1 activation (28). In fact, NHE1 activity in primary cultures of cardiomyocytes has been shown to be elevated following the induction of transient as well as sustained acidosis (57, 58). NHE1 activity can also be regulated through a variety α1 adrenergic receptor (α1-AR) and growth factors, interaction with binding proteins, and most commonly, through phosphorylation and dephosphorylation by protein kinases/phosphatases (48,

59). Since the expression/activity of NHE1 appears to play a major role in both physiological and pathological conditions, it has become increasingly important to elucidate the pathways known to regulate its activity.

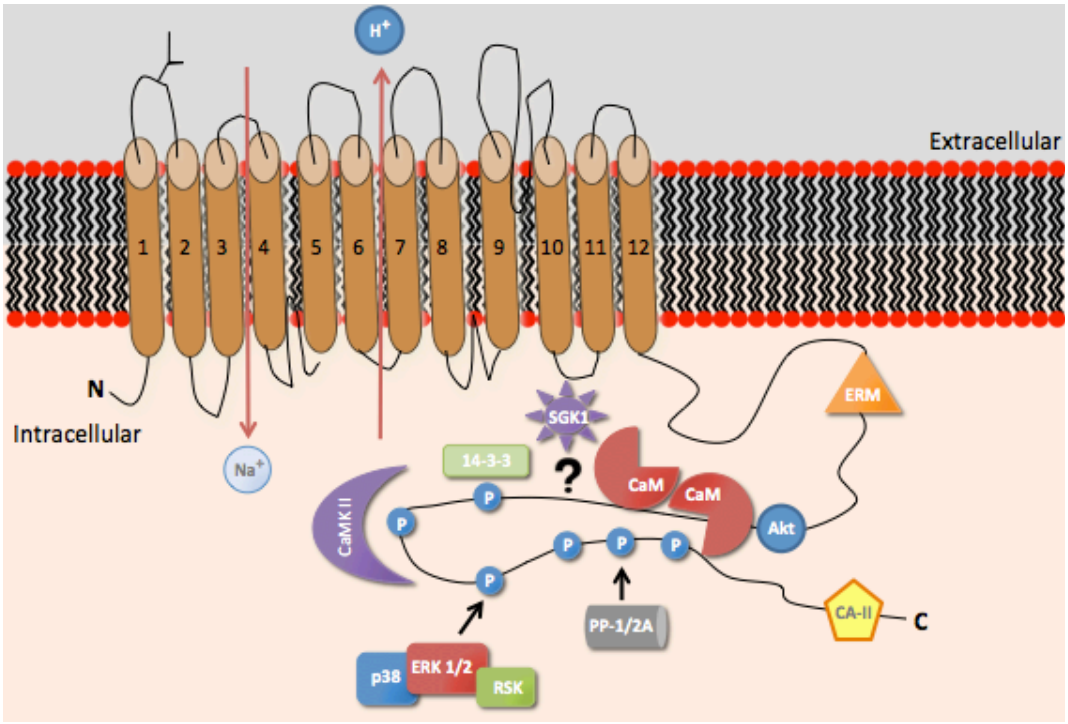

Fig. 1.1: A representative topology model of the NHE1. Displayed are the extracellular, membrane and intracellular cytosolic domains. The major binding sites for binding proteins and kinases known to regulate NHE1 activity are displayed along the cytoplasmic C-terminal terminal displays the major protein-protein interactions and kinases. **ERM**, Ezrin/Radixin/Moesin; **Akt**, protein kinase B; **CaM**, calmodulin; **CaMK II**, Ca^{2+}/CaM kinase II; ERK 1/2, extracellular regulated kinase 1/2; RSK, p90 ribosomal S6 kinase; **PP-1/2A**, protein phosphatase 1/2A; **CAII**, carbonic anhydrase II; **SGK1**, serum and glucorticoid-inducible kinase 1; **?**, putative sites of phosphorylation, circled **Ps**, sites of phosphorylation. This figure was adopted from Malo et al. (25) (2010).

1.2.2.3.1 Regulation of NHE1 Activity through Binding Proteins

The C-terminal domain of NHE1 is known to regulate the activity of the exchanger. The regulation of NHE1 activity can occur through interaction of the exchanger with binding proteins including calmodulin (CaM), carbonic anhydrase II (CAII) and the 14-3-3 protein binding motif (30). Bertrand et al. were the first to identify two CaM binding sites located on the middle of NHE1's C-terminal (60). These binding sites include a high affinity binding region between residues 637–657 and a low affinity binding region between 657–700. Upon binding of CaM to the high affinity binding site, it exerts an autoinhibitory effect by reducing the affinity of NHE1 for intracellular H^+ (60). On the other hand, binding of Ca^{2+} bound CaM to the low affinity binding site, causes activation of NHE1 (61). These findings illustrate that Ca^{2+}/CaM can act as direct regulators of NHE1 activity. CAII catalyzes the hydration of CO_2 ($CO_2 + H_2O \leftrightarrow H_2CO_3 \leftrightarrow H^+ + HCO_3^-$), thereby generating H^+ (62). It has been detected in the rat cardiac papillary muscles as well as neonatal and adult rat ventricular cardiomyocytes (NRVMs and ARVMs) (63). A CAII binding site has been identified on NHE1 at amino acids 790-802 (62, 64). Binding of CAII to NHE1 has been shown to enhance its activity through phosphorylation of NHE1 at Ser^{796} (62). CAII has also been suggested to enhance the activity of NHE1 by providing the necessary H^+ upon enzymatic hydration of CO_2 (63). NHE1 also contains a consensus sequence specific for binding of the 14-3-3 protein binding motif (65). Taken together, the previous data illustrates one of the possible mechanisms of regulating NHE1 activity through protein interaction.

1.2.2.3.2 Phosphorylation and Dephosphorylation of NHE1

NHE1 activity has also been shown to be regulated through direct phosphorylation and dephosphorylation by several kinases and phosphatases (66). Sardet et al. were the first to demonstrate that the activity of NHE1 was significantly increased following phosphorylation in response to thrombin and growth factor stimulation (reviewed in (25)). Moreover, treatment of fibroblasts with okadaic acid, a protein phosphatase 1 and 2A inhibitor, was able to alkalinize pH_i, suggesting enhanced activity of NHE1 (reviewed in (25)). Wakabayashi et al. later reported that the major sites of NHE1 phosphorylation were located between amino acid 636 and 815 on the C-terminal and that deletion of these sites reduced growth factor-induced cytoplasmic alkalinization by 50% (67). Several Ser/Thr kinases have already been shown to regulate the activity of NHE1 including the CaMK II and the mitogen activated protein kinases (MAPK) particularly the extracellular regulated kinase (ERK) 1/2 and its downstream effector, the p90 ribosomal S6 kinase (RSK) (57, 68, 69). In fact, α1-AR agonists and growth factors have been shown to stimulate the activity through *G protein-coupled receptors* (GPCRs) and the subsequent activation of the ERK pathway (30, 70). In response to phosphorylation-mediated activation of NHE1, protein phosphatases, including protein phosphatase 1 and 2A, have been shown to play a role in terminating NHE1 activity (59). A better understanding of the different pathways of NHE1 phosphorylation/dephosphorylation is essential, as it will highlight targets for the regulation of NHE1 activity in the healthy and diseased myocardium.

MAPKs, including ERK 1/2, c-Jun N-terminal kinases (JNK1/2/3) and p38 MAPKs (p38), are considered important contributors to GPCRs mediated regulation

of NHE1 activity (71). GPCRs are a family of seven transmembrane cell surface receptors composed of an extracellular domain, associated with ligand binding, and an intracellular domain that signals through guanine nucleotide-bound protein intermediates (G proteins) (72). GPCRs are composed of an α, β and γ subunit. Upon ligand binding to the extracellular domain, the α subunit dissociates from the β and γ subunits, thus converting guanosine triphosphate (GTP) into guanosine diphosphate (GDP) leading to the activation of downstream signaling pathways (73). Gα subunit is comprised of four primary families $G\alpha_s$, $G\alpha_i$, $G\alpha_q$, and $G\alpha_{11/12}$ (72). Dissociation of the Gα subunit can activate effectors and enzymes including adenylyl cyclase and phospholipase C (PLC) (73). The activation of $G\alpha_q$ and muscarinic receptors is thought to stimulate NHE1 activity through a change in NHE1's sensitivity to pH_i (25). $G\alpha_q$ is known to be activated by a variety of α1-AR agonists including phenylephrine (PE), angiotensin II (Ang II) and endothelin (ET-1) (73). Several stimuli that activate the ERK pathway, such as PE and growth factors, appear to increase NHE activity in both NRVMs and fibroblasts (57, 70). Because Ras, the small GDP bound protein, is activated upstream of both NHE and ERK, it has been suggested that ERK acts as a funnel for extracellular stimuli that leads to the activation of the effector NHE1 (70). This has been attributed to the interaction of the βγ subunits with ERK and subsequent phosphorylation and activation of NHE1 (70). These findings strongly suggest that MAPK stimulation regulates NHE1 activity through an ERK 1/2 dependent pathway.

Another very important family of kinases that has been implicated in the regulation of NHE1 activity is *RSK* family (35). RSK is a downstream effector of ERK 1/2 and has been shown to phosphorylate and activate NHE1 (25). The RSK

family is comprised of four principle isoforms, RSK 1-4 (35). Activation of RSK 1 and 2 have also been shown to phosphorylate the Ser^{703}, residue on the 14-3-3-protein binding motif, which in turn activates NHE1 (57, 69, 74). Activation of the Ang II receptor type 1 is also thought to activate NHE1 through RSK phosphorylation. Moreover, NHE1 activity was significantly inhibited in NRVMs overexpressing cardiac-specific dominant negative (DN) RSK following treatment with hydrogen peroxide H_2O_2, a stimulator of NHE1 activity, further confirming the role of RSK in activating NHE1 (75). Taken together, these findings suggest that RSK is an important regulator of NHE1 activity. As such, RSK may prove to be a beneficial target to reduce NHE1 activity, in cardiovascular diseases associated with enhanced activity of RSK and NHE1.

The *p38* kinase is considered the second major group of MAPKs. p38 signaling was initially thought to be critical for normal immune and inflammatory responses in mammalian cells (76). In the heart, p38 signaling is rather similar to the ERK 1/2 in that the cascade is initiated by activation of GDP-bound Ras (76). Cardone et al. recently demonstrated that downregulation of p38 was necessary for the activation of NHE1 in NIH3T3 fibroblasts (77). As such, the emerging role of the p38 MAPK in the regulation of NHE1 activity remains less defined and may require further studies.

In the heart, several isoforms of *CaMK* have been detected including CaMK I, II and IV (17). Interestingly, activation of the CaMK signaling cascade has been associated with several models of CH and heart failure (17). In addition, CaMK II is another kinase that has been reported to phosphorylate and activate the C-terminal of NHE1 *in vitro* and *in vivo* (17, 68). The Fliegel group was the first to demonstrate that

CaMK II directly phosphorylates and activates the Ser^{324} site on the C-terminal of NHE1 *in vivo* (25). In parallel with these findings, a study using ARVMs overexpressing the CaMK II revealed a faster pH_i recovery from acidosis compared to ARVMs overexpressing βcompared to AR (68). Moreover, Vila-Petroff et al. recently indicated that CaMK II stimulated the activity of NHE1 following sustained intracellular acidosis independent of ERK 1/2 and RSK in cardiomyocytes (68). Interestingly, inhibition of both ERK 1/2 and CaMK II pathways in isolated cardiomyocytes significantly reduced NHE1 activity (68). Taken together, these findings indicate that while CaMK II-induced activation of NHE1 occurs independent of MAPK activation, both pathways may be working additively to regulate the activity of NHE1. Thus, it is critical to further investigate whether these hypertrophic kinases interact to mediate the detrimental effects of NHE1 in CH.

Protein kinase C (*PKC*), a serine/threonine kinase, has been suggested to be a regulator of NHE1 activity (25, 71). In addition to the ERK pathway, GPCR stimulation of NHE1 been suggested to occur through PKC (70). Stimulation of GPCRs is known to induce the hydrolysis of PIP_2 by PLC producing diacylglycerol (DAG), a potent PKC activator, as well as inositol 1,4,5-triphosphate, which is responsible for releasing the Ca^{2+} stored in the endoplasmic reticulum (ER) (73). As discussed in Section 1.2.2.3.1, Ca^{2+}_i activates NHE1 through the direct interaction of the Ca^{2+}-bound CaM to the C-terminal of NHE1 (61). In order to validate the involvement of PKC in the regulation of NHE1 activity, pretreatment of NRVMs with GF109203X, a PKC inhibitor, was used to confirm that inhibition of PKC prevented PE-induced increase in NHE1 activity *in vitro* (71). Rather than the DAG/PKC-induced activation of NHE1, Wakabayashi et al. suggested that activation of NHE1

occurs through interaction of DAG with a lipid interacting domain (LID) along the C-terminal of the exchanger (78). It is, however, important to note that NHE1 does not carry a consensus site for direct phosphorylation by PKC. Therefore, at present, evidence for the involvement of PKC in the activation of NHE1 and the exact molecular mechanism underlying this pathway remains inconclusive.

In addition to PKC, several groups have implicated *protein kinase B/Akt* in the regulation of NHE1 activity (79, 80). Avkiran and co-workers were the first to identify NHE1 as a substrate for Akt (80). The group confirmed that Akt-phosphorylation of NHE1 occurred through the Ser^{648} binding motif and that it leads to inhibition of NHE1 activity in ARVMs. On the other hand, Barber's group revealed that phosphorylation of NHE1 by Akt increased NHE1 activity (H^+ extrusion) in PS120 fibroblasts (79). The fact that these studies were conducted on different cell lines could explain the opposing conclusions reached, however, the findings clearly indicate that Akt regulates NHE1 activity through interaction with the Ser^{648} binding motif.

While numerous studies have attempted to elucidate the kinases involved in regulation of NHE1 activity, only a few have examined the role of *phosphatases* that dephosphorylate the protein in order to inactivate it. Phosphatases are a family of serine/threonine protein phosphatases (PP) that regulate a magnitude of cellular processes (59). PPs including PP1, PP2A, and calcineurin (CaN) are expressed in the heart and have been shown to regulate NHE1 activity (59). Misik et al. have previously demonstrated that treatment of primary cultures of cardiomyocytes with the phosphatase inhibitor, okadaic acid, increased NHE1 activity following the induction of an acid load (59). CaN, a Ca^{2+}-dependent serine/threonine protein

phosphatase, has been suggested to regulate NHE1 activity (reviewed in (25)). Of more importance, however, is the fact that CaN has been shown to dephosphorylate and induce nuclear translocation of the NFAT family of transcription factors (81). The family of NFAT transcription factors encompasses five proteins NFAT1-4 (also known as NFATc1-c4) all of which are expressed in the myocardium (81). NFATc1 and NFATc4 mRNA and protein levels have been shown to be elevated in murine models of CH (13, 14, 81). Stimulation of GPCRs has previously been shown to activate the CaN/NFAT pathway (82). Moreover, NHE1-induced CH has been suggested to occur through the CaN/NFAT pathway in NRVMs (14, 17). Taken together, these findings indicate that CaN may act as both a regulator of NHE1 activity and possibly a mediator of NHE1-induced CH.

1.3 NHE1 in Cardiac Remodeling

Since the identification and characterization of NHE1 in the myocardium, numerous studies have focused on the physiological and pathological roles of NHE1 in the heart (83). In addition to the regulation of pH_i in the heart, NHE1 plays a major role in regulating cell volume and survival, inducing cell differentiation as well as acting as a plasma membrane anchoring protein (30, 37). Enhanced NHE1 activity has been well established during the process of cardiac remodeling in CH and following I/R injury (18, 54). As a result, activated NHE1 has been suggested to contribute to the process of heart failure (17). Due to the involvement of NHE1 in the pathogenesis of several cardiac pathologies, NHE1 has become a valuable therapeutic target.

1.3.1 NHE1 in Cardiac Hypertrophy

The importance of NHE1 in CH has been clearly defined in the literature (17, 18, 22, 84). NHE1 activity has been shown to be upregulated in response to pressure/volume overload on the heart as well as neurohormonal activation (16). In addition to enhanced activity of NHE1, mRNA levels as well as protein expression have been shown to be elevated in several *in vitro* and in *vivo models* of CH (14, 15, 21, 23, 54). The importance of NHE1 was further emphasized through the direct inhibition of NHE1 (16, 85). In a study by Snabaitis et al. (80), inhibition of NHE activity significantly attenuated CH post-MI in the rat myocardium. In a later study, Cingolani et al. demonstrated the α1-AR blocker, enalapril regressed CH and this was accompanied by the normalization of NHE1 activity (86). Ennis et al. further confirmed these findings by demonstrating that NHE1 inhibition by BIIB723 prevented isoproterenol-induced CH in male Wistar rats (84). These findings suggest that inhibition of NHE1 activity may be beneficial in reversing NHE1-induced CH both *in vitro* and *in vivo*. Interestingly, both pressure overload and dexamethasone-induced CH in WT serum and glucocorticoid-inudcible kinase 1 (SGK1) mice resulted in enhanced ANP and NHE1 gene expression as well as NHE1 activity (21, 22). Taken together, these findings indicate that NHE1 mediates CH in response to mechanical and neurohormonal stimulation. Moreover, the activity of NHE1 during CH appears to be an important factor in the remodeling of the heart.

1.3.1.1 NHE1 Activation of Mechanisms in Cardiac Hypertrophy

The importance of the the *activation* of NHE1 during CH was confirmed by Mraiche et al. who have established that overexpression of the active form of NHE1

induces CH (18). NRVMs infected with an adenovirus expressing active NHE1 demonstrated parameters of CH including elevated cell area and protein synthesis compared to NRVMs overexpressing the WT NHE1 (15). Similialy, transgenic mice overexpressing active NHE1 promoted CH to a much larger extent than WT NHE1 mice (18, 23), further implicating activated NHE1 in the induction of CH *in vivo*. Moreover, Voelkl et al. recently revealed that dexamethasone-induced upregulation of SGK1 enhances NHE1 gene expression as well as activity in HL-1 cardiomyocytes (21). Upregulation of SGK1 has been found to play a role in CH, however, whether its hypertrophic effects are mediated through NHE1 activation is yet to be established (87). Taken together, these findings further confirm that elevated levels of NHE1 alone is not detrimental in the myocardium and that rather, the activity of NHE1 is necessary for the induction of CH.

One possible mechanism by which NHE1 could induce CH has been attributed to the *elevated* pH_i and *intracellular* Na^+ (Na^+_i) following the activation of NHE1 (14). Elevated Na^+_i is thought to activate the reverse mode of the Na^+/Ca^{2+} exchanger (NCX) thereby increasing levels of Ca^{2+}_i (17, 88). This has been previously demonstrated in a model of human hereditary cardiomyopathy in which NHE1 expression and activity was associated with elevated Na^+_i and Ca^{2+}_i (89). Elevated Ca^{2+}_i can in turn activate key factors that promote the process of CH, including CaN and CaMK II, which are also key regulators of NHE1 activity as described in Section 1.2.2.3.2 (4, 14, 17). However, it is not abundantly clear how the upregulation of NHE1 can affect the homeostasis of Ca^{2+} and the activation of pro-hypertrophic signaling pathways.

Another pathway that could be considered for the implication of NHE1 in CH is the *activation of pro-hypertrophic kinases* such as ERK 1/2, RSK and Akt (17, 54, 90). In fact, PE-induced activation of ERK 1/2 and its downstream effector, RSK has recently been shown to induce hypertrophic gene expression in NRVMs (91). Moreover, in guanlyl cyclase-A (GC-$A^{-/-}$) deficient mice, a hypertrophic phenotype of mice, NHE1 activity was enhanced, which was associated with elevated Ca^{2+}_i and subsequent activation of CaMK II, the CaN/NFAT pathway as well as phosphorylation of ERK 1/2, p38 and Akt (92). Interestingly, inhibition of NHE1 using cariporide significantly reversed NHE1-induced CH and the activation of Akt only, suggesting that Akt and CaMK II are key mediators of NHE1-induced CH. Taken together, these findings further emphasize the influence of enhanced NHE1 activity on the activation of pro-hypertrophic kinases including MAPKs and Akt.

Hisamitsu et al recently demonstrated that in NRVMs, enhanced expression/activity of NHE1 induced the activation of the *CaN/NFAT pathway* leading to enhanced ANP gene expression and CH (14). Interestingly, treatment of NRVMs with ginsenosides, a group of triterpenoid saponins extracted from ginseng, significantly reduced PE-induced upregulation of NHE1 and activation of the CaN/NFAT, further confirming the role of CaN/NFAT in NHE1-induced CH (93). More importantly, the inhibition of NHE1 or CaN activity using EIPA or FK506, respectively, significantly inhibits NFAT translocation as well as ANP gene expression (14). These findings strongly suggest that that the hypertrophic effects of enhanced NHE1 activity during CH may be occuring through activation of the pro-hypertrophic CaN/NFAT pathway.

1.3.2 NHE1 in Ischemia/Reperfusion Injury

During I/R injury, the heart switches from fatty acid oxidation, as a means to generate energy, to glycolysis in an attempt to generate more Adenosine-5'-triphosphate (ATP) and compensate for the damage induced by ischemia (94). The reduction in pH_i that occurs during ischemia secondary to the anaerobic metabolism and hydrolysis of ATP has been suggested to increase NHE1 activity and subsequently, elevate Na^+_i and Ca^{2+}_i (48). The exact role of enhanced NHE1 activity during I/R injury is subject to major controversy. While some studies have suggested that activation of NHE1 protects against I/R injury, other have indicated that inhibition the exchanger protects against I/R injury and the progression of cardiac dysfunction.

An increasing number of studies have reported an important pathophysiological role for enhanced NHE1 activity in the *development* of myocardial dysfunction during CH, I/R injury and heart failure (17, 18, 94). Karki et al. suggested that upregulation of NHE1 and ER stress-associated proteins in a hypoxia-reoxygenation model of I/R injury in NRVMs predisposed to severe damage as well as apoptosis (43). Furthermore, administration of the highly selective and potent NHE1 inhibitor, sabiporide, to mice undergoing coronary artery occlusion exhibited significantly reduced infarct size and ischemia-induced arrhythmia and activated ERK 1/2 levels (95). Moreover, using an NHE1 knock out (KO) mouse line, Prasad et al. have recently shown that long-term inhibition of NHE1 activity reduced oxidative stress and enhanced metabolic substrate handling following high-fat diet-induced stress on the heart (54). Taken together, these findings suggest that enhanced activity

of NHE1 mediates cardiac remodeling and predisposes the heart to dysfunction following /R injury.

Recently, much controversy has surrounded the role of NHE1 in I/R injury. Mraiche et al. recently demonstrated that transgenic mice overexpressing cardiac specific NHE1 subjected to ischemia and reperfusion exhibited enhanced fatty acid oxidation, glycolysis as well as ATP levels compared to the NHE1 WT mice (94). While enhanced rates of glycolysis are considered detrimental during I/R injury as a result of elevated H^+_i, enhanced activity of NHE1 would be cardioprotective as it would regulate the pH_i and thus, reduce the proton load on the heart (94). These findings were in agreement with an earlier study in which Cook et al. demonstrated that the *cardioprotective* effects of upregulated NHE1 following I/R was preserved even in the presence of zoniporide (96). This interesting observation was associated with the upregulation of endoplasmic reticulum (ER) stress-associated proteins including calreticulin, glucose-regulated protein (GRP78), protein disulfide isomerase (PDI) and C/EBP homologous protein, proteins that have been implicated in enhanced protection against I/R injury. However, whether the observed cardioprotection is due to enhanced NHE1 activity or if it is mediated through an alternative pathway is yet to be determined (Figure 1.2).

1.3.2.1 NHE1 In Clinical Trials

The apparent therapeutic potential of NHE inhibitors, coupled with the perceived need for cardioprotective therapy in the management of CH, has led to the initiation of clinical trials using the different inhibitors of NHE1 discussed in 1.2.2.2. The first trial conducted using the NHE1 inhibitor cariporide was "The GUARD

During Ischemia Against Necrosis (GUARDIAN)" trial (97). 11,590 patients who had been diagnosed with either unstable angina/ non–Q-wave MI or were in need for high-risk percutaneous interventions, or high-risk coronary artery bypass grafting were enrolled. The results of the study revealed that here was no overall improvement in mortality. As a result, the trial had failed to demonstrate any clinical significance for the use of cariporide in the inhibition of NHE1 (98). The second large-scale trial was the "Evaluation of the Safety and Cardioprotective effects of eniporide in the Acute Myocardial Infarction (ESCAMI)" (47). In this study, patients undergoing thrombolysis or angioplasty for acute MI received different doses of eniporide as a 10-minute infusion. The results of the ESCAMI study published in 2001 concluded no meaningful benefits for the use of eniporide as an inhibitor for NHE1 on its own before reperfusion therapy (99). The most recent trial "The Na^+/H^+ Exchange inhibition to Prevent coronary Events in acute cardiac conDITIONs (EXPEDITION)", addressed the ability of cariporide in preventing death or nonfatal MI in patients who were undergoing coronary artery bypass graft (CABG) (100). The results from the EXPEDITION trial showed a reduction in the incidence of death or MI from 20.3% - 16.6%, which was accompanied by an elevation in the occurrence of cerebrovascular insults (101). Murphy E recently suggested that failure of the clinical trials involving the use of NHE1 inhibitors may be attributed to the timing of administration of the inhibitors, indicating that administration of the inhibitors on reperfusion may have proven to be more beneficial than during ischemia (102). Moreover, the inhibition of basal NHE1 activity and the house keeping properties of exchanger may in reality not be ideal. Despite the challenges of using NHE1 inhibitors in clinical trials, it is very important not undermine the importance of

inhibiting the enhanced activity of NHE1, which appears to be a major culprit leading to CH. Therefore, it is important to identify the different mediators and NHE1 activity in order to highlight a potential therapeutic target that may be inhibited instead of NHE1 during CH.

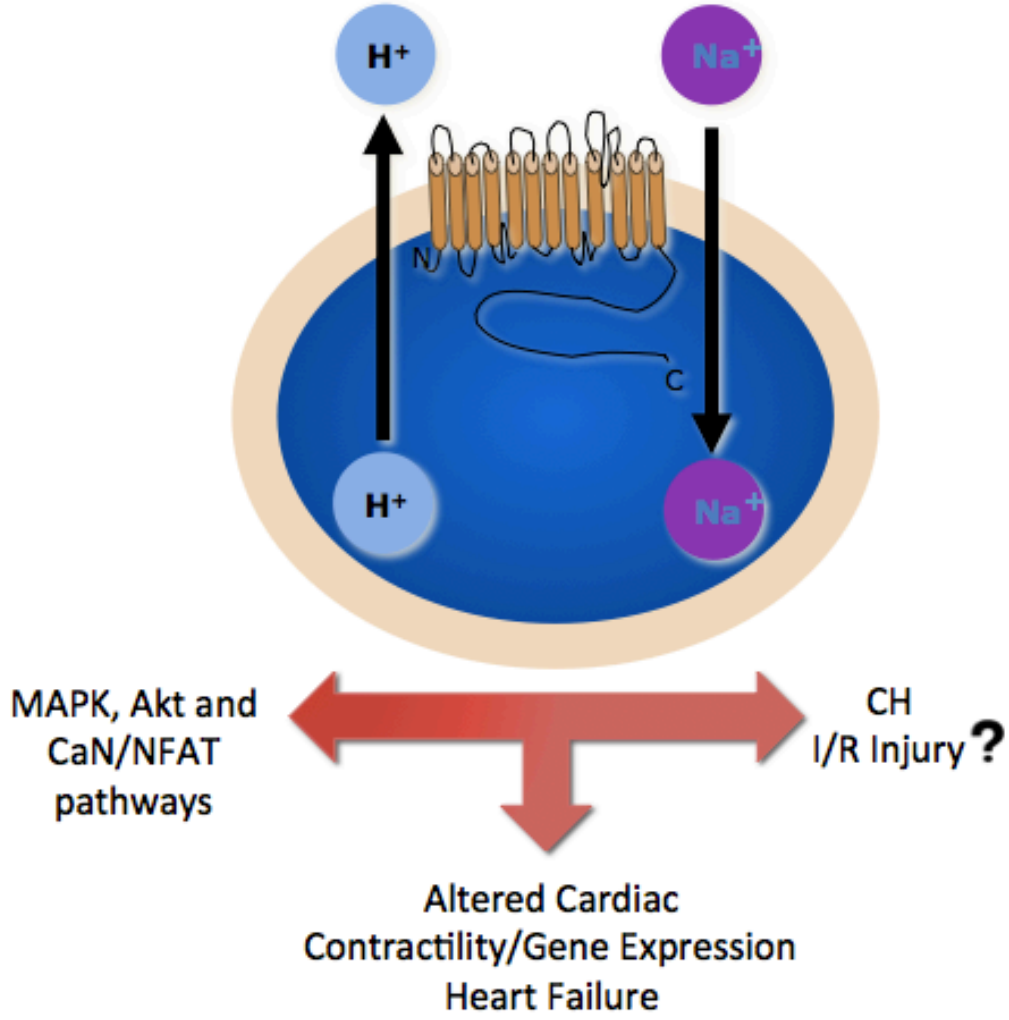

Fig. 1.2: Role of NHE1 in cardiovascular diseases. Enhanced activity of NHE1 has been shown to contribute cardiac hypertrophy ischemia/reperfusion injury through the activation of hypertrophic pathways including mitogen activated protein kinases and Calcineurin/Nuclear factor activated T-cells pathways. Impaired cardiac contractility as well as altered gene expression can lead to heart failure. **CH**, cardiac hypertrophy; **I/R**, ischemia/reperfusion; **MAPK**, mitogen activated protein kinases; **CaN/NFAT**, Calcineurin/Nuclear factor activated T-cells.

1.4 Osteopontin (OPN)

1.4.1 Structure of OPN

OPN, also known as secreted phosphoprotein I (SPP1) and early T-lymphocyte activation 1(Eta-1), was first isolated from bovine mineralized bone matrix in 1985 (103). OPN is a 44 to 75 kDa arginine-glycine-aspartate (RGD) containing glycoprotein expressed by cells in numerous tissues. Cardiomyocytes have been shown to express very basal levels of OPN in the heart (104). However, OPN is mainly expressed by cardiac fibroblasts, endothelial and smooth muscle cells (105). OPN is also secreted by a variety of cells including osteoblasts, osteoclasts, macrophages and T cells, thus highlighting its role inflammatory processes and interactions with the immune system (106). As a matricellular protein of the ECM, OPN is involved in cell signaling as well as structural tissue remodeling and wound healing (107, 108). As such, OPN is considered a multifunctional protein involved in many biological processes.

The OPN protein is a negatively charged, acidic hydrophilic protein that is synthetized by numerous tissues and secreted into the body fluids (109). The total number of amino acids in the OPN protein sequence ranges between 300-317 in rats and human (106). There appears to be a discrepancy in the predicted mass and apparent molecular weight of OPN (110, 111). The degree of sequence homology of the OPN coding sequence seems to be highly conserved amongst species (112). The N terminal contains the RGD cell binding sequence, which mediates many of OPN's cellular functions through its interaction with cell surface integrin receptors including $\alpha_v\beta_1$, $\alpha_v\beta_3$, and $\alpha_v\beta_5$.(103). The N-terminal also contains a non-RGD serine-valine-

valine-tyrosine-glutamate-leucine-arginine (SVVYGLR) domain between the RGD cell binding sequence and a thrombin cleavage site, which has been suggested to allow for the interaction between OPN and integrin receptors $\alpha_4\beta_1$ and $\alpha_9\beta_1$ (113). In addition, OPN contains 2 putative heparin bindings sites and a Ca^{2+} binding site towards the C-terminal of the protein (114). It is widely believed that these sites serve as binding sites for hyaluronic acid receptor 44 (CD44), along with OPN's N-terminal, thus allowing OPN to regulate CD44 surface expression (115).

OPN has an unusually high content of serine, threonine and glutamate residues rendering it a perfect candidate for *post-translational modifications* (PTM) through phosphorylation, sulfation and glycosylation (109). Some studies have suggested that OPN must undergo significant PTM in order to become functional (103, 106). This was demonstrated in a study in which phosphorylation of OPN was necessary to induce cell spreading in the MH-S murine macrophage cell line (116). PTMs can also lead to tissue-specific isoforms of OPN that differ in their phosphorylation patterns, function and overall cellular response to OPN (115). In fact, adhesion of the mouse transformed embryonic fibroblasts to immortalized osteoblasts (ObOPN) was significantly higher than adhesion to the *ras*-transformed fibroblasts (FbOPN) (117). This was attributed to the different degree of phosphorylation between OPN produced by ObOPN osteoblasts compared to FbOPN fibroblasts. On the other hand, several studies have indicated that exposure of the RGD and SVVYGLR through cleavage is more important for the activation of OPN through integrin and CD44 binding (115). Taken together these findings highlight the impact of PTM on the role of OPN in numerous biological processes. In addition, PTM helps in regulate OPN's function in physiological and pathological processes.

OPN is differentially expressed as two *isoforms*, a *secreted* full length OPN (sOPN) and an *intracellular* (iOPN) form found in the cytoplasm and nucleus (118). sOPN is a major regulator of biological functions including cell motility, immunity and survival (113). Interaction of sOPN with its integrin $\alpha_v\beta_3$, $\alpha_v\beta_5$ and CD44 receptors has previously been shown to activate cytokine and chemokine expression (119). In addition, the interaction of circulating sOPN with cell surface receptors, growth factor and cell survival pathways has been suggested to play a pivotal role in tumor progression and malignancies (120). Moreover plasma levels of OPN were found to be upregulated in several animal and human models of heart failure, suggesting a pivotal role for sOPN in remodeling (105, 118). On the other hand, iOPN has been suggested to play a role in cytoskeletal rearrangement (119). However, the exact function of iOPN in immunity and the signaling pathways activated by it remain quite unclear (113). Taken together these findings suggest that even though the secreted and intracellular forms of OPN are generated from the same OPN mRNA species, their functional and overall cellular response differ. It is, important to note that it is rather difficult to differentiate between sOPN and iOPN protein/gene expression *in vitro*. This is due to the fact that sOPN binds to cell surface proteoglycans and is a matricellular protein of the ECM. Therefore, a large portion of the secreted protein remains associated with the surface of the cell and ECM (121). As a result, in the majority of *in vitro* studies, OPN expression is more readily examined in the cell lysates (110, 121-123).

1.4.2 Physiological Role of OPN

OPN has important roles in both normal physiological as well as pathological

processes. OPN was initially identified as a cytokine with pro-inflammatory actions (114). More recently, OPN has emerged as a matricellular protein of the ECM (107). OPN is also heavily involved in the regulation of bone tissue mineralization and differentiation of both osteoblasts and osteoclasts under normal physiological conditions (106). In addition, OPN appears to be involved in several diseases including inflammatory and autoimmune diseases, cancers and more recently, cardiovascular diseases (103, 124). Thus, OPN has become a key phosphoprotein in several physiological processes and in pathologic conditions including cardiovascular diseases and cancer.

1.4.2.1 OPN as a Matricellular Protein of the Extracellular Matrix

As a matricellular proteins of the ECM, OPN has been suggested to play a major role in mediating cell attachment and signaling between cells through a number of receptors including integrins and CD44 (125). In the heart, the ECM surrounds cardiomyocytes and is mainly composed of glycoproteins, fibronectin, matricellular proteins, proteoglycans, and collagens (namely I and III) (126). A growing body of evidence suggests that ECM proteins play a vital role in the regulation of cellular proliferation, migration and adhesion (107). In addition to its role in maintaining the myocardial static structure, the myocardial ECM has become widely recognized as a complex microenvironment that plays a fundamental role in the cardiac remodeling process (127). The induction of extracellular proteins such as MMPs have been suggested to be of biological significance in a variety of pathological conditions including cancer and cardiovascular diseases (128). Interestingly, in several animal models of MI, CH as well as cardiomyopathies, MMP-2 and 9 have been shown to be

upregulated (Reviewed in (128)). Several α1-AR agonists that are hallmarks to cardiac remodeling have been shown to induce the transcription of MMPs including Ang II, ET-1 and NE (129). Moreover, during cardiac remodeling, thrombin, another protein of the ECM, functions to cleave collagen I and degrade the ECM, aggravating the inflammatory and fibrotic processes (107). Taken together, these findings indicate that the wide variety of functions attributed to OPN may in part be mediated by its interaction with other proteins of the ECM, thus highlighting the importance of OPN in cell signaling and remodeling.

1.4.2.2 Inflammation and Tissue Remodeling

OPN expression by macrophages and immune cells is thought to promote cell adhesion, chemotaxis and cytokine expression, processes that are known to mediate *inflammation* (106, 119). In fact, OPN expression appears to be elevated in response to infection and cell injury (130). Several studies have shown that pro-inflammatory cytokines including interleukin 1 and 6 (IL-1, IL-6), tumor necrosis factor alpha (TNF-α) and interferon- γ (IFN-γ) can induce the expression of OPN during chronic inflammatory diseases (107). It has also been shown that OPN can modulate the immune response by macrophage recruitment and differentiation, phagocytosis, enhanced expression of Th1 cytokines and matrix degrading enzymes (124). The mechanism by which OPN mediates expression of inflammatory cytokines has suggested to be in part due to the activation of OPN through integrin binding (114). This in turn phosphorylates the Nuclear Factor-Kappa β (NFkB)-inducing kinase (NIK) and inhibitor of nuclear factor kappa-β kinase β kinases (IKKβ), leading to NFkB mediated expression of inflammatory cytokines. Taken together, these findings

strongly implicate OPN in mediating cellular migration and infiltration during inflammation.

Recent research has defined a role for OPN in mineralized and soft *tissue remodeling* (107). In the bone, OPN plays a major role in preventing hydroxyapatite formation (131) suggesting that it is more readily involved in the process of bone resorption rather than bone formation (108). On the other hand, an upregulation of OPN in calcified atherosclerotic lesions blocks hydroxyapatite crystal growth and can thus regress arterial mineral deposition (132). OPN has also recently been suggested to mediate wound healing (124). Studies have shown that OPN KO mice suffer from insufficient wound healing (124). Moreover, OPN is essential for the differentiation of fibroblasts into myofibroblasts (122, 133). During the process of post-MI remodeling, activated fibroblasts and myofibroblasts become the source of ECM proteins necessary for scar formation and healing of infarct regions (134), suggesting a crucial role for OPN for remodeling of the heart post-MI injury. Taken together, these findings highlight OPN as an emerging key regulator in biomineralization and tissue remodeling.

1.4.2.3 Cell Survival and Migration

Cell migration plays an important role in numerous biological processes essential for development, repair, and pathogenesis (123). Cell-ECM interactions mediated through transmembrane cell adhesion receptors and extracellular matricellular proteins is essential for cell migration (125). OPN is involved in cell adhesion, migration, invasion and proliferation through interaction of its GRGDS sequence with integrin receptors (106). Jalvy et al recently demonstrated that OPN

mediates platelet derived-growth factor (PDGF) migration in vascular smooth muscle cells (VSMCs) (123). OPN expression has also been shown to play a major role in atherosclerotic lesion formation (135). This has been attributed to OPN's ability to promote macrophage and VSMC accumulation as well as VSMC and endothelial cell migration and proliferation, thus contributing to vasculature remodeling (124). OPN has also been shown to mediate cell migration and invasion of cancer cells (130). Behera et al. demonstrated that OPN promoted $\alpha_v\beta_3$ integrin-mediated Signal transducer and activator of transcription (STAT3), an oncogenic gene induction of tumor progression through Janus kinase 2 (JAK2) phosphorylation (136). Upon pretreatment of MDA-MB-468 and MCF-7 breast cancer cells with a JAK2 inhibitor, apoptosis was enhanced and cell migration reduced. These findings suggest that activation of $\alpha_v\beta_3$ is necessary to stimulate migration induced by OPN in cancer. As such, it has become widely accepted that OPN could serve both as a mediator and oncogenic marker for cancer (137).

There is compelling evidence that OPN promotes the *cell survival* in numerous settings. This may be physiologically beneficial, as is the case with regulation of bone resorption (108), or detrimental, during tumor progression (138). In adherent cells such as VSMCs and epithelial cells, OPN has both pro-survival and proliferative functions (139). A recent study has recently demonstrated that OPN mediated cell survival occurs through binding of $\alpha_v\beta_3$ integrin and NFkB activation (140). In this study, the addition of a neutralizing anti-β_3 integrin antibody blocked NFkB activation, which resulted in death of endothelial cells plated on osteopontin-coated dishes. The OPN-mediated NFkB induction and survival may serve beneficial for cell cycle progression, which is important for tissue development and regulation

(139). OPN has also been shown to act through the Ca^{2+}-NFAT pathway to promote osteoclast survival and increase bone resorption (141). This has been demonstrated in Czech-II/Ei mouse bone tumors in which the invasiveness of the tumor resembling human osteosarcoma was attributed to the ability of OPN to activate NFAT (142). Therefore, OPN seems to play a functional role in the progression of cancer through the promotion of cell migration and survival.

1.4.2.4 Angiogenesis

The formation of new blood vessels is critical for supplying the healing *myocardium* with oxygen and nutrients necessary to sustain metabolism (143). Structural and functional remodeling of the infarcted and non-infarcted myocardium through angiogenesis is one of the most critical phases of the post-MI infarct healing and LV remodeling processes (118, 144). In addition, angiogenesis is considered beneficial following I/R injury in an attempt to replenish the blood and oxygen starved myocardium (107). OPN acts as a chemo-attractant for vascular endothelial and smooth muscle cells and is shown to promote vascular cell adhesion and spreading (143). Absence of OPN, however, was shown to significantly reduce markers of angiogenesis both *in vivo* and *in vitro* (118). In OPN KO mice myocardial angiogenesis measured using Matrigel implantation in the LV post-MI induction was associated with a significant decrease in vessel-like area percentages compared to hearts from OPN WT mice (143). Furthermore the reduction in *in vitro* tube formation in cardiac microvascular endothelial cells (CMECs) isolated from the OPN KO hearts was regained following treatment with purified OPN protein (143). In a recent study, Wang et al. demonstrated that patients undergoing mitral valve

replacement surgery who presented with elevated plasma OPN levels were protected against I/R injury (145). Moreover, administration of exogenous OPN to neonatal rat pups who had undergone hypoxic/ischemic injury significantly reduced the size of the infarct in the brain and improved long-term neurological impairment (146). Taken together, these findings suggest that OPN-mediated angiogenesis may serve as a protective mechanism following MI and I/R-injury.

As discussed in Section 1.4.4.2, the involvement of OPN in the prognosis and progression of *cancer* has received wide attention lately (137, 138). Angiogenesis is one of the key steps known to promote tumor metastasis and development. In several malignancies including breast, prostate and gastric cancers, upregulation of OPN was correlated with the progression and metastasis of the tumor (136, 147). Peng et al. have recently demonstrated the role of OPN antibodies in suppressing the angiogenic properties of OPN both *in vitro* and *in vivo* (120). In addition to inhibiting angiogenesis, the OPN antibodies significantly reduced both primary tumor growth rate as well as the tumor lung metastasis. These studies suggest that OPN antibodies could be a potential therapeutic approach to target tumors that are OPN-dependent.

1.4.3 Regulation of OPN Activity

The functional motifs of the OPN protein illustrated in Figure 1.3 highlight the different pathways that can be sought in order to regulate the activity of OPN. OPN is also known to be a substrate for proteolytic cleavage by several proteases that form an integral part of the ECM as discussed in Section 1.4.1.

1.4.3.1 Phosphorylation and Dephosphorylation of OPN

An integral aspect of the regulation of this activity is through phosphorylation and dephosphorylation (106, 115-117). OPN is phosphorylated by tyrosine or serine/threonine kinases including mammary gland casein kinase (MGCK) and casein kinase II (CKII), protein kinase G (PKG), PKA as well as PKC along the N-terminal (106). Christensen et al. have previously demonstrated that phosphorylation of OPN purified from bovine milk occurs mainly through MGCK and CKII as revealed by mass spectrometry (MS) studies (148). *In vitro* experiments have shown that phosphorylation of OPN can be mediated by PKG (106). Activation of PKG and PKA secondary to elevated levels of cyclic guanosine monophosphate (cGMP) and cyclic adenosine monophosphate (cAMP) was associated with a downregulation of OPN rat aortic smooth muscle cells (RASMCs) (148). Phosphorylated OPN has been known to multiple roles including preventing mineralization and ultimately ectopic calcification of VSMCs and impaired bone mineralization (132, 149). Therefore, it is important to understand how to maintain physiologically balanced levels of phosphorylated OPN in order to avoid its pathological effects.

OPN activity has also been shown to be regulated by phosphatases. Alkaline and acidic phosphatases such as TNAP (tissue-nonspecific alkaline phosphatase) and TRAP (tartrate resistant acid phosphatase) expressed by osteoblasts and osteoclasts are known to dephosphorylate and terminate the activity of milk and bone derived OPN (115). In transgenic mice, functional ablation of TNAP ($Alpl^{-/-}$) resulted in enhanced phosphorylation of OPN (131). Taken together, these findings emphasize one of the possible mechanisms of regulating OPN activity. Through phosphorylation and dephosphorylation the activity of OPN can be maintained, creating a balance

between the beneficial vs. the detrimental effects of OPN.

1.4.3.2 Mediators that Cleave OPN and Alter its Activity.

OPN also serves as a substrate for several proteases which have been shown to have significant implications on the binding of OPN to integrin $\alpha_v\beta_1$, $\alpha_v\beta_3$, and $\alpha_v\beta_5$ receptors (105). OPN has been found to be a substrate for proteolytic cleavage by *matrix metalloproteinases* (MMPs) 2, 3, 7 and 12 (110, 121). Interestingly, MMP-cleavage of OPN has been suggested to modulate the activity of the phosphoprotein (115). Agnihotri et al. were the first to demonstrate that the MMP-cleaved OPN fragments increased both cell adhesion and migration in the MH-S murine macrophage cell line compared with full-length OPN (110, 121) More recently, Wolak et al. revealed that in highly inflamed carotid plaques from hypertensive human subjects, the MMP-12 cleaved N-terminal fragment was more abundant than the full form (135). These studies indicate that rather than degradation of OPN, MMP-cleavage can modify, and even enhance the biological activity of OPN.

As mentioned in Section 1.4.1, OPN contains a *thrombin* cleavage site that severs the phosphoprotein into an RGD and SVVYGLR containing N-terminal and a C-terminal fragment (Figure 1.3) (105). Thrombin has been thought to regulate OPN activity through enhanced accessibility of the RGD and SVVYGLR binding domains to the $\alpha_v\beta_1$, $\alpha_v\beta_3$ or $\alpha_v\beta_5$ and $\alpha_4\beta_1$ or $\alpha_9\beta_1$ integrin receptors, respectively (113). Increased thrombin generation, has been implicated in the risk of MI and is often overexpressed on the surface of cancer cells (150). In the inflamed atherosclerotic plaque, an abundance of the thrombin cleaved OPN N-terminal has been demonstrated (135). Moreover, in the MDA-MB-435 human melanoma cell line,

thrombin cleavage of OPN resulted in enhanced cellular adhesion through $\alpha_v\beta_3$ (151). On the other hand, MDA-MB-468 human breast cancer cells transfected with mutant OPN lacking the thrombin cleavage domain exhibited decreased cell adhesion in another study (152). Collectively, these findings strongly suggest that thrombin cleavage of OPN provides another mechanism for the regulation of OPN activity, which is likely to be of great physiological importance. This has proven to be relevant in physiological processes such as inflammation and tissue remodeling, and in pathologic conditions including cardiovascular diseases and cancer.

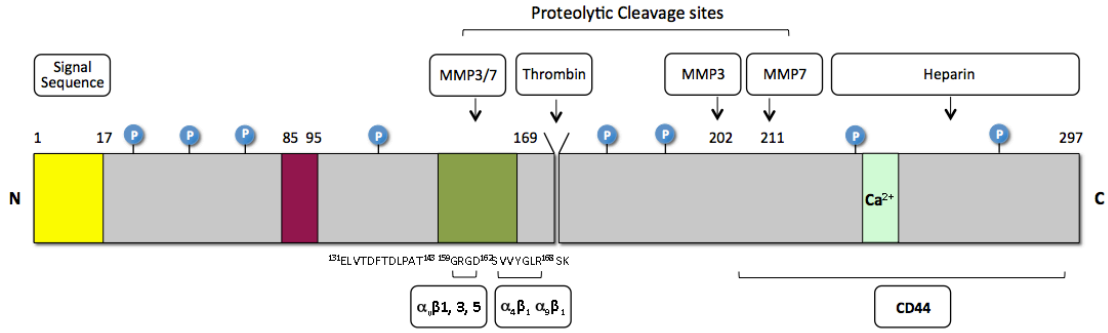

Fig. 1.3: A representative topology model of osteopontin. Displayed is the N-terminal signal sequence regulating OPN secretion, which is cleaved off when the protein is secreted. The GRGDs sequence responsible for integrin binding; the thrombin cleavage site nearest to the C-terminal; the likely region of interaction with CD44 variants towards the C-terminal region of the protein are also displayed. Sites susceptible to matrix metalloproteinases cleavage are also indicated; circled Ps indicate potential regions of serine/threonine phosphorylation. **MMP3/7**, matrix metalloproteinases; **$\alpha_v\beta1, 3, 5$** and **$\alpha_4\beta_1$ $\alpha_9\beta_1$,** integrin; circled **Ps,** sites of phosphorylation. This figure was adopted from Wang et al. (114) (2009).

1.5 OPN in Cardiac Remodeling

Under normal physiological conditions, the adult heart expresses only basal levels of OPN (107). The main sources of OPN expression are non-myocytes, which include fibroblasts, endothelial and smooth muscle cells (105, 107). OPN does not play a role in the development of the heart; however, its expression appears to be markedly increased during cardiac pathologies (118). Enhanced expression of OPN by cardiomyocytes has also been associated with left ventricular hypertrophy (153-155), DCM (20), as well as diabetic cardiomyopathy (82). Increased expression of OPN has also been correlated with the progression of CH to heart failure and the severity of the condition (19, 156). Upregulation of OPN in the infarcted myocardium post-MI has been suggested to contribute to excessive scaring and accumulation of ECM and fibrotic tissue leading to heart failure (134, 156) In addition, tissue from failing hearts of rats revealed that the upregulation of OPN mRNA was originating from infiltrating macrophages and fibroblasts in the interstitium (105, 107). Taken together, these findings clearly indicate that the expression of OPN is critical for cardiac remodeling.

1.5.1 OPN in Post-Myocardial Infarction Injury

The role of OPN in post-MI cardiac remodeling is becoming increasing more evident. Plasma levels of OPN has been shown to be elevated during the early stages of acute ST-elevation MI (STEMI) as well as in patients who have underwent reperfusion within 12 h after the onset of anterior-wall acute MI (AMI) (157, 158). In patients who underwent successful reperfusion following AMI, reduction in OPN plasma levels was significantly correlated with LV end-systolic and diastolic volume

index as well as ejection fraction (158). Collectively, these observations strongly indicate that OPN plays an important role in the remodeling process post-MI injury.

The intricate process by which OPN may mediate its effects in post-MI injury may include the coordination of intracellular signals necessary for the differentiation of fibroblasts into myofibroblasts and their proliferation (122), promoting angiogenesis (143), wound healing and tissue regeneration (125) as well as protecting against LV dilatation (104). During MI, increased proliferation and increased ECM synthesis are the key characteristics of cardiac fibroblasts within the infarct zone (129). The cardiac renin-angiotensin (RAS) system also plays a critical role in structural and functional remodeling post-MI (6). Previous studies have demonstrated that Ang II induces the expression of OPN in both neonatal and adult rat cardiac fibroblasts (NRCFs and ARCFs) (105). During the early stages of post-MI remodeling, mechanical stress and the release of Ang II from injured cardiomyocytes activate fibroblasts, which are then considered the main sources of OPN post-MI (105, 107, 134). The Ang II induced activation of OPN has been suggested to occur through the ERK1/2 and JNK pathways in ARCFs (159). These findings emphasize the role of OPN during post-MI injury cardiac remodeling, which maybe in part mediated by Ang II.

1.5.2 OPN in Cardiac Hypertrophy

The process of fibroblast activation and differentiation into myofibroblasts post-MI is intended to initiate a swift response to injury while avoiding fibrotic scarring and excessive ECM deposition (134). OPN is essential for the differentiation of fibroblasts into myofibroblasts, as demonstrated by Lenga et al.(122). During the

process of post-MI remodeling, activated fibroblasts and myofibroblasts also become the source of ECM proteins necessary for scar formation and healing of infarct regions (134). Failure to terminate this wound-healing process has been shown to result in persistent activation of fibroblasts, excessive cardiac remodeling associated with impaired ventricular relaxation (127). This cascade of events has been suggested to result in the release of OPN from cardiomyocytes and the initiation of CH (103, 105). During cardiac remodeling post-MI, the upregulation of Ang II by cardiomyocytes has also been found to activate fibroblasts (6, 160). Treatment of cardiac fibroblasts with Ang II has previously been shown to stimulate OPN gene expression (161). Moreover, in a model of Ang II induced-CH, fibrosis, collagen deposition as well as LV dilatation were significantly reduced in OPN KO mice (155). These findings suggest that during CH, OPN appears to be an important mediator of Ang II-induced cardiac fibrosis and hypertrophy. Despite these advances, it is still unknown whether Ang II is the only stimulus responsible for the upregulation of OPN expression during hypertrophy of the heart.

Several *in vivo* and *in vitro* models have demonstrated an essential role for OPN in CH (20, 153, 154, 162). In fact, ablation of OPN in transgenic mice has been shown to reduce CH (154, 162). The importance of OPN in CH was also demonstrated in hearts explanted at the time of cardiac transplantation for idiopathic cardiomyopathies, which revealed an upregulation of OPN in cardiomyocytes (156). Although the exact role of OPN and the mechanism underlying its implication in CH is rather unknown, several *in vitro* and *in vivo* studies have highlighted the activation of *pro-hypertrophic kinases and pathways* in response to the upregulation of OPN (82, 154, 155, 163).

The role of OPN in mediating an array of cardiomyopathies has received much attention lately. Gadeau et al. have recently demonstrated that cardiac specific overexpression of OPN in transgenic mice leads to the progression of DCM associated with LV dilatation and fibrosis (20). Moreover, OPN has been previously shown to mediate diabetic cardiomyopathy *in vivo* (162, 163). In one study, Subramanian et al. suggested that activation of *PKC-βII* mediates the upregulation of OPN in diabetic cardiomyopathy in mice (163). The authors demonstrated that phosphorylation of PKC-βII isoform was significantly elevated in WT transgenic mice compared to the OPN KO mice (163). Similarly, Soetikno et al. revealed that curcumin attenuated diabetes-induced cardiomyopathy in mice through the reduction of OPN expression and PKC-βII activity (162). Collectively these findings suggest that OPN mediates diabetic cardiomyopathy possibly through the activation of PKC-βII as well as ERK 1/2. However, whether this is the only mechanism through which elevated OPN expression in cardiomyocytes induces cardiomyopathies is yet to be determined.

Phosphorylated *Akt* and *glycogen synthase kinase-3β* (GSK-3β) have been suggested to contribute to the OPN-induced hypertrophic response (105). In one study, heart weight/body weight ratio, cell surface area as well as ANP gene expression were significantly lower in OPN KO mice compared to OPN WT mice following aortic banding (AB) (154). Interestingly, levels of phosphorylated Akt and glycogen synthase kinase-3β (GSK-3β) were significantly higher in the OPN WT mice following AB. GSK-3β is normally active in unstimulated cells, however, upon phosphorylation by Akt, GSK-3β becomes inactive (154). Inhibition of GSK-3β enhances the translocation of NFAT and GATA-4 transcription factors to the nucleus,

inducing hypertrophic gene expression (155). Taken together, these findings suggest that upregulation of OPN during CH causes the activation of Akt, which contributes to GSK-3β-mediated hypertrophic gene expression, possibly through the interaction of NFAT and GATA-4.

As discussed in section 1.1.3.1, the *CaN/NFAT pathway* is thought to activate hypertrophic gene expression leading to CH (10, 11). Interestingly, OPN expression was significantly reduced in arteries from the diabetic NFAT KO mice (82). Moreover, Nilsson-Berglund et al. recently identified two NFATc3 responsive sequences in the OPN promoter in streptozotocin-induced diabetic NFAT WT mice (82). The role of NFAT in the OPN-induced hypertrophic response was further emphasized in a study in which the activation of NFATc1 and GATA-3 was severely impaired in OPN deficient mice (164). Both NFATc1/c4 and GATA-3/4 mRNA and protein levels have been shown to be elevated CH (13, 14, 81). Based on these findings, not only does OPN appear to mediate cardiac fibrosis and LV dilatation during CH; the phosphoprotein appears to further enhance hypertrophic gene expression through an NFAT/GATA-dependent pathway.

1.5.3 OPN in Heart Failure

During heart failure, the heart's function as a pump is inadequate to deliver oxygen rich blood to the body. OPN expression has been correlated with the onset of heart failure in both animal models and clinical settings (165, 166). In a rat model of congestive heart failure, Trueblood et al. demonstrated that OPN levels dramatically increase after the transition from LV hypertrophy to cardiac decompensation, suggesting that OPN expression is an important mediator of heart failure (104).

Furthermore, in a recent study where the role of OPN in hypertension-induced heart failure was investigated, plasma levels of OPN appeared to be significantly higher in hearts of patients with heart failure compared to control hearts (166). These finding confirm the importance of OPN in the heart and the progression of heart failure.

Cardiac resynchronization therapy (CRT) is an effective treatment for heart failure in patients with ventricular dyssynchrony (167). CRT promotes LV reverse remodeling and contributes to myocardial collagen turnover (167). In patients undergoing CRT, plasma OPN levels were significantly lower in responders to CRT compared to non-responders (168). Such results further implicate OPN in heart failure and imply that plasma OPN levels may serve as a biomarker for the severity of heart failure and an indicator of the response to heart failure therapies (Figure 1.4).

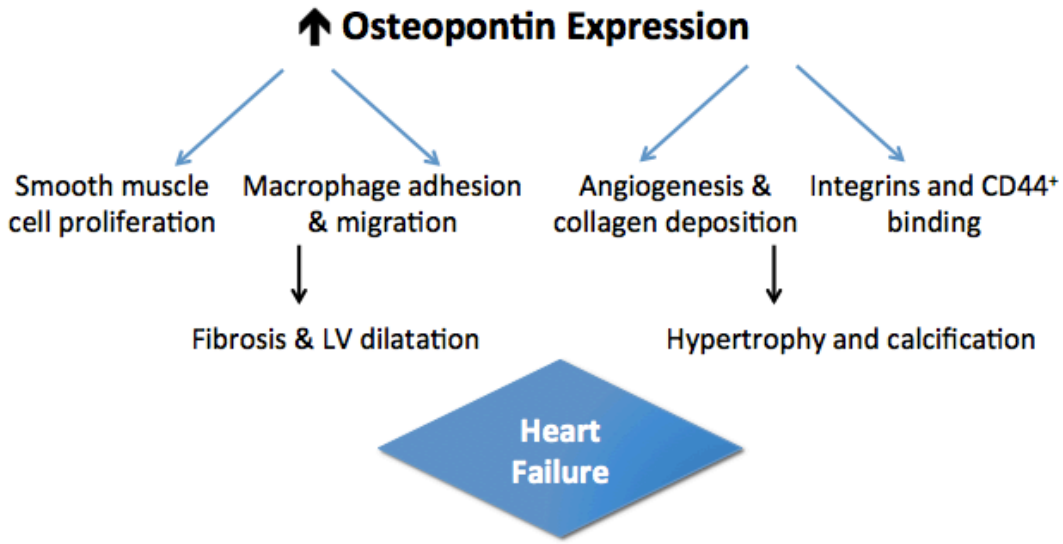

Fig. 1.4: Role of OPN in cardiac remodeling and hypertrophy. Upregulation of OPN has been shown to contribute fibrosis, left ventricular dilatation and calcification, which can ultimately lead to heart failure. This figure was adopted from Waller et al. (103) (2010).

1.6 The Role of NHE1 and OPN in Cardiac Hypertrophy

To date, there have been several studies that highlight an association between NHE1 and OPN in CH (21-24) In fact, the earliest report highlighting the cellular interplay between NHE1 and OPN in CH demonstrated that administration of deoxycorticosterone acetate to mice upregulated both NHE1 and OPN expression, an effect that was significantly reduced upon inhibition of NHE1 (24). Recently, Mraiche et al. suggested that the NHE1-induced hypertrophic response may be in part due to OPN (23). In their study, transgenic mice expressing cardiac specific active NHE1 showed alterations in gene expression that led to both CH and an upregulation of OPN and OPN related molecules (23). Another model of CH induced by the action of SGK1 demonstrated enhanced expression/activity of NHE1 associated with an upregulation of OPN gene expression (21, 22). In an additional study, Voelkl et al. revealed that upregulation of SGK1 in HL-1 cardiomyocytes significantly increased NHE1 activity and OPN gene expression, effects that were abrogated in the presence of an SGK1 inhibitor (21). These findings further implicate the activity of NHE1 in CH, an effect that may be mediated through OPN. However, the relevance of SGKI in this cascade remains questionable since an earlier study demonstrated that mineralocorticoid treatment of pressure-overload induced hypertrophic mice exhibited marked CH associated with fibrosis and enhanced OPN gene expression independent of SGK1 and NHE1 (169). These findings are questionable and inconsistent with several studies that have identified both SGK1 and NHE1 as mediators of CH (17, 18, 22, 84, 170). Taken together, the findings presented here clearly demonstrate an association between NHE1 and OPN in CH.

The importance of NHE1 and OPN in CH is quite clear. Previous reports have

revealed that enhanced activity of NHE1, rather than expression, produces a prominent cardiac hypertrophic phenotype (18, 21-23). OPN has also been shown to play an important role in CH (20, 153, 154, 162). Moreover, OPN has been shown to upregulated in the hypertrophic phenotype of mice associated with enhanced expression/activity of NHE1 (21-23). Although, the exact mechanism by which OPN contributes to the hypertrophic effects of NHE1 are yet to be determined, SGK1 seems to be implicated in the pathway (21, 22). In fact, enhanced SGK1 expression and activity has been suggested to contribute to CH in vivo (87). Moreover, some reports have attributed NHE1-induced CH to the activation of the CaN/NFAT pathway (14, 17). Interestingly, OPN has been shown to function through the CaN/NFAT NFAT/GATA pathway as well (82, 155, 164). However, whether OPN contributes to NHE1-induced CH through upregulation of SGK1 or hypertrophic gene expression through NFAT/GATA is yet to be determined.

1.7 Thesis Objective

Understanding the signaling pathways mediating NHE1-induced CH is critical to provide therapeutic targets that will ultimately lead to an improvement in the management of HF. Although several studies have suggested that NHE1 inhibition could serve as an effective strategy to attenuate CH *in vivo*, clinical trials revealed increased incidence of mortality and reported cerebrovascular side effects with direct NHE inhibition (47). Based on previous studies that revealed enhanced NHE1 expression/activity was associated with CH and upregulation of OPN (21-23), the purpose of this project was to delineate the role of OPN in regulating NHE1 activity and the hypertrophic response induced by NHE1. Our hypothesis was that

OPN contributes to the hypertrophic effects of NHE1 during CH. To investigate whether OPN mediates NHE1-induced CH, NHE1 and OPN were overexpressed in NRVMs using adenoviruses. NRVMs infected with OPN and NHE1 were characterized for changes in NHE1 and OPN protein expression patterns and NHE1 activity. We then analyzed cell area, which serves as a parameter of CH. To confirm the role of OPN in contributing to NHE1-induced CH, the effects of downregulating OPN on the NHE1-induced hypertrophic response in H9c2 cardiomyocytes was investigated. For this set of studies, NHE1 was over expressed using an NHE1 containing adenovirus and an siRNA against OPN was used to downregulate OPN expression. Initially we examined the effects of downregulating OPN on NHE1 protein expression as well as activity. We then characterized our cardiomyocytes for parameters of CH including cell area, protein content and ANP mRNA levels. The *gain* and *loss* of function *in vitro* models were important tools that allowed us to further investigate the importance of OPN on the NHE1-induced hypertrophic response in cardiomyocytes (Figure 2.1). Identifying a novel regulator of NHE1 activity is of great value, as it will provide a potential target for inhibiting NHE1 activity and reversing NHE1-induced CH. This approach could prove to be more beneficial than the direct inhibition of the housekeeping glycoprotein, NHE1.

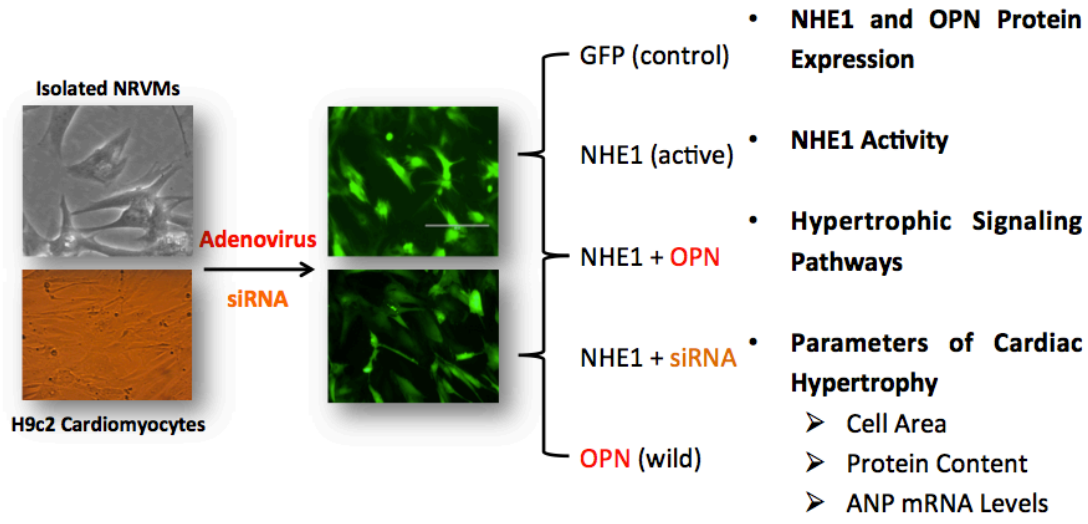

Fig. 2.1: Experimental Model used to determine the role of OPN in NHE1-induced cardiac hypertrophy in cardiomyocytes. Adenovirus infected and/or siRNA OPN transfected cardiomyocytes were characterized by analysis of protein expression and NHE1 activity. Cardiomyocytes were also characterized for parameters of cardiac hypertrophy including cell area, protein content and ANP mRNA levels. Hypertrophic signaling pathways were also examined to determine whether their involvement in NHE1-induced cardiac hypertrophy.

Chapter 2: Materials and Methods

2.1 Effects of Enhanced NHE1 and OPN Expression on Cardiac Hypertrophy in Neonatal Rat Ventricular Cardiomyocytes

2.1.1 Isolation of Neonatal Rat Ventricular Cardiomyocytes (NRVMS)

Isolation of NRVMs was conducted in the laboratory of Dr. Gary Lopaschuk (Heritage Medical Research Center, University of Alberta, Alberta, Edmonton, Canada). All experimental procedures involving animals were in accordance with guidelines set out by the Canadian Council on Animal Care. Ventricular cardiomyocytes from 1-3 day-old neonatal rat heart pups were isolated as described previously with minor modifications (171). Hearts were extracted and placed in ice-cold 1 × phosphate-buffered saline solution (PBS). The PBS was aspirated and the ventricles were separated from the atria and finely minced with scissors. The minced ventricles were then transferred into a T-25cm^2 tissue culture flask containing 1 x PBS. A solution of (2%) DNase (w/v), (0.5%) collagenase (w/v), and (2%) trypsin (w/v) was used to digest the tissue in the T-25cm^2 flask. The flask was placed in an incubator shaker at 37°C for 20 minutes. Following the initial digestion, the tissue was transferred to a 50mL falcon tube containing *isolating media* (DMEM/F12 1:1, 20% fetal bovine serum (FBS), 1% penicillin/streptomycin, and 50µg/mL gentamycin mixed stock solution). The 50mL falcon tube containing the digested tissue was centrifuged at 800rpm for 1 minute at 37°C. The supernatant was discarded, and the pellet was subsequently resuspended in 1 x PBS and transferred into a second T-25cm^2. The DNase/collagenase/trypsin mix was added to the flask for a second

digestion. The flask was placed in an incubator shaker at 37°C for 20 minutes. After the second digestion, the tissue was transferred to a 50mL falcon tube containing *isolating media*, which was centrifuged at 800 rpm for 1 minute at 37°C. The supernatant from the second digestion was separated from the pellet, transferred into a 50mL falcon tube and centrifuged at 17,000rpm for an additional 7 minutes at 37°C. The supernatant was discarded and the remaining pellet was resuspended in *isolating media*. The pellet from the second digestion was resuspended in 1 x PBS, transferred into a T25cm^2 and a third digestion using DNase/collagenase/trypsin was preformed. The flask was placed in an incubator shaker at 37°C for 20 minutes. The digested cell mixture from the third digestion was combined to the cell suspension from the second digestion in a 50mL falcon tube. This cell mixture was then centrifuged at 17,000rpm for 7 minutes at 37°C, after which the supernatant was discarded and the remaining pellet was resuspended in 20 mL *plating media* (DMEM/F12 1:1, 11% horse serum, 5% FBS, 1% penicillin/streptomycin, and 50μg/mL gentamycin mixed stock solution). The cell suspension was filtered using a 70μm cell strainer and the cells were incubated at 37°C in a T-75cm^2 tissue culture flask for 2 hours of differential plating. After 2 hours, the supernatant was transferred to a 50mL falcon tube and the contents of the flask were rinsed 3 times with 1 x PBS, which was added to the supernatant. The cell suspension in the 50mL falcon tube was centrifuged at 1,000 rpm for 2 minutes at 37°C. The supernatant was discarded and the pellet containing the NRVMs was resuspended in *plating media*. NRVMs were seeded in 35mm Primaria-coated dishes (Falcon) at a density of 2.0×10^6 cells/well.

2.1.2 Construction of Adenoviruses Expressing NHE1 and OPN

The pAdTrack plasmids were used to engineer the OPN and NHE1 (15) containing adenoviruses. Mrs. Amy Barr, from Dr. Jason R. B. Dyke's laboratory (474 Heritage Medical Research Centre, University of Alberta, Edmonton, Alberta), was generous enough to assist in the preparation, precipitation, purification and determination of viral titer (plaque formation unit *PFU/mL*) of the GFP, active NHE1 (K3R4E) (15, 32) and wild type OPN adenoviruses as previously described. The OPN and NHE1 containing adenoviruses carried either the human NHE1 plasmid (K3R4E) (a generous gift from Dr. Larry Fliegel, University of Alberta, Edmonton, Alberta) (15, 18, 32) or the mouse OPN (BC057858) plasmid (a generous gift from Dr. Alain Gadeau, INSERM, Pessac, France) (20). Both adenoviruses contained a hemagglutinin (HA) tag and the green fluorescent protein (GFP). The NHE1 adenovirus contained the cytomegalovirus promoter (CMV), a polyadenylation signal (PA) as well as the long terminal repeat (LTR). The NHE1 (K3R4E) plasmid contained mutations in the Lys^{641}, Arg^{643}, Arg^{645} and Arg^{647} sites (to glutamic acid) that rendered the protein active (Figure 2.2) (15). Since previous studies have indicated that the expression active NHE1 produces a more prominent cardiac hypertrophic response compared to the expression of wild type NHE1 (15, 17), we decided to use the active NHE1 adenovirus to simulate NHE1-induced hypertrophic conditons. The NHE1 plasmid also contained an inhibitor resistant mutation created through a double mutation of the $Leu^{163}Phe/Gly^{174}Ser$ region of NHE1 that allows the protein to maintain activity even in the presence of 10 μM EMD87850 (32, 57). Meanwhile, the OPN plasmid carried the wild type form of the plasmid, PST I and Xho I site

sequences between the stop codon and the Sal I and BamH I restriction enzyme site sequences (Figure 2.2). The GFP adenovirus was used in all experiments as a control.

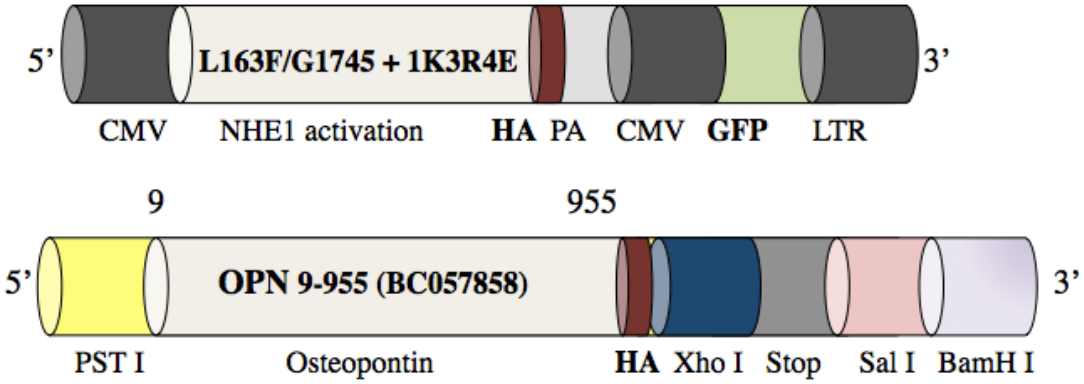

Fig. 2.2 Representative constructs of the NHE1 and OPN plasmids. **A** The NHE1 cDNA plasmid contains mutations at the Lys^{641} (K), Arg^{643}, Arg^{645} and Arg^{647} (R) sites to glutamic acid residues (4) (as indicated by 1K3R4E) rendering the plasmid active at alkaline pH. The plasmid contained an inhibitor resistant mutation region (IRM) that enables the protein to maintain activity even in the presence of an inhibitor and a HA tag. **B** The OPN cDNA contains the wild type HA tagged OPN plasmid. **CMV,** cytomegalovirus promoter; **HA,** hemagglutinin tag; **PA,** polyadenylation signal; **GFP,** green fluorescent protein; **LTR,** long terminal repeat; **PST I**; **Xho I**; **Sal I** and **BamH I**, restriction enzyme site sequences.

2.1.3 Determination of NHE1 and OPN Adenoviral Multiplicity Of Infection and Characterization of NRVMs Infected with NHE1 in the Presence and Absence of OPN Adenovirus

To investigate whether OPN mediates NHE1-induced CH, NHE1 and OPN were overexpressed in NRVMs using adenoviruses. In order to determine the most adequate multiplicity of infection (MOI) and duration of infection for each adenovirus, NRVMs were infected using an MOI of 10, 20 and 30 for the GFP, NHE1 and OPN adenoviruses. Plated NRVMs were supplied with fresh *plating media* for 24 hours prior to infection. On the day of infection, NRVMs were dissociated using 0.25% trypsin EDTA solution and counted using a Hemocytometer. The volume of purified virus required for infection per well was calculated using the formula below:

***mL virus** = (number of cells per dish * MOI) / viral titer (PFU/mL)*

The volume of viral stock calculated was diluted into a 10-25μL solution of 1x PBS and 1% sterile-filtered glycerol and added to 2mL per plate of *infection media* (DMEM/F12, 0.5% FBS, 1% penicillin/streptomycin and 50 μg/mL gentamycin mixed stock solution). Following infection with GFP (as control) or NHE1 in the presence and absence of OPN, NRVMs were incubated at 37°C in a humidified atmosphere (95% O2-5% CO2) for both 24 and 48 hours. Infected NRVMS were then lysed as described in Section in 2.1.3.2.1 and immunoblotting against anti-HA tag was preformed to determine expression of *exogenous* NHE1 and OPN proteins. Based on exogenous protein expression and GFP fluorescence, NRVMs were infected with the GFP adenovirus using an MOI of 10, an MOI of 20 for the NHE1 adenovirus and an MOI of 20 for the OPN adenovirus.

2.1.3.1 Immunoblot Analysis of NHE1 and OPN Proteins in Infected NRVMs

In order to investigate whether OPN mediates NHE1-induced CH, NHE1 and OPN protein expression was analyzed in NRVMs infected with adenoviruses containing NHE1 in the presence and absence of OPN, or GFP (as a control). NRVMs infected with the respective adenoviruses and MOIs identified in Section 2.1.3, were lysed using *Radio-Immunoprecipitation Protein Assay (RIPA) buffer* (50mM Tris (pH at 7.4), 150mM NaCl, 1mM ethylene glycol bis(b-aminoethylether)-N,N,N',N'-tetraacetic acid (EGTA), 0.25% (w/v) sodium deoxycholate, 0.1% (v/v) Triton X-100, 1% (v/v) Nonidet P-400, 1mM benzamidine, 0.1mM phenylmethylsulfonyl fluoride (PMSF), and 0.1% (v/v) protease inhibitor cocktail) as described earlier with a few modifications (15). NRVMs were washed using ice cold 1 x PBS and the cells were incubated in 100μL RIPA buffer for 3 minutes on ice, followed by 2 minutes of cell scrapping. Cell lysates were then collected and centrifuged at 14,000rpm for 5 minutes at room temperature. The supernatants were collected and stored at –20°C. Total amount of protein presented by each adenoviral-infected samples was quantified using the protein assay kits supplied by Biorad (Hercules, CA) according to the manufacturer's instructions. 40 μg of protein was resolved on 10% Sodium dodecyl sulfate polyacrylamide gel electrophoresis (SDS-PAGE) and transferred on to nitrocellulose membranes. The nitrocellulose membranes were then incubated in mouse-anti-HA-tag antibody to determine the expression of *exogenous* NHE1 or OPN, or in mouse-anti-NHE1 and rabbit-anti-OPN to determine the expression of *endogenous* NHE1 or OPN. Anti-glyceraldehyde-3-phosphate dehydrogenase (GAPDH) was used as a loading control. All primary antibodies used were diluted to a factor of 1:1,000-1:2,000 in 1% non-fat milk 1 x TBST solution and incubated

overnight at 4°C with gentle rocking. The membranes were washed 5 times for 5 minutes with 1 x TBST solution at room temperature, after which they were incubated with goat-anti-mouse IGg-HRP (GAM) or goat-anti-rabbit IGg-HRP (GAR). All secondary antibodies used were diluted to a factor of 1:5,000 in 1% non-fat milk 1 x TBST solution and incubated for 1.5 hours at room temperature with gentle rocking. Membranes were washed 5 times for 5 minutes with 1 x TBST solution and immunoreactive proteins were visualized using enhanced chemiluminescence (Amersham Biosciences). Imaging and densitometry analyses were carried using the Alpha Innotech FluorChem Imager (R&D Systems). NHE1 and OPN protein expression was were normalized to GAPDH and expressed as % of GFP ± %SEM.

2.1.3.2 Immunoblot Analysis of ERK 1/2, RSK and Akt, Proteins in Infected NRVMs

The activation of kinases previously implicated in the regulation of NHE1 activity and the mediation of CH was examined. The expression of phosphorylated-ERK/total ERK, phosphorylated-RSK/total RSK as well as phosphorylated-Akt/total Akt proteins was measured in NRVMs infected with GFP, NHE1 alone or in the presence of OPN. Cells were sonicated at constant duty with an output of 30 using a Branson Sonifier (Danbury, CT) in 1mL of *MAPK cell lysis buffer* (50mM Na-pyrophosphate, 50mM NaF, 50mM NaCl, 5mM EDTA, 5mM EGTA, 0.1mM sodium orthovandate, 0.1% Triton X-100, 10mM Hepes pH 7.4, 0.5mM PMSF, 10mg/mL leupeptin) as described previously with minor modifications (18). Protein concentration was determined and western blots were run and developed as described in Section 2.1.3.1. Immunoblotting was against phospho-ERK1/2 and ERK 1/2 (Thr^{202}/Tyr^{204}), phospho-p90RSK (Ser^{380}) and both RSK 1 and RSK 2 as well as

phospho-Akt (Ser^{473}) and Akt (Table 1.1). Anti-GAPDH was used as a loading control. The expression of phosphorylated protein was normalized to the corresponding total protein expression and GAPDH. ERK 1/2, RSK and Akt protein expression was expressed as % of GFP ± %SEM.

Table 1. Primary and secondary antibodies for the analysis of protein expression of NHE1, OPN and hypertrophic kinases

	Primary Antibody	**Secondary Antibody**	**Company**
HA tag	Mouse mAb 6E2	Goat anti-mouse	Cell Signaling (#2367)
NHE1	Mouse IgG1	Goat anti-mouse	BD Pharmingen (#611775)
OPN	Rabbit polyclonal Osteopontin	Goat anti-rabbit	Abcam (#ab14176) (#ab8448)
pERK 1/2	Phosphorylated-ERK (Thr^{202}/Tyr^{204}) Goat polyclonal	Donkey anti-goat	Cell Signaling Technology (#9106)
ERK 1/2	ERK 1/2 (p44/p42 MAPK) Rabbit polyclonal	Goat anti-rabbit	Cell Signaling Technology (#9102)
pRSK	Phosphorylated-RSK (Ser^{380}) Rabbit polyclonal	Goat anti-rabbit	Cell Signaling Technology (#9323)
RSK 1	Rabbit RSK-1 (SC-21)	Goat anti-rabbit	Santa Cruz (#sc231)
RSK 2	Goat Rsk-2 (C-19)	Donkey anti-goat	Santa Cruz (#sc1430)

pAkt	Rabbit Akt (Ser^{473})	Goat anti-rabbit	Cell Signaling Technology (#9271)
Akt	Rabbit polyclonal Akt	Goat anti-rabbit	Cell Signaling Technology (#9272)
GAPDH	Rabbit polyclonal GAPDH	Goat anti-rabbit	Abcam (#ab9485)
α -tubulin	Rabbit polyclonal α -tubulin	Goat anti-rabbit	Abcam (#4074)

2.1.3.3 NHE1 Activity of Infected NRVMs

In order to characterize NHE1 and OPN adenoviruses used to infect NRVMS, NHE1 activity of NRVMs infected with NHE1 in the presence and absence of OPN or GFP (as a control) was measured. NRVMs were isolated and plated on to 35 mm dishes as described in Section in 3.1.1 in the presence of two coverslips. 24 hours post infection, each coverslip was incubated in 0.5% FBS *plating media* and loaded with 3μg/mL pH sensitive dye 2,7-bis(carboxyethyl)-5(6)-carboxyfluorescein acetoxymethyl ester (BCECF-AM) for 30 minutes at 37 °C in a humidified atmosphere (95% O_2-5% CO_2) (172). The change in proton concentration was measured using a PTI Deltascan spectrofluorometer (Photon Technology International; London, Ontario). The PTI fluorometer excitation wavelengths were set at 502.5 nm and 440 nm and the emission wavelength was set at 528.7 nm. Cells were subjected to an acid load using 50mM ammonium chloride (NH_4Cl). Following acidification, coverslips were placed in a 37°C pre-warmed solution of *Na^+-free buffer* (135mM N-methyl-D-glucamine, 5mM KCl, 1.8mM $CaCl_2$, 1mM $MgSO_4$, 5.5mM Glucose, 10mM HEPES) that was pre-warmed to 37°C and adjusted to a pH of 7.3 until a steady acidic pH was reached. The coverslip was then removed and placed in a cuvette containing a 37°C pre-warmed solution of *Na^+-normal buffer* (135mM NaCl, 5mM KCl, 1.8 mM $CaCl_2$, 1mM $MgSO_4$, 5.5mM Glucose, 10mM HEPES) for 3 minutes to allow for cell recovery (173). Each coverslip was then equilibrated in a three-step pH calibration buffer solution (135mM N-methyl-D-glucamine, 135mM KCl, 1.8mM $CaCl_2$, 1mM $MgSO_4$, 5.5mM Glucose, 10mM HEPES) adjusted to a pH of 8, 7 or 6 using KOH and HCl and 10μM nigericin, a K+ ionophore (174). This calibration data was then used to generate a standard curve that

was used to convert fluorescence output measurements into pH readings (Figure 2.3) (32, 57). A linear slope was then calculated which represented the rate of cell recovery, indicative of NHE1 activity, following the induction of an acid load (Figure 2.3). Average NHE1 activity of NRVMs infected with NHE1 in the presence and absence of OPN was expressed as % of GFP control ± %SEM.

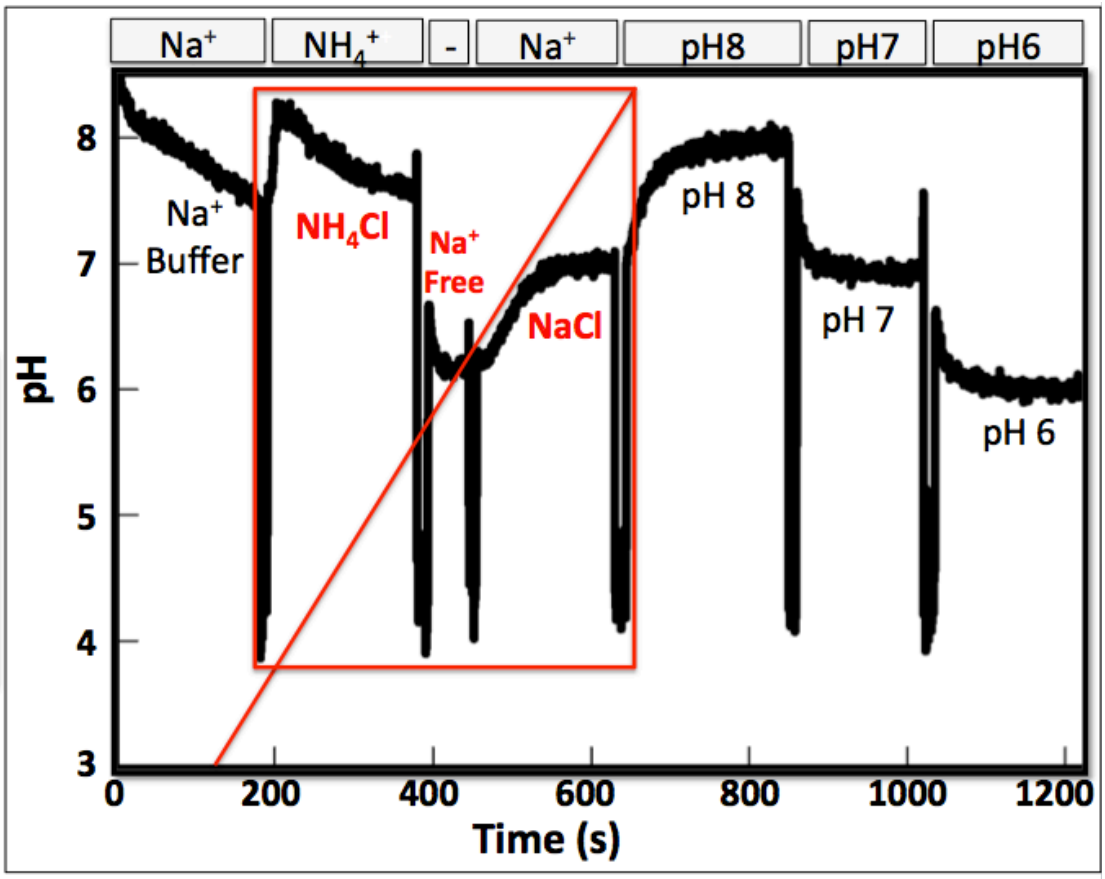

Fig. 2.3: Representative NHE1 activity trace. NHE1 activity, identified as the rate of recovery of adenovirus infected and/or transfected cardiomyocytes was measured following the induction of an acid load using 50mM ammonium chloride as described in Section 2.1.3.2.3. The calculated pH_i trace is shown and the slope of the curve, represented as a linear red line, indicates rate of recovery and NHE1 activity. **Na^+ Buffer** and **NaCl**, Na^+ normal buffer; **NH_4Cl**, ammonium chloride; **Na^+ Free**, Na^+ free buffer.

2.1.4 Characterization of Cell Area, a Parameter of Cardiac Hypertrophy, in Infected NRVMs

In order to characterize the role of OPN in the NHE1-induced hypertrophic response, we analyzed the changes in cell area; a parameter of CH. The average cell area of 50-70 randomly selected cells out of 3-4 preparations was taken. Cells were visualized with an inverted microscope equipped with a monochrome digitalized camera for the detection of fluorescence signals using 20X magnification. Cell area was determined using the AxioVision Imaging Software (Carl Zeiss Microimaging, New York, NY). Average cell area of NRVMs infected with NHE1 in the presence or absence or OPN was expressed as % of GFP control ± %SEM.

2.2 Effects of Downregulating OPN on NHE1-induced Cardiac Hypertrophy in the Rat Embryonic Myoblast Cell Line H9c2

2.2.1 H9c2 Cell Culture and Differentiation into Cardiac Phenotype

H9c2 myoblasts, a clonal cell line derived from the embryonic BD1X rat heart tissue (175), were obtained from European Collections of Cell Cultures (ECACC) and used for the OPN *loss* of function model. H9c2 myoblasts were cultured in DMEM/F12 1:1 supplemented with 10% FBS and 1% penicillin/streptomycin 10% at 37 °C in a humidified atmosphere (95% O_2-5% CO_2). Upon becoming confluent, cells were seeded at a density of 2.0×10^6 cells per 35mm culture dishes containing the 10% FBS *culture medium* used earlier in Section 2.1.1 for 1 day. H9c2 myoblasts were then differentiated into the cardiac phenotype by culturing in DMEM/F12 1:1 supplemented with 1% horse serum and 1% penicillin/streptomycin in the presence of 0.1μM all-trans-retinoic acid (RA) according to the method described earlier (176). The 1% horse serum *culture media* was replaced every other day and 0.1μM RA was supplied daily for 5 days. Following differentiation, H9c2 cardiomyocytes were cultured in DMEM/F12 1:1 supplemented with 1% FBS, devoid of antibiotics in preparation for transfection (Figure 2.4).

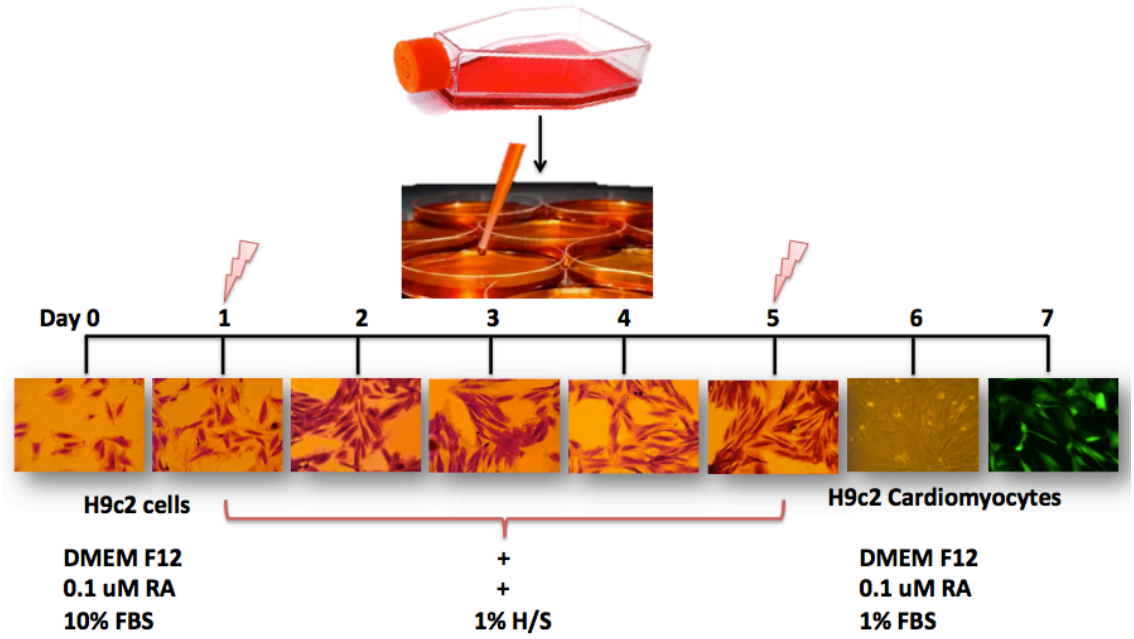

Fig. 2.4: Differentiation of H9c2 rat myoblasts into their cardiac phenotype. Cells were seeded in 10% FBS DMEM *culture medium* for 24 hours prior to differentiation in 1% horse serum DMEM *media* for a duration of 5 days, according to the method described by Me´nard et al (176). Differentiating cells were supplied with 0.1μM all-trans-retinoic acid on a daily basis.

In order to confirm the differentiation of H9c2 cells into the cardiac phenotype, the changes in cell morphology from day 0 to day 5 were analyzed using crystal violet staining (177). H9c2 cardiomyocytes were washed twice with 1 x PBS and incubated in a solution of 4% formaldehyde at room temperature for 10 minutes. Excess formaldehyde was aspirated and cardiomyocytes were washed and fixed in cold methanol for 20 minutes at room temperature. Excess methanol was aspirated and fixed cardiomyocytes were stained using a solution of crystal violet (Sigma) for a further 20 minutes. Images of cell cultures were then taken using an inverted microscope at a magnification of 20X to compare the morphological changes that took place over the course of the differentiation process. The color and hue of the original images was enhanced using Photoshop CS 5.0 in order to improve the quality of the images. The size, fusion and nucleation of the cells were examined to allow for comparison between the myoblasts and cardiomyocytes.

2.2.2 Assessment of NHE1 and OPN Basal Expression in H9c2 Cells

To determine basal NHE1 and OPN protein expression of H9c2 cells in both the differentiated and undifferentiated states, H9c2 were lysed prior to or following differentiation and proteins were separated by western blotting as described in Section 2.1.3.1. To determine the expression of *total* NHE1 or OPN proteins, immunoblotting was preformed against mouse-anti-NHE1 and rabbit-anti-OPN. Anti-α tubulin was used as a loading control for normalization of NHE1 and OPN protein expression.

2.2.3 Characterization of H9c2 Cardiomyocytes Infected with NHE1 and/or Transfected with Silencing RNA (siRNA) OPN

Previous studies have indicated that OPN expression was elevated secondary to enhanced NHE1 expression and activity in several models of CH (21-24). In order to confirm the role of OPN in NHE1-induced CH, we infected H9c2 cardiomyocytes with active NHE1 adenovirus to simulate NHE1-induced hypertrophic conditions and downregulated OPN using a silencing RNA (siRNA) against OPN.

2.2.3.1 Determination of Adenoviral Multiplicity of Infection for H9c2 Cardiomyocytes

Initially, we needed to determine the most ideal MOI and duration of infection for the GFP, NHE1 and OPN adenoviruses in H9c2 cardiomyocytes. Differentiated H9c2 cardiomyocytes were infected with GFP (as control), NHE1 or OPN containing adenoviruses using an MOI of 10, 20 and 30, respectively for 24 hours. Cardiomyocytes were then lysed and western blots were run and developed as described in Section 2.1.3.1 The nitrocellulose membranes were incubated with mouse-anti-HA-tag to examine *exogenous* NHE1 and OPN protein expression. Anti-α tubulin was used as a loading control for normalization of exogenous NHE1 and OPN protein expression. The amount of GFP fluorescence was also monitored using fluorescent microscopy. Based on exogenous protein expression and GFP fluorescence, H9c2 cardiomyocytes were infected with the GFP adenovirus using an MOI of 20, and NHE1 or OPN adenoviruses using an MOI of 30 and 40, respectively.

2.2.3.2 siRNA OPN Transfection of H9c2 Cardiomyocytes

Previous studies have indicated that the use of 2 siRNA targeting the same mRNA is more effective at downregulating the target gene than the use of a single siRNA duplex (123, 178, 179). Moreover, the siRNA against OPN has previously been used both *in vitro* and *in vivo* to silence the OPN gene specifically in VSMCs and epididymal adipose tissue macrophages (123, 180, 181). As a result, in order to downregulate OPN expression in H9c2 cardiomyocytes, the OPN siRNA-1 5'-GAUGAUAGGUAUCUGAAAUTT-3' and OPN siRNA-2: 5'-CGGAUGACUUUAAGCAAGATT-3' targeting the OPN mRNA was used (Eurogentec, http://www.eurogentec.com). 40nM of siRNA OPN were reconstituted in 800μL ultrapure double distilled water to a final concentration of 50μM (or 0.067μg/μL). H9c2 cardiomyocytes were also transfected with 30nM universal scrambled siRNA as a negative control. Lipofectamine 2000 (Invitrogen) was selected as a means to transfect the siRNA OPN. A previous report has suggested it as the most adequate lipid based reagent for siRNA OPN delivery into H9c2 cardiomyocytes (178). Following differentiation, as described in Section 2.2.1, transfection of H9c2 cardiomyocytes using Lipofectamine was performed as described by the manufacture (178). H9c2 cardiomyocytes were cultured in DMEM/F12 1:1 supplemented with 1% FBS devoid of antibiotics 1 day before transfection. On the day of transfection, 1.58μg of siRNA OPN was diluted in OPTI-MEM media (GIBCO) for 5 minutes at room temperature. 4.75μg Lipofectamine was also diluted in OPTI-MEM media for 5 minutes at room temperature. The siRNA OPN:Lipofectamine solutions were then mixed and allowed to complex at room temperature for 20 minutes. H9c2

cardiomyocytes were then transfected with siRNA OPN and incubated at 37 °C in a humidified atmosphere (95% O_2-5% CO_2) for 24 hours.

Prior to carrying out any our experiments, it was essential to determine the most ideal siRNA OPN:Lipofectamine ratio that would produce adequate downregulation of OPN whilst preserving cardiomyocyte health and viability. Thus, in order to determine the most adequate and effective siRNA OPN:Lipofectamine ratio to downregulate OPN, several combinations were put to trial including: 1:0.6, 0.5:1 and 1:3 (178, 179, 182). Following transfection of H9c2 cardiomyocytes with the respected ratios, the cardiomyocytes were lysed and western blots were run and developed as described in Section 2.1.3.1. The nitrocellulose membranes were then incubated in rabbit-anti-OPN. Anti-α tubulin was used as a loading control for normalization of OPN protein expression since the siRNA OPN appeared to markedly downregulate GAPDH expression as well. A decrease of at least 40% was considered most comparable with real-life settings for downregulation of OPN. Cell viability of transfected H9c2 cardiomyocyteswas evaluated using 0.4% Trypan blue solution (Sigma) according to manufacturer's instructions (183). NHE1 infected and/or siRNA OPN transfected H9c2 cardiomyocytes were washed in 1 x PBS before trypsinzation using 0.25% Trypsin-EDTA solution (Sigma). The total number of cardiomyocytes in 10μL of cell suspension were counted using a Hemocytometer. 10μL of cell suspension were mixed with 20μL of Trypan blue solution and allowed to complex for 3 minutes at room temperature. Dead cardiomyocytes stained with Trypan blue in 10μL of cell suspension were counted using a Hemocytometer. Cell viability was expressed using the following calculation:

***% Cell Viability** = (total number of cells/mL – (number of dead cells/mL * 3)) * 100 (PFU/mL)*

Cell viability of no less than 80% was considered most optimum (183). In all subsequent transfections involving siRNA OPN, a ratio of 1:3 was used.

To ensure effective inhibition of OPN, a set of experiments were also run identify the optimum concentration and contact time to use for the siRNA OPN. Several studies have suggested the use of either 30nM or 100nM siRNA OPN for transfection (123, 181). As a result, we examined the effect of downregulating OPN using 30nM vs. 100nM siRNA OPN for 24 and 48 hours . Cardiomyocytes were lysed in RIPA buffer and immunoblotting was preformed as described in Section 2.1.3.1. H9c2 cardiomyocytes infected with OPN (40 MOI) was used as a positive control. Based on the cell health and extent of OPN downregulation, siRNA OPN was used at a concentration of 100nM for a duration of 24 hours in all subsequent experiments.

2.2.3.3 Co-transfection of H9c2 Cardiomyocytes with NHE1 Adenovirus and siRNA OPN

In order to analyze the effects of downregulating OPN on the NHE1-induced hypertrophic response, we decided to overexpress NHE1 using the active NHE1 adenovirus (as discussed in Section 2.1.3) and downregulate OPN using the siRNA against OPN (as discussed in Section 2.2.3.2). We had established that using an MOI of 20, 30 and 40 for adenoviruses containing GFP, NHE1 and OPN, respectively, for 24 hours was most ideal for infection of H9c2 cardiomyocytes (as described in Section 2.2.3.1). Moreover, transfection of H9c2 cardiomyocytes with 100nM siRNA OPN using a 1:3 ratio of siRNA OPN:Lipofectamine for 24 hours was most adequate to downregulate OPN. We then needed to determine the most optimum time frame of co-transfection of NHE1 adenovirus and siRNA OPN that would produce least cell

death and adequate downregulation of OPN. As a result we tried different combinations including: transfection with NHE1 (30 MOI) and siRNA OPN (100nM) at the same time (0 hours), transfection with NHE1 then siRNA OPN 0.5 hours later (0.5 hours), transfection with NHE1 then siRNA OPN 4 hours later (4 hours) and transfection with NHE1 then siRNA OPN 24 hours later (24 hours). After 24 hour incubation at 37°C in a humidified atmosphere (95% O_2-5% CO_2), cardiomyocytes were lysed in RIPA buffer and immunoblotting against anti-OPN was preformed to determine protein expression of OPN (as described in section 2.1.3.1). H9c2 cardiomyocytes infected with OPN (40 MOI) were used as a positive control.

In order to further verify that transfecting H9c2 cardiomyocytes using a concentration of siRNA OPN 100nM was suitable for co-transfection with the NHE1 adenovirus, H9c2 cardiomyocytes were co-transfected with NHE1 adenovirus and siRNA OPN using concentration of both 30 and 100 nM for 24 and 48 hours. H9c2 cardiomyocytes were infected with the NHE1 adenovirus using an MOI of 30 and siRNA OPN 30 and 100nM, 4 hours post infection (using the 4 hour time frame) for 24 and for 48 hours. Cardiomyocytes were lysed in RIPA buffer and immunoblotting was preformed as described in Section 2.1.3.1. Based on cell health and extent of OPN downregulation, cardiomyocytes were transfected with siRNA OPN (100 nM) 4 hours post infection with NHE1 adenovirus (30 MOI). siRNA OPN transfected cardiomyocytes were maintained at 37 °C in a humidified atmosphere (95% O_2-5% CO_2) for 24 hours prior to immunoblotting, measurement of NHE1 activity as well as parameters of CH; cell area, protein content and ANP mRNA expression.

2.2.3.3.1 Immunoblot Analysis of NHE1 and OPN Proteins in NHE1 infected and/or siRNA OPN Transfected H9c2 Cardiomyocytes

H9c2 cells infected with the NHE1 adenovirus and transfected with siRNA OPN (as described in Section 2.2.3.3) were characterized by examining NHE1 and OPN protein expression. Lysates were collected from differentiated H9c2 cardiomyocytes infected with GFP (as control), NHE1 or OPN containing adenoviruses or co-transfected with both NHE1 and siRNA OPN as described in Section 2.1.3.1. Western blots were run and developed as described in Section 2.1.3.1. In order to determine changes in expression patterns of NHE1 and OPN proteins, primary and secondary antibodies were incubated as described in Section 2.1.3.1, with anti-α tubulin used as a loading control. NHE1 and OPN protein expression of H9c2 cardiomyocytes infected with OPN or NHE1 in the presence or absence or siRNA OPN was normalized to α tubulin and expressed as % of GFP control ± %SEM.

2.2.3.3.2 NHE1 Activity of NHE1 Infected and/or siRNA OPN Transfected H9c2 Cardiomyocytes

In order to characterize the effect of downregulating OPN on NHE1 activity in H9c2 cardiomyocytes, NHE1 activity was measured as described in Section 2.1.3.3. The activity of NHE1 following the induction of an acid load was measured in cardiomyocytes infected with NHE1, in the presence and absence of siRNA OPN, and those infected with GFP or OPN containing adenoviruses, as controls. Average NHE1 activity of infected and/or siRNA OPN transfected H9c2 cardiomyocytes was expressed as % of GFP control ± %SEM.

2.2.4 Characterization of Parameters of Cardiac Hypertrophy in NHE1 Infected and/or siRNA OPN Transfected H9c2 Cardiomyocytes

2.2.4.1 Measurement of Cell Surface Area of NHE1 Infected and/or siRNA OPN Transfected H9c2 Cardiomyocytes

To assess the effects of downregulating OPN on the NHE1-induced hypertrophic response, surface area of H9c2 cardiomyocytes infected with NHE1 and transfected with siRNA OPN was measured as described in Section 2.1.4. An MOI of 20, 30 and 40 was used for GFP, NHE1 and OPN adenoviruses respectively. 100nM/L siRNA OPN was added 4 hours post NHE1-infection for 24 hours. The average cell area of 50-70 randomly selected cells out of 3-4 experiments was taken. Average cell area of H9c2 cardiomyocytes infected with OPN or NHE1 in the presence or absence or siRNA OPN was expressed as % of GFP control ± %SEM.

2.2.4.2 Measurement of Protein Content in NHE1 Infected and/or siRNA OPN Transfected H9c2 Cardiomyocytes

Protein content of H9c2 cardiomyocytes transfected with siRNA OPN and infected with NHE1 was measured as described previously with some modifications (184). Seeded cardiomyocytes were infected with GFP, NHE1 and OPN adenoviruses using an MOI of 20, 30 and 40 respectively. 100nM/L siRNA OPN was added 4 hours post NHE1-infection for 24 hours. H9c2 Cardiomyocytes were washed twice in 1 x PBS and trypsinized with 0.25% trypsin-EDTA solution (Sigma). 10uL of cardiomyocytes was then loaded onto Countess® Cell Counting Chamber Slides (Invitrogen) and total number of cells was calculated. Protein concentration in total

cell lysate from another set of infected/transfected H9c2 cardiomyocytes was measured using the DC protein assay kit from Biorad (184). Protein content per 10 x 10^6 cells was determined by dividing the total amount of protein in μg by the cell number. Average protein content of H9c2 cardiomyocytes infected with OPN or NHE1 in the presence or absence or siRNA OPN was expressed as % of GFP control ± %SEM.

2.2.4.3 Expression of ANP and OPN mRNA in NHE1 Infected and/or siRNA OPN Transfected H9c2 Cardiomyocytes

Semi-quantitative Reverse Transcription-Polymerase Chain Reaction (RT-PCR) was used to analyze ANP and OPN mRNA expression. Elevated ANP gene expression is considered a marker of CH both *in vivo* and *in vitro* (14, 90, 93). We also wanted to examine OPN gene expression in order to confirm the results of protein expression following NHE1 upregulation and OPN downregulation. Semi-quantitative Reverse Transcription-Polymerase Chain Reaction (RT-PCR) was used to analyze ANP mRNA expression. RNA was extracted from infected/transfected cardiomyocytes using the Total RNA Purification Kit (Norgen) according to manufacturer's instructions. 1μg of total RNA was reverse transcribed into cDNA using SuperScript-III First Strand Synthesis SuperMix (Invitrogen) according to manufacturer's protocol. 100ng from the cDNA product was used for each PCR reaction. PCR was performed with the 2X PCR Master Mix (Norgen) according to the manufacturer's instructions. Following an initial denaturation of 3 minutes at 95 °C, the samples were denatured at 95°C for 30 seconds, annealed at 60°C for 30 seconds and extended at 72°C for 1 minute. For the expression of each gene, 35 cycles were

preformed to ensure the products were collected just before plateau was reached. A final extension of 72°C for 5 minutes was preformed in order to ensure maximum recovery of products. ANP cDNA was amplified using sense 5′-CTGCTAGACCACCTGGAGGA-3′ and antisense 5′-AAGCTGTTGCAGCCTAGTCC-3′ primer sequence (185) and OPN cDNA with sense 5'-CAGTCGATGTCCCTGACGG-3' and antisense 5'-GTTGCTGTCCTGATCAGAGG-3' primer sequence. The β-actin gene has been demonstrated to be highly stable and conserved and was selected as an internal reference gene (123). β-actin cDNA was primed with sense 5′-ACGCAGCTCAGTAACAGTCC-3′ and antisense 5′-AGATCAAGATCATTGCTCCTCCT-3′ primer sequence (186) (Table 2). RT-PCR products were electrophoresed on 2% agarose gels stained with 0.5g/mL ethidium bromide. ANP, OPN and β-actin were detected 320, 206 and 174bp respectively and quantified using the Alpha Innotech FluorChem Imager. Changes in ANP and OPN mRNA levels of H9c2 cardiomyocytes infected with OPN or NHE1 in the presence or absence or siRNA OPN was expressed as % of GFP control ± %SEM.

Table 2. Semi-quantitative Reverse Transcription-PCR primer sequences and conditions used for analysis of ANP and OPN mRNA levels. β-actin was used as an internal reference gene.

Gene		**Primer Sequence**
ANP	Sense	5′-CTGCTAGACCACCTGGAGGA-3′
	Antisense	5′-AAGCTGTTGCAGCCTAGTCC-3′
OPN	Sense	5’-CAGTCGATGTCCCTGACGG-3’
	Antisense	5’-GTTGCTGTCCTGATCAGAGG-3’
β-actin	Sense	5′-ACGCAGCTCAGTAACAGTCC-3′
	Antisense	5′-AGATCAAGATCATTGCTCCTCCT-3’

Initial Denatur.	**Cycles**	**Denatur.**	**Ann.**	**Extension**	**Final Extension**
95 °C x 3 min	35	95°C x 30 sec	60°C x 30 sec	72°C x 1 min	72°C x 5 min

Denatur, denature; **Ann**, annealing.

2.3 Statistical Analysis

All values expressed were compared to control GFP infected cardiomyocytes ± SEM or SEM%. Since the data represented values with unequal variances that followed a normal distribution, the upaired student's *t* tests was used to compute differences between control GFP, NHE1 and OPN infected groups. A ***P*** value <0.05 was considered a significant difference.

Chapter 3: OPN Facilitates the NHE1 Induced Cardiac Hypertrophic Response in Neonatal Rat Ventricular Cardiomyocytes

3.1 Rationale

CH is a condition associated with an increase in heart mass following chronic and acute morbidities such as hypertension, valvular dysfunction, and post-MI injury (as discussed in Sections 1.1.2 and 1.1.3 (4, 6, 16)). NHE1 has been implicated in several models of CH (14, 17, 22, 23, 84). Interestingly, elevated NHE1 activity, rather than protein expression, has been shown to be a mediator of CH (17, 18, 21, 54). However, since NHE1 is a ubiquitously expressed housekeeping protein that also functions to regulate numerous physiological cell functions (discussed in Section 1.2.2.1 and in (25, 28, 37, 39), the direct inhibition of NHE1 activity may not be ideal to reverse NHE1-induced CH, justifying the failure of several clinical trials (47). In search of a more ideal therapeutic target, much research focusing on the mechanism by which NHE1 induces CH is currently underway. The elevation of OPN in transgenic mice expressing cardiac specific active NHE1 (23) has led us to believe that the NHE1-induced hypertrophic response may in part be due to the expression of OPN. Moreover, Voelkl et al. have previously demonstrated that the activation of SGK1 was associated with the upregulation of both NHE1 and OPN both *in vitro* and *in vivo* (21, 22). In fact, inhibition of NHE1 in deoxycorticosterone acetate treated mice caused a significant reduction in OPN (24). As mentioned in Sections 1.4.1 and 1.4.4, OPN is a matricellular protein component of the ECM involved in mediating inflammation and cellular adhesion (107, 114, 139). Overexpression of OPN has been

shown to result in DCM (20), CH (154, 155, 162) and has been correlated with the severity of heart failure (19, 166, 168). The importance of both NHE1 and OPN in CH intrigued us to further investigate whether OPN mediates the hypertrophic effects induced by NHE1 using an *in vitro* model of NRVMs. We sought to demonstrate that this may occur through OPN's ability to regulate NHE1 expression and activity. Since previous studies have indicated that the expression active NHE1 produces a more prominent cardiac hypertrophic response compared to the expression of wild type NHE1 (15, 17), we decided to use to the active NHE1 adenovirus to simulate the NHE1-induced hypertrophic response, in the presence and absence of OPN. Initially, we analyzed the effect of upregulating OPN on NHE1 expression and activity in NRVMs. Our study also allowed us to characterize NRVMs for parameters of CH, such as cell area, in order to investigate the impact of OPN on the hypertrophic effects induced by NHE1. The results of our experiments are outlined in the section below.

3.2 Results

3.2.1 Characterization of NHE1 and OPN Adenoviruses in NRVMs Infected with NHE1 in the Presence and Absence of OPN

In order to investigate whether OPN contributes to the hypertrophic response induced by NHE1, NRVMs were infected with NHE1 in the presence and absence of OPN or a GFP containing adenovirus (as a control). NRVMs were then characterized for infection by measuring OPN and NHE1 protein expression and activity, and assessed for parameters of CH.

3.2.1.1 NHE1 and OPN Adenoviral Multiplicity of Infection

In order to determine the most idea MOI and duration of infection for the GFP, NHE1 and OPN adenoviruses, we examined *exogenous* NHE1 and OPN protein expression at different MOIs (10, 20, 30) and contact times (24 and 48 hours). NRVMs were infected with active NHE1 alone, NHE1 in the presence of OPN or a GFP containing adenovirus. Both plasmids used to construct the NHE1 and OPN adenoviruses contained an HA tag (as discussed in Section 2.1.2 and illustrated in Figure 2.1) that enabled us to detect and confirm exogenous protein expression. Exogenous protein expression was detected using the HA-tagged antibody (Figure 2.2). All proteins expressed were corrected with the total protein expression of GAPDH. Figure 3.1 A *Upper panel* demonstrates NRVMs infected with NHE1 in the presence and absence of OPN or GFP adenoviruses at 10, 20 and 30 MOI following 24 hour infection. NRVMs infected with the GFP containing adenovirus did not express any NHE1 protein. On the other hand, infection of NRVMs with active NHE1 in the presence and absence of OPN produced the glycosylated and partially glycosylated NHE1 proteins appearing at 110 and 90 kDa respectively. NRVMs infected with NHE1 and OPN also expressed the full form OPN protein at 66 kDa and the cleaved fragment at 32 kDa. Due to extensive PTM, OPN appears to have several isoforms appearing in the form a doublet at 66 and a single band at 50 kDa (as described in Section 1.4.1 and in (113, 154)), in addition to the 32 kDa cleaved form of the full form of OPN (110, 121). An MOI of 20 appeared to produce the most optimum expression of exogenous NHE1 in NRVMs infected with active NHE1 in the presence and absence of OPN adenovirus. Similarly, NRVMs infected with NHE1 and OPN adenoviruses also revealed that an MOI of 20 was the most adequate for

OPN protein expression. To confirm the transfection efficiency, GFP fluorescence was monitored in our respective groups. Figure 3.1 A *Lower panel* demonstrates representative fluorescent images of NRVMs infected with the GFP and NHE1 in the presence and absence of OPN adenoviruses at 10, 20 and 30 MOI following 24 hour infection. These images clearly reflect the high transfection efficiency of the GFP, NHE1 and OPN adenoviruses using an MOI of 20 for 24 hours in the NRVMs. Similar experiments were carried out investigating the *exogenous* protein expression of NHE1 and OPN in NRVMs infected with the respective adenoviruses using 10, 20 and 30 MOI for 48 hours. Figure 3.1 B shows both the glycosylated and partially glycosylated NHE1 proteins appearing at 110 and 90 kDa in NRVMs infected with active NHE1 in the presence and absence of OPN. NRVMs infected with NHE1 and OPN also expressed the full form OPN protein at 66 kDa. Our results indicated that infection of NRVMs with NHE1 adenovirus alone using an MOI of 30 produced the highest NHE1 protein expression. However, infection of NRVMS with both NHE1 and OPN adenoviruses using an MOI of 20 produced more adequate NHE1 and OPN protein expression. Cleary at 48 hours post adenoviral infection, the NHE1 and OPN protein expression is less than that expressed at 24 hours. Therefore, in all our experiments, we infected NRVMs using an MOI of 20 and contact time of 24 hours.

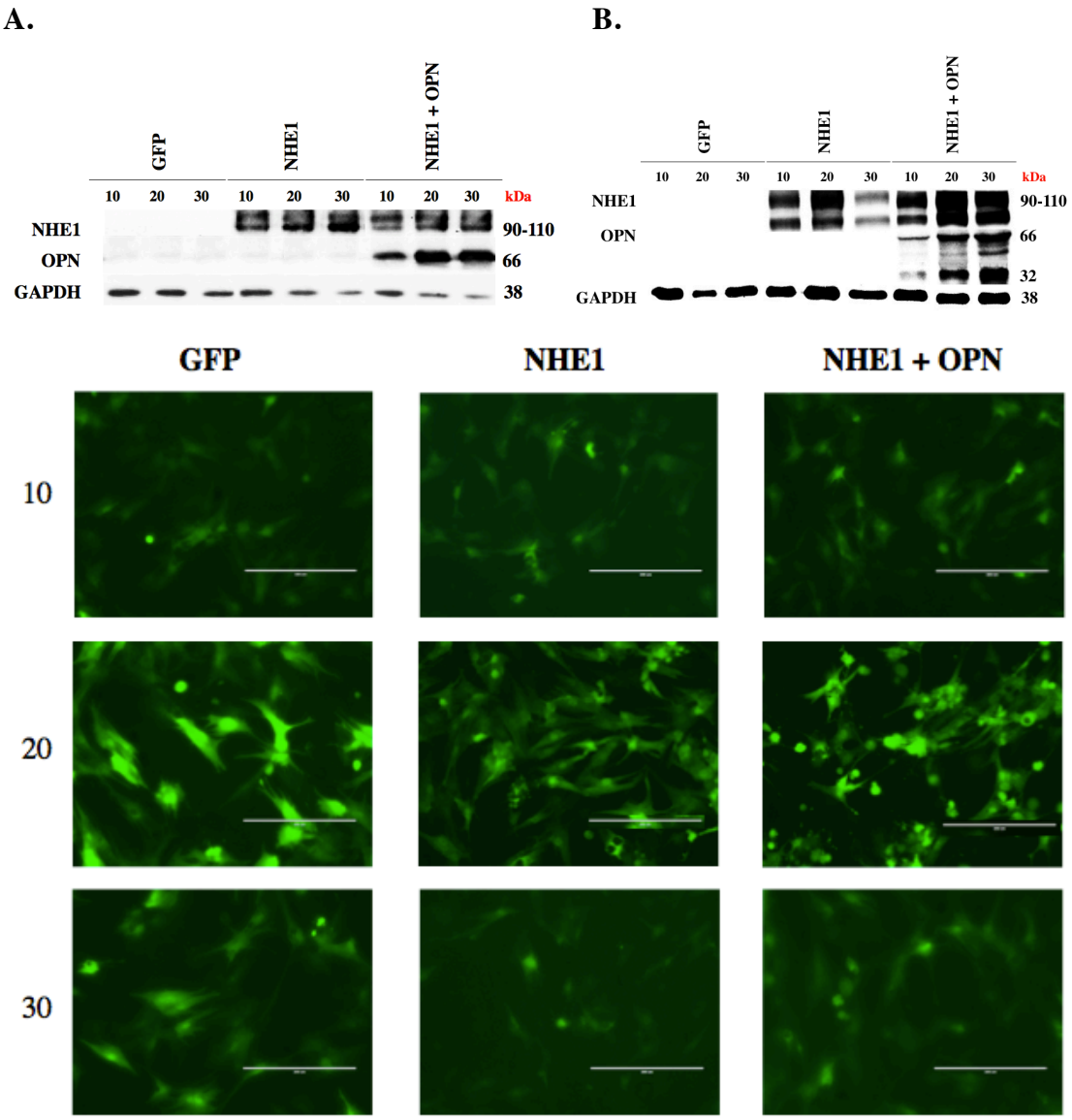

Fig. 3.1: Multiplicity of infection (MOI) and protein expression of *exogenous* NHE1 and OPN in NRVMs. **A.** *Upper panel:* Representative western blot of NRVMs infected with GFP or active NHE1 ± OPN adenovirus 24 hours post infection using an MOI of 10, 20 and 30. Protein expression was determined by immunoblotting against anti-HA; normalization was against GAPDH. Exogenous NHE1 protein was detected between 90-110 kDa, OPN between 66 and/or 32 kDa and GAPDH, as loading control, at 38 kDa. *Lower panel:* Representative fluorescence microscopy images of NRVMs infected with GFP or active NHE1 ± OPN adenovirus examined 24 hours post infection. **B.** Representative western blot of NRVMs infected with GFP or active NHE1 ± OPN adenovirus 48 hours post infection using an MOI of 10, 20 and 30. n=3/group (representative of one preparation).

3.2.1.2 Total NHE1 and OPN Protein Expression in Infected NRVMs

In order to characterize our infected NRVMs; *total* NHE1 and OPN protein expression were measured in NRVMs infected with active NHE1, in the presence and absence of OPN, or an adenovirus containing GFP only. Immunoblotting was preformed using the anti-NHE1 and OPN antibodies (Figure 3.2). Figure 3.2 A *Upper panel* is a representative western blot illustrating the total expression levels of both the glycosylated and partially glycosylated NHE1 and total expression levels of the OPN proteins in the infected NRVMs. NRVMs infected with the GFP containing adenovirus did not express any NHE1 protein. However, NRVMs infected with the active NHE1 adenovirus expressed NHE1 protein with both the glycosylated and partially glycosylated proteins appearing at 110 kDa and 90 kDa respectively. Interestingly, NHE1 protein expression in was significantly increased in NRVMs infected with both NHE1 and OPN adenovirus compared to NRVMs infected with GFP alone (636.5±128.75% NHE1 and OPN infected NRVMs vs. 100.0±10.9% GFP infected NRVMs; $P<0.05$) as well as NHE1 alone (636.5±128.75% NHE1 and OPN infected NRVMs vs. 215.8±72.64% NHE1 infected NRVMs; $P<0.05$) (Figure 3.2 B *Lower panel*), thus implicating OPN in the regulation of NHE1 expression in cardiomyocytes.

We also examined total OPN protein expression levels following overexpression of NHE1 in NRVMS. Although NRVMs infected with the GFP containing adenovirus did express basal levels of the OPN protein at 66 kDa (Figure 3.2 A *Upper panel*), OPN protein expression appeared to be significantly elevated in NRVMs infected with NHE1 alone (342.7%±69.22% NHE1 infected NRVMs vs. 100.0±33.93% GFP infected NRVMs; $P<0.05$) (Figure 3.2 A *Lower panel*). OPN

expression appeared to increase in NRVMs infected with NHE1 in the presence and absence of OPN. A second band was also detected with the anti-OPN antibody (ab14176) at 32 kDa. Our results revealed than upon overexpression of NHE1 and OPN, OPN cleavage showed a trend towards increase (372.6±234.36% NHE1 and OPN infected NRVMs vs. 100±77.1% GFP infected NRVMs). Thus, our data further confirms previous findings that indicated that upregulation of NHE1 enhances OPN expression. Moreover, upregulation of both NHE1 and OPN resulted in elevated cleavage of OPN, suggesting a cross talk between NHE1 and OPN in cardiomyocytes.

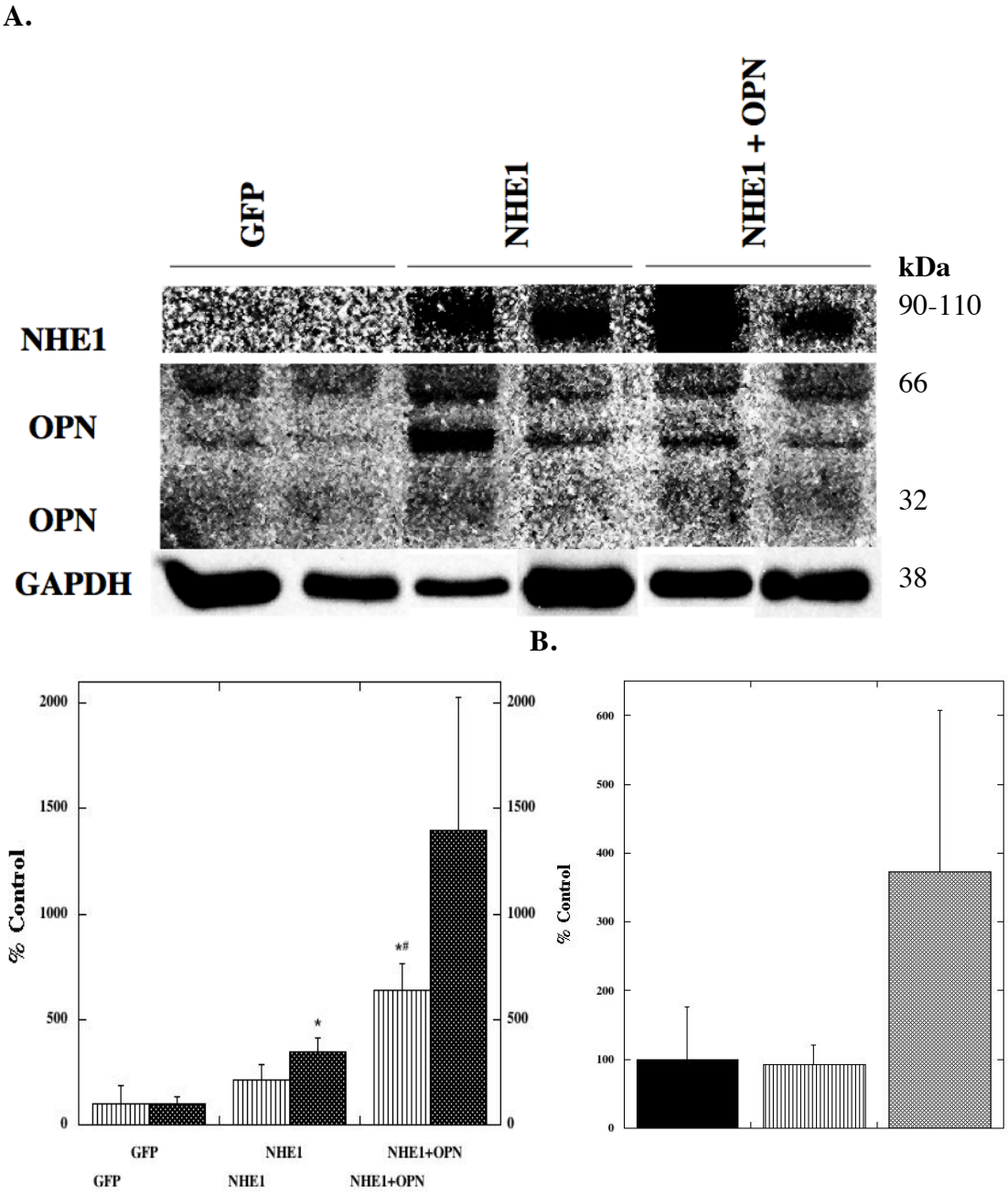

Fig. 3.2: Protein expression of *total* NHE1 and OPN in NRVMs infected with active NHE1 ± OPN adenovirus(es). **A.** *Top panel:* Representative western blot of NRVMs infected with GFP or active NHE1 ± OPN adenovirus 24 hours post infection using an MOI of 20. Protein expression was determined by immunoblotting against anti-NHE1 or OPN; normalization was against GAPDH. NHE1 protein was detected between 90-110 kDa, OPN between 66 kDa and 32 kDa, and GAPDH, as loading control, at 38 kDa. *Bottom panel:* Quantification of relative levels of NHE1 (*stripped*) and OPN at 66 kDa (*dotted*) protein expression. **B.** Quantification of relative levels of cleaved OPN at 32 kDa. Results expressed as % of GFP control ± SEM *** *P* < 0.05** vs. GFP, # vs. NHE1 infected NRVMs (representative of 2-3 preparations).

3.2.1.3 NHE1 Activity of Infected NRVMs

In order to further characterize the effect of enhanced OPN expression on NHE1, we examined NHE1 activity of NRVMs infected with active NHE1, in the presence and absence of OPN, or an adenovirus containing GFP only (Figure 3.3). NHE1 activity was measured as described in Section 2.1.3.2.3 following loading of plated NRVMs with 3g/mL pH sensitive dye BCECF-AM for 30 minutes. The rate of cell recovery, inductive of the ability of NHE1 to exchange one H^+ for one Na^+, was measured following the induction of an acid load using 50mM NH_4Cl. Data from a series of pH calibration curves were used to generate a standard curve, indicating the change in pH over time, and a linear slope to represent NHE1 activity (Figure 2.3). Figure 3.3 *Upper panel* illustrates an example of the representative traces from each adenovirus infected group. Figure 3.3 *Lower panel* quantitatively compares the rate of recovery in NRVMs infected with the respective adenovirus. Interesting, NHE1 activity was significantly highest in NRVMs infected with both the NHE1 and OPN adenoviruses (163.1±19.49% NHE1 and OPN infected NRVMs vs. 100.0±10.90% GFP infected NRVMs; $P<0.05$). Furthermore, NHE1 activity was significantly increased in the presence of both the NHE1 and OPN adenoviruses when compared to NRVMs infected with active NHE1 alone (163.1±19.50% NHE1 and OPN infected NRVMs vs. 114.7±9.48% NHE infected NRVMs; $P<0.05$). Taken together, our data strongly suggests that OPN regulates both NHE1 protein expression (Figure 3.2) as well as activity.

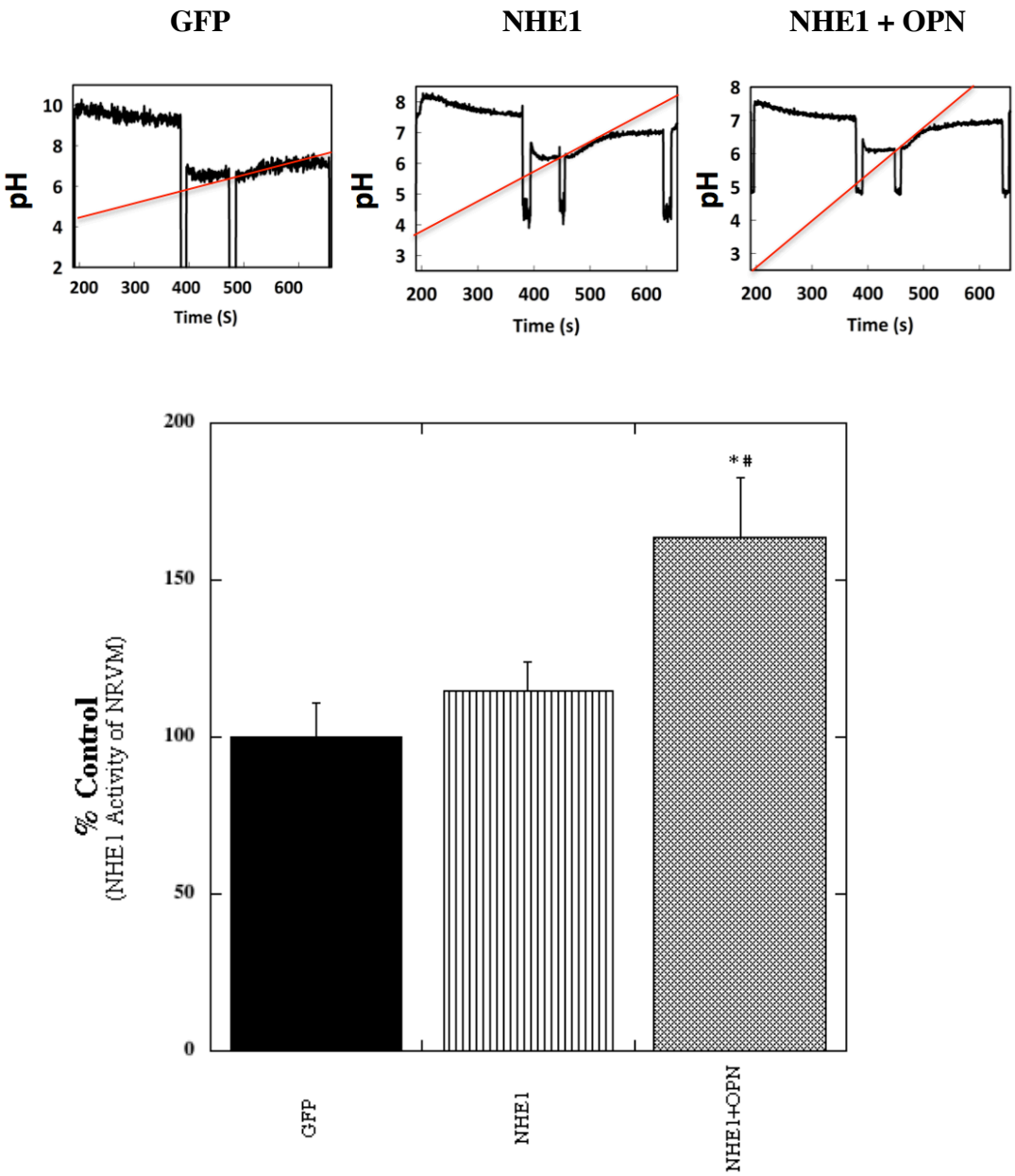

Fig. 3.3: NHE1 activity of NRVMs infected with active NHE1 ± OPN adenovirus(es) 24 hours post infection using an MOI of 20. NRVMs plated on coverslips were incubated with BCECF-AM as described in Section 2.1.3.3. To induce an acid load, 50mM NH_4Cl was added. Cells were immersed in Na^+ free buffer before the reintroduction of Na (NaCl) and calculation of the rate of recovery, indicative of NHE1 activity. *Upper panel* Representative traces of NHE1 activity assay of infected NRVMs. The true, calculated pH_i trace and rate of recovery slopes are indicated. *Lower panel* Quantification of a series of experiments was conducted, NHE1 activity was expressed as a % of GFP control ± %SEM. ***P < 0.05** vs. GFP, # vs. NHE1 (representative of 10-14 coverslips, from 3-4 preparations).

3.2.2 Characterization of Cell Area, a Parameters of Cardiac Hypertrophy in Infected NRVMs

Cell area has been used as a parameter of CH *in vitro* in several studies (15, 63). In order to determine the ability of OPN to mediate the hypertrophic effects of NHE1 during CH, cell area in NRVMs infected with GFP or active NHE1 in the presence and absence of OPN was analyzed (Figure 3.4). Our results indicated that the expression of active NHE1 in NRVMs caused a significant increase in cell area vs. NRVMs infected with the GFP adenovirus (157.9±2.63% NHE1 infected NRVMs vs. 100.0±7.34% GFP infected NRVMs; $P< 0.05$). Cell area of NRVMs overexpressing both NHE1 and OPN was also significantly high when compared to GFP (158.4±3.59% NHE1 and OPN infected NRVMs vs. 100.0±7.34% GFP infected NRVMs; $P<0.05$). The lack of difference between the cell area in NRVMs infected with NHE1 alone or in the presence of OPN probed us to examine more parameters of CH in later experiments, including protein content and ANP mRNA. Nevertheless, our data suggests that OPN contributes to the hypertrophic effects of NHE1 through enhancing NHE1 expression and activity.

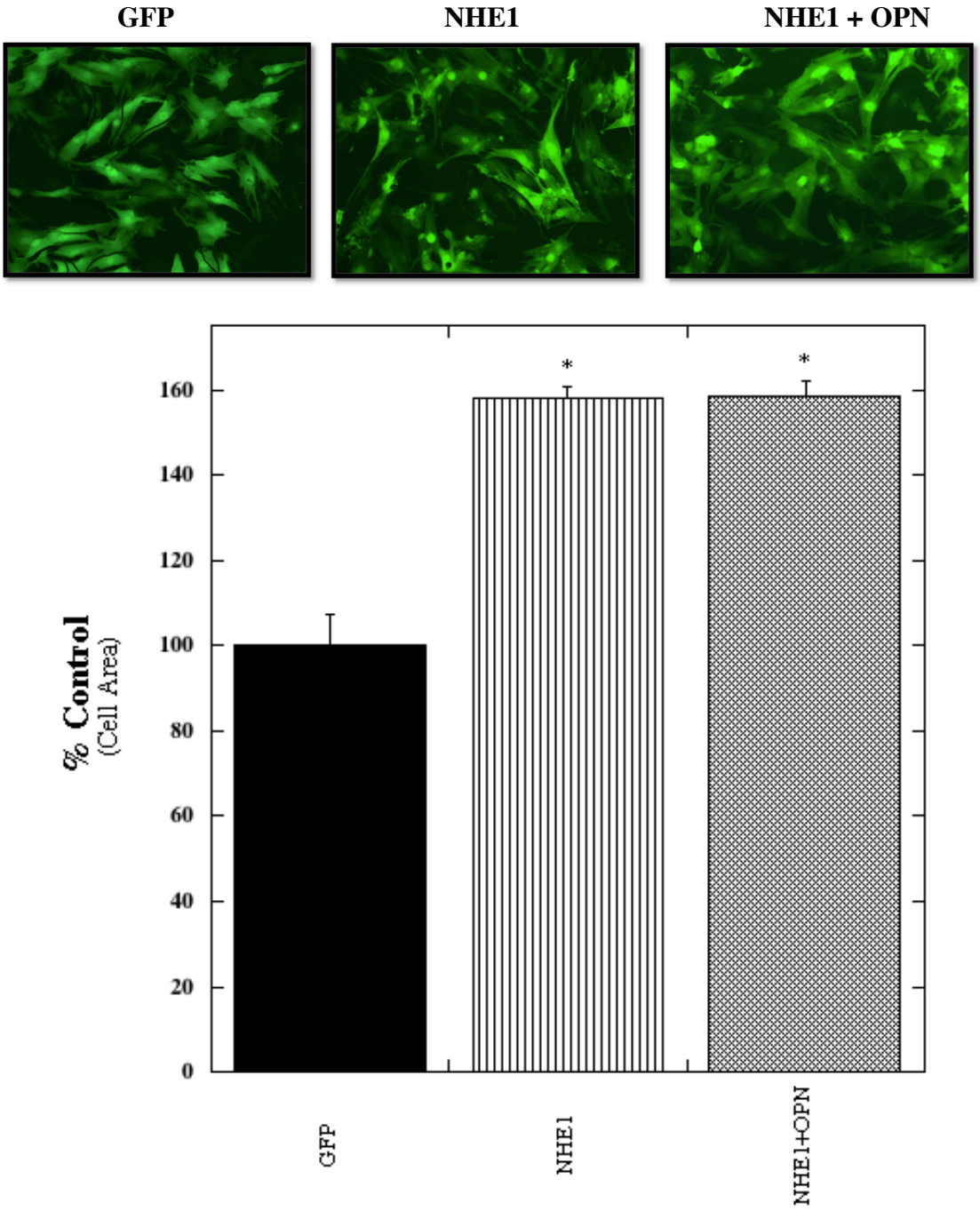

Fig. 3.4: Analysis of cell area of NRVMs infected with active NHE1 ± OPN adenovirus(es) 24 hours post infection using an MOI of 20. *Upper panel* Representative fluorescence microscopy images of infected NRVMs. *Lower panel* Quantification of cell area of infected NRVMs. Results expressed as %GFP ± %SEM. ***** ***P* < 0.05** vs. GFP (representative of at least 50-70 cells measured from 4-6 individual dishes from 3 preparations).

3.2.3 Signaling Pathways Contributing to NHE1-Induced Cardiac Hypertrophy in Infected NRVMs

Several kinases in their phosphorylated forms have been shown to regulate NHE1 activity and have been implicated in CH including RSK, Akt and ERK 1/2 (as discussed in Section 1.3.1 and (69, 70, 79)). Interestingly, ERK 1/2 has been suggested to regulate OPN gene expression in ARCFs in response to Ang II (105, 159). In addition, enhanced activation of Akt in OPN WT mice in response to AB has been suggested to mediate the cardiac hypertrophic effects of OPN (154). Both RSK 1 and RSK 2 have been implicated in the regulation of NHE1 activity and have been found to be expressed in the heart (35, 57). However, RSK 2 is the main isoform implicated in CH and thus, was our isoform of interest (91). In order to eliminate the involvement of such kinases in the NHE1 and OPN induced hypertrophic response in NRVMs, we investigated their activation by measuring the expression of their phosphorylated and total proteins (Figure 3.5). Although expression of the phosphorylated of ERK 1/2, Akt and RSK 2 proteins appeared to increase in NHE1 and OPN infected NRVMs, this increase was not significant. Taken together, our data suggests that OPN contributes to the hypertrophic response of NHE1 in NRVMs, which appears to be independent of hypertrophic kinases including ERK 1/2, RSK and Akt.

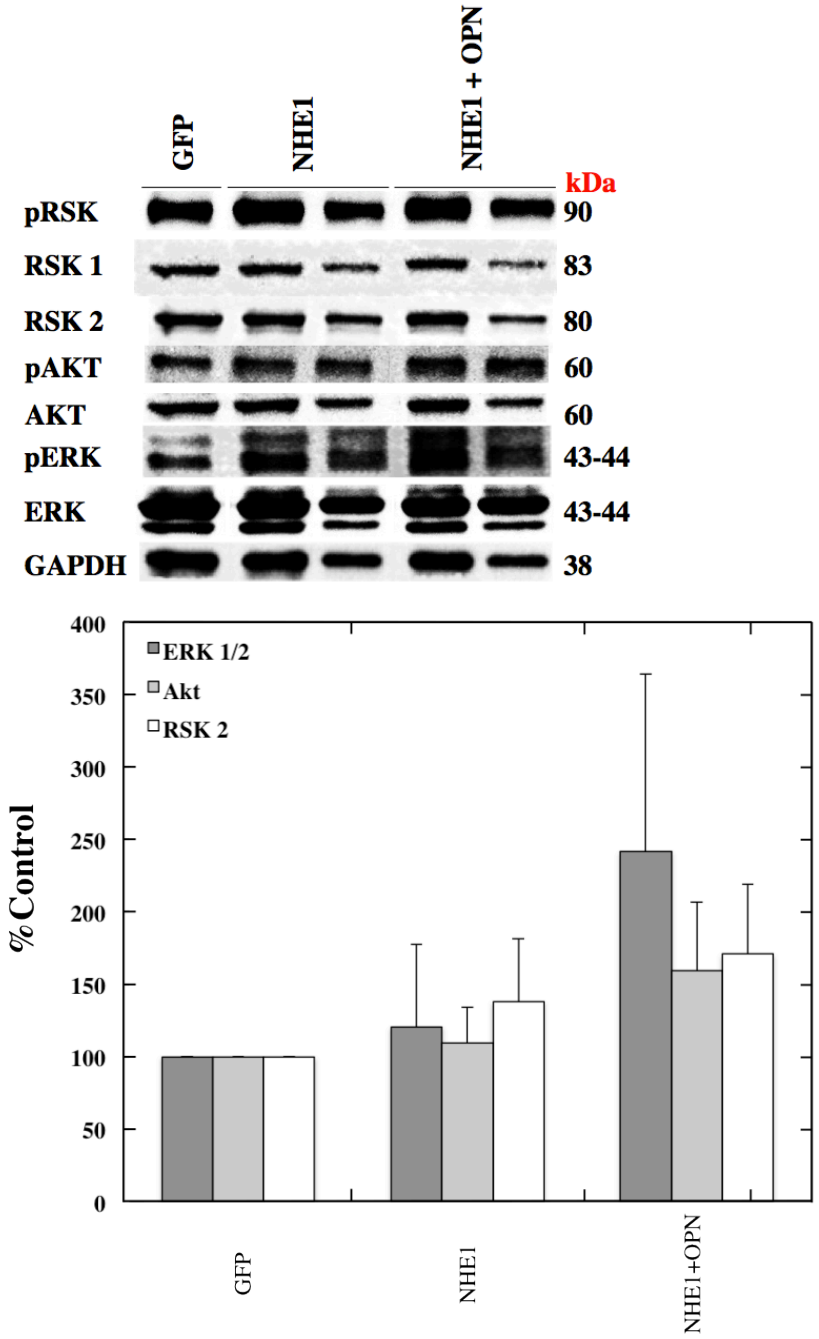

Fig. 3.5: Western blot analysis of relative amounts of RSK, Akt and ERK 1/2 protein expression in NRVMs infected with active NHE1 ± OPN adenovirus(es) 24 hours post infection using an MOI of 20. *Upper panel* Representative western blot of *phosphorylated* as well as *total* protein expression, protein expression was determined by immunoblotting against phosphorylated and total anti-RSK, Akt or ERK 1/2; normalization was against GAPDH. RSK protein was detected between 80-90 kDa, Akt between 60 kDa, and ERK 1/2 between 43-44 kDa, GAPDH, as loading control, at 38 kDa. *Lower panel* Quantification of relative levels of RSK, Akt or ERK activation in infected NRVMs. Results expressed as % of GFP control ± %SEM (n=2/group representative of 2 preparations).

3.3 Discussion

Although CH is a beneficial adaptive response of the heart to intrinsic and extrinsic stimuli, chronic hypertrophy can lead to DCM and eventually to heart failure if left unresolved (7). NHE1 has been known to contribute to various pathological conditions including myocardial I/R injury and hypertrophy (14, 22, 23, 43, 51). Previous reports have demonstrated that active expression of NHE1 produces a prominent cardiac hypertrophic phenotype (17, 18, 21, 54, 95). Inhibition of NHE1 expression/activity has been shown to attenuate CH *in vitro* and *in vivo* (53, 54, 84). However, the use of NHE1 inhibitors in patients undergoing coronary CABG demonstrated a high incidence of cerebrovascular side effects (101), suggesting that the clinical applicability of NHE1 inhibitors is questionable. Establishing the mechanism by which enhanced NHE1 activity induces CH is important, as it will provide a better understanding of the detrimental role of NHE1 in CH and identify potential therapeutic targets.

A possible approach to decrease the activity of NHE1 and attenuate the hypertrophic response is through the inhibition of the regulators of NHE1 activity. Several kinases, including ERK 1/2, its downstream effector RSK and Akt, have been suggested to be regulators of NHE1 activity (25). These kinases are themselves considered to be mediators of CH and being investigated as possible means of regressing NHE1 induced CH (4, 6, 90). Clearly, the role of NHE1 activity in CH is critical and identifying different regulators of NHE1 activity would assist with identifying alternative therapeutic targets to indirectly inhibit NHE1 induced CH.

A recent study by Mraiche et al. demonstrated that transgenic mice expressing cardiac specific active NHE1 exhibited alterations in gene expression that leads to

both CH and an upregulation of OPN expression (23). Furthermore, upregulation of SGK1 has been associated with CH and upregulation of both NHE1 and OPN (21, 22). Taken together, these findings strongly suggest that OPN may in part be responsible for mediating the hypertrophic effects of NHE1 in CH. In fact, the expression of OPN has been shown to be markedly increased during CVDs including left and right ventricular dysfunction associated with pressure overload as well as hypertrophy of the heart (154, 155, 162). More specifically, cardiomyocytes have been described as the sources of OPN during pressure overload hypertrophy and streptozotocin-induced diabetic cardiomyopathy (153, 162). Despite the importance of NHE1 and OPN in cardiac hypertrophy, no reports have investigated whether the two proteins work additively to induce CH and how OPN facilitates the NHE1 induced hypertrophic response. As a result we aim to delineate the cellular interplay between NHE1 and OPN in CH. Our findings suggest that OPN regulates NHE1 expression/activity and contributes to the hypertrophic effects of NHE1 in cardiomyocytes. Therefore our findings highlight OPN as a potential mechanism by which NHE1 induces CH.

The aim of our first objective was to determine the effects of enhanced NHE1 and OPN expression in cardiomyocytes. As such, we decided to utilize adenoviruses as tools to upregulate NHE1 and OPN expression in NRVMs. In order to characterize the NRVMs infected with NHE1 in the presence and absence of OPN, we analyzed changes in OPN protein expression as well as NHE1 expression/activity. We established that an MOI of 20 for active NHE1 and OPN adenoviruses were the most ideal viral load required to overexpress active NHE1 and OPN in NRVMs (Figure 3.1). We then moved our attention to the role of OPN in contributing to the

hypertrophic effects of NHE1. Therefore, we examined the changes in cell area, a parameter of CH, in our infected NRVMs.

3.3.1 Upregulation of NHE1 Enhances OPN Protein Expression

In our study, overexpression of NHE1 in NRVMs caused an increase in both NHE1 expression and activity (Figure 3.2). This upregulation of NHE1 was associated with a significant increase in sOPN protein expression, since our antibody of choice (ab14176) detects the secreted form of the protein (Figure 3.2). This is consistent with previous findings in which enhanced NHE1 expression/activity caused an upregulation in OPN (21-24). Interestingly, the expression of OPN in NRVMs infected with both NHE1 and OPN was much higher than that observed in NRVMs infected with NHE1 alone, suggesting that enhanced NHE1 expression could upregulate OPN expression.

3.3.2 Enhanced OPN Expression Stimulated NHE1 Expression and Activity

An association between enhanced NHE1 expression/activity and OPN has been demonstrated in CH (21-24). However, the importance of the NHE1-induced upregulation of OPN on NHE1 has never been investigated. Our study indicated that infection of NRVMs with the NHE1 adenovirus alone did not significantly increase NHE1 activity. This is consistent with previous data in which NHE1 activity of NRVMs infected with a NHE1 adenovirus was not significantly higher following intracellular acidosis (32). Even though the findings by Coccaro et al. and our study suggested that NHE1 activity was not significantly increased following infection of

NRVMs with active NHE1, the plasmid has been proven to produce enhanced NHE1 expression and activity (14, 17, 23).

Our study demonstrated for the first time that the upregulation of OPN in the presence of NHE1 significantly increases NHE1 protein expression and activity, compared to NHE1 infection alone (Figure 3.2 and 3.3). The mechanism by which OPN induces NHE1 activity and expression requires further investigation. Voelkl et al. previously demonstrated that activation of SGK1 was associated with enhanced expression/activity of NHE1 and elevated OPN gene expression both *in vitro* and *in vivo* (21, 22). Whether OPN regulates the expression and activity of NHE1 through SGK1 is yet to be determined. Taken together our findings reveal for the first time that the NHE1-induced upregulation of OPN enhances NHE1 protein expression and activity.

3.3.3 Enhanced NHE1 and OPN Expression Induces Cleavage of OPN

OPN has been shown to be cleaved by MMP-3/7, into an N-terminal 40 kDa and a C-terminal 32 kDa fragment (110, 121). The anti-OPN antibody used in these experiments only detected the LRSK epitope on the C-terminal 32 kDa fragment. Therefore, we were only able to detect the C-terminal OPN cleaved fragment at 32 kDa. In our study, expression of NHE1 alone in NRVMs demonstrated no cleaved form of OPN (Figure 3.2 and 3.3 B). Interestingly, expression of both NHE1 and OPN resulted in enhanced cleavage of OPN, suggesting that enhanced expression of NHE1 may enhance cleavage of the full form of the phosphoprotein when sufficient amounts of OPN are present. Cleaved fragments of OPN have been suggested to be more biologically active than the full form of the phosphoprotein (110, 113, 135).

Whether the cleaved form of OPN or the full form of the phosphoprotein is responsible for mediating the hypertrophic effects of NHE1 is yet to be established. Furthermore, we are yet to determine whether NHE1, MMPs or other mediators are responsible for the cleavage of OPN during CH.

3.3.4 OPN Contributes to the Hypertrophic Effects of NHE1 in Cardiomyocytes

Using adenoviruses as tools to upregulate NHE1 and OPN in NRVMs, we established that a two-way crosstalk exists between NHE1 and OPN. Our findings indicated that upregulation of NHE1 enhances OPN protein expression, which in turn, regulates NHE1 protein expression and activity. This intrigued us to further examine the role of OPN in contributing to the NHE1-induced hypertrophic response. We chose to investigate the effects of enhanced NHE1 expression in the presence and absence of OPN on cell area, a parameter of CH. We demonstrated that infection of NRVMs with active NHE1 significantly increases cell area, a parameter of CH (Figure 3.4). Our findings were consistent with several *in vitro* studies (17, 18, 63). This effect as also observed in NRVMs infected with both active NHE1 and OPN compared to GFP, however, they were not significantly different from NRVMs infected with NHE1 alone. Although NHE1 is a cardiac specific exchanger mainly expressed in cardiomyocytes (33), fibroblasts are thought to be the main sources of OPN in the myocardium (105, 107). Therefore, our model may not be taking into consideration the interaction between cardiomyocytes and fibroblasts, thereby limiting the extent to which OPN contributes to the NHE1-induced hypertrophic response in cardiomyocytes. This could justify why the increase in cell area was not equivalent to the increase in activity that was demonstrated when we enhanced NHE1

and OPN expression in NRVMs. Nevertheless, our findings indicate that OPN enhances NHE1 expression and activity and may in part facilitate the NHE1-induced cardiac hypertrophic response.

3.3.5 Upregulation of OPN Contributes to the Hypertrophic Effects of NHE1 Independent of ERK 1/2, RSK and Akt Activation

In order to eliminate the involvement of kinases known to regulate NHE1 activity and induce CH (25, 54, 90), we investigated the expression of their phosphorylated and total proteins in NRVMs infected with NHE1 in the presence and absence of OPN (Figure 3.5). Even though immunoblotting does not provide an indication of the functional activity of kinases, it is considered an ideal method to measure protein expression of the phosphorylated and active forms of kinases (54, 57, 90). Although protein expression of phosphorylated ERK 1/2, RSK and Akt appeared to be increased in NRVMs infected with NHE1 and OPN, these changes were not significant. This is inconsistent with previous studies that associated enhanced NHE1 expression/activity with elevated levels of ERK 1/2 both in NRVMs (58) and H9c2 cells (90). On the other hand, Coccaro et al. revealed that sustained intracellular acidosis-induced activation NHE1 occurred independent of the RSK pathway, which is in part in agreement with our findings (58). This discrepancy may be due to the timing in which the experiments where carried out. In our experiments, it was necessary to infect NRVMs for a period of 24 hours, however, other studies have indicated that peak activation of ERK 1/2 and RSK occurred within minutes of stimulation (58, 90). Since the changes detected in our experiments were not significant, our findings suggest that OPN contributes to the hypertrophic effects of

NHE1 through the regulation of NHE1 expression/activity and independent of hypertrophic kinases. However, further studies in which the activation of ERK 1/2, RSK and Akt is measured in a time dependent manner is necessary in order to rule out their involvement. Furthermore, in order to confirm the ability of OPN to facilitate the hypertrophic effects of NHE1 during CH, a model in which OPN expression is inhibited is necessary.

Chapter 4: Downregulation of OPN Reverses NHE1 Induced Cardiac Hypertrophy in the Rat Embryonic Myoblast Cell Line H9c2

4.1 Rationale

The concept of NHE1 inhibition as an effective therapeutic option for CH has been pursued in several *in vitro* and *in vivo* studies (14, 63, 80, 84). Although the notion to inhibit NHE1 proved to be successful on the bench side, the use of NHE1 inhibitors in clinical trials was not successful (97, 99, 101, 102). OPN has recently been implicated in several cardiovascular diseases (20, 153-155, 162). In failing human hearts, elevated levels of OPN were correlated with the severity of heart failure suggesting that OPN mediates the remodeling process of the myocardium leading to heart failure (19, 166, 168). Furthermore, elevated levels of OPN has been correlated with enhanced expression/activity of NHE1 in CH both *in vitro* and *in vivo* (21-24). In addition, our results with NRVMs revealed that OPN contributes to the hypertrophic effects of NHE1 by upregulating NHE1 expression/activity and enhancing parameters of CH including cell area. We also demonstrated that OPN contributes to the NHE1-induced hypertrophic response independent of hypertrophic kinases such as ERK 1/2, RSK and Akt. Therefore, based on our findings as well as previous studies, a cellular interplay between NHE1 and OPN exists during CH.

To verify that OPN contributes to the hypertrophic effects of NHE1 during CH, OPN was downregulated in H9c2 cardiomyocytes overexpressing the active form of NHE1. Through the use of the active NHE1 adenovirus, we were able to infect H9c2 cardiomyocytes and simulate NHE1-induced hypertrophic conditions. We then chose

to use an siRNA against OPN to downregulate OPN protein expression. The effects of downregulating OPN on NHE1 expression and activity were examined. We were also able to characterize H9c2 cardiomyocytes for parameters of CH including cell area (90), protein content (184) as well as ANP mRNA levels (90, 175). We establish that downregulating OPN causes a reduction in NHE1 activity as well as expression confirming that OPN regulates NHE1 activity and expression. We also demonstrate downregulating OPN reverses the NHE1-induced hypertrophic response through attenuation of parameters of CH in cardiomyocytes.

4.2 Results

4.2.1 Differentiation of H9c2 Cells into the Cardiac Phenotype

H9c2 myoblasts derived from the embryonic rat ventricular tissue are undifferentiated in nature, however, they acquire a myogenic phenotype following serum starvation of media (187). In order to differentiate H9c2 cells into their cardiac phenotype, several studies have adopted the use of RA as suggested by Me´nard et al. (described in Section 2.2.1 and Figure 2.4) (176, 184, 187). H9c2 cardiomyocytes have also been shown to display hypertrophy-associated traits comparable to primary cultures of cardiomyocytes when stimulated with α1-AR agonists as well as high glucose treatment (175, 188). As such, we chose to investigate the effects of downregulating OPN on NHE1-induced CH in H9c2 cardiomyocytes. Changes in cell morphology, expression of cardiac specific L-type voltage-dependent Ca^{2+} channels (VDCCs) and the cardiac sarcomeric heavy chain can be used as parameters to confirm differentiation of H9c2 cells into cardiomyocytes (176, 189, 190). In our

study we confirmed the differentiation of H9c2 cardiomyocytes into the cardiac phenotype using the changes in cell morphology; shape, fusion and nucleation. Figure 4.1 shows the crystal violet stained H9c2 cells between day 0 and 5 of the differentiation process. At day 0, H9c2 myoblasts appeared relatively large and seemed to grow as single mono nucleated cells. Between day 3-5 of serum deprivation and the addition of RA to induce differentiation, H9c2 cardiomyocytes appeared to become more elongated and branched. By day 5 of the differentiation process, multinucelation of the H9c2 cardiomyocytes was prominent. Examining cell elongation, branching and multinucleation was used to confirm the differentiation of H9c2 myoblasts into the cardiac phenotype (176, 190).

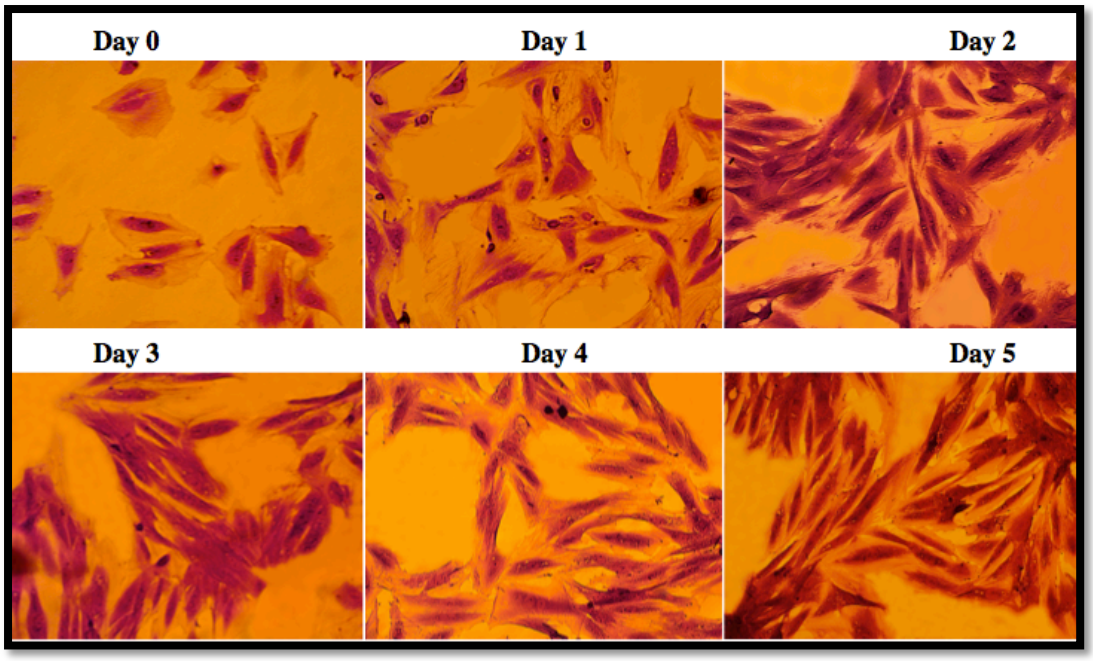

Fig. 4.1: Crystal violet stained cell culture images of the differentiation process of H9c2 cells. H9c2 myoblasts were cultured for 24 hours in DMEM supplemented with 10% FBS. The medium was then replaced with DMEM supplemented with 1% horse serum every 2 days. Differentiation into cardiomyocytes was induced by adding 0.1μM all-trans-retinoic acid (RA) daily for 5 days.

4.2.1.2 Basal NHE1 and OPN Expression in H9c2 Cells

Initially, we wanted to examine the basal protein expression of NHE1 and OPN proteins in undifferentiated H9c2 cardiomyocytes (Figure 4.2). The addition of RA, during serum reduction, favors differentiation of the cells into a cardiac phenotype (176, 184, 187). Both NHE1 and OPN were expressed in the undifferentiated and differentiated H9c2 cells. Upon differentiation, protein expression of NHE1 and OPN showed a trend towards increasing in H9c2 cardiomyocytes. Upon examination of cleaved OPN at 32 kDa, no protein expression was detected.

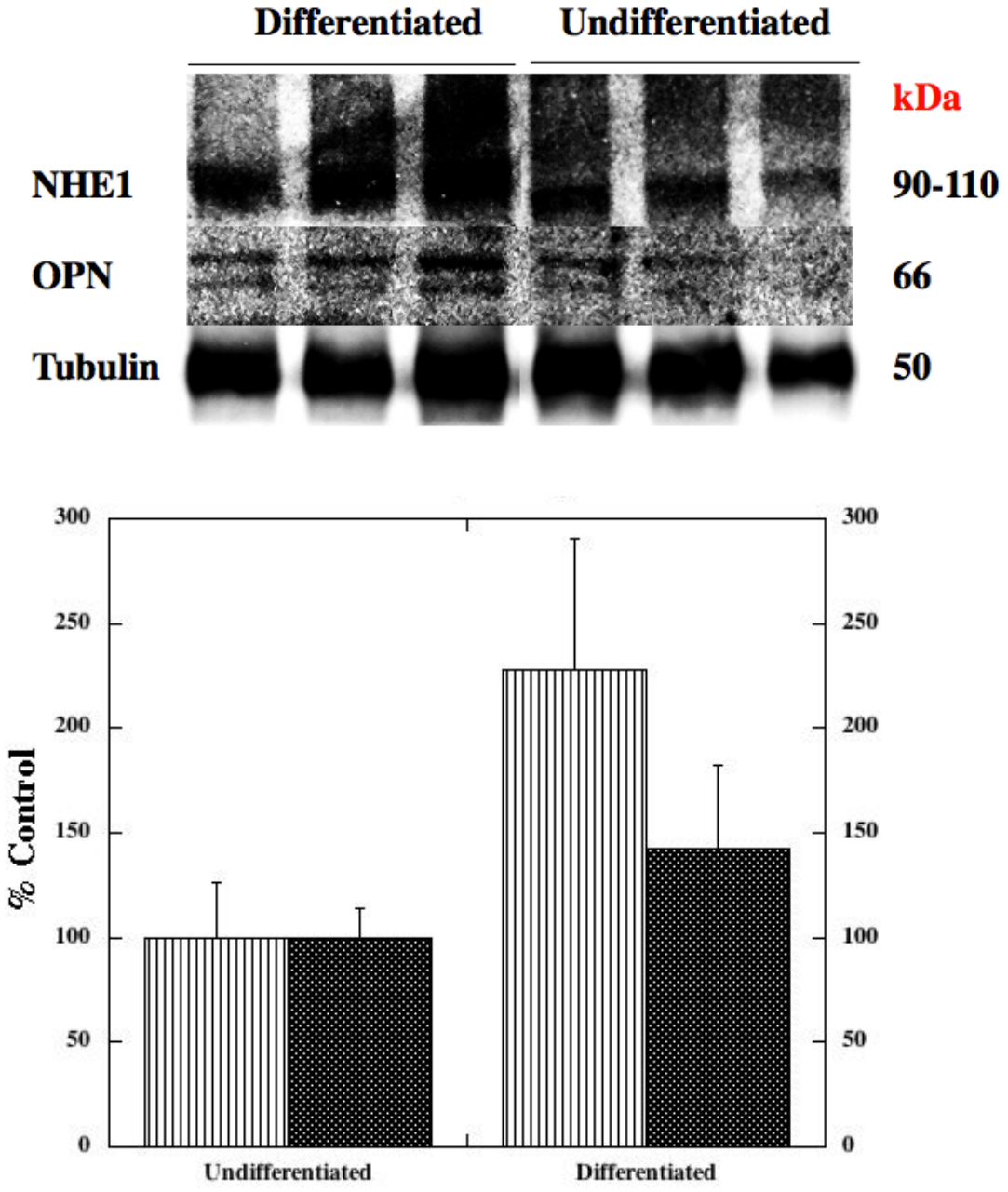

Fig. 4.2: Basal expression of NHE1 and OPN proteins in H9c2 cells. Protein expression was determined by immunoblotting against anti-NHE1 or OPN; normalization was against α-tubulin. NHE1 protein was detected between 90-110 kDa, OPN between 66 kDa and α-tubulin, as loading controls, at 50 kDa, respectively. *Upper panel:* Representative western blot of basal expression of NHE1 and OPN proteins in differentiated vs. undifferentiated H9c2 cells. *Lower panel:* Quantification of relative levels of NHE1 (*stripped*) and OPN (*dotted*) protein expression. Results expressed as % undifferentiated H9c2 cells ± SEM% (representative of 2-3 experiments).

4.2.2 Characterization of H9c2 Cardiomyocytes Infected with NHE1 and/or Transfected with siRNA OPN

In order to confirm that OPN mediates the NHE1-induced cardiac hypertrophic response in H9c2 cardiomyocytes, we used the active NHE1 adenovirus to simulate NHE1-induced CH and the siRNA against OPN to downregulate OPN expression. The siRNA against OPN has previously been used both *in vitro* and *in vivo* to silence the OPN gene (123, 180, 181). Moreover, based on the ability of the NHE1 adenovirus to enhance NHE1 protein expression (Section 3.2.1.2), activity (Section 3.2.1.3) and result in the induction of CH in NRVMs (Section 3.2.3), we continued to use the active NHE1 adenovirus. The GFP adenovirus was used as a control.

4.2.2.1 Adenoviral Multiplicity of Infection

Initially, the GFP, NHE1 and OPN adenoviruses were characterized in H9c2 cardiomyocytes to determine the most appropriate MOI. We examined the exogenous NHE1 and OPN protein expression at different MOIs (10, 20, 30) for 24 hours using an antibody against HA tag (Figure 4.3 *Upper panel*). The presence of the HA tag on all adenoviral constructs was a feasible tool to monitor exogenous protein expression (Figure 2.1). Moreover, the GFP adenovirus acted as a great control to ensure we have no non-specific bands (Figure 4.3). Our results indicated that an MOI of 30 produced the most adequate overexpression of NHE1. In some experiments, the H9c2 cells were infected with the OPN adenovirus to act as a positive control for experiments in which we silenced OPN. As such, the MOI of OPN in H9c2 cells was also examined. Upon examination of OPN protein expression, our results revealed that an MOI of 10,

20 and 30 where not sufficient to overexpress OPN. Since an MOI of 50 resulted in marked cell toxicity and cell death, infection of H9c2 cardiomyocytes using an MOI of 40 for the OPN adenovirus was used. The amount of GFP fluorescence was monitored using fluorescent microscopy (Figure 4.3 *Lower panel*). Based on exogenous protein expression and cell health, H9c2 cardiomyocytes were infected with the GFP adenovirus using an MOI of 20 and NHE1 or OPN adenoviruses using an MOI of 30 and 40, respectively.

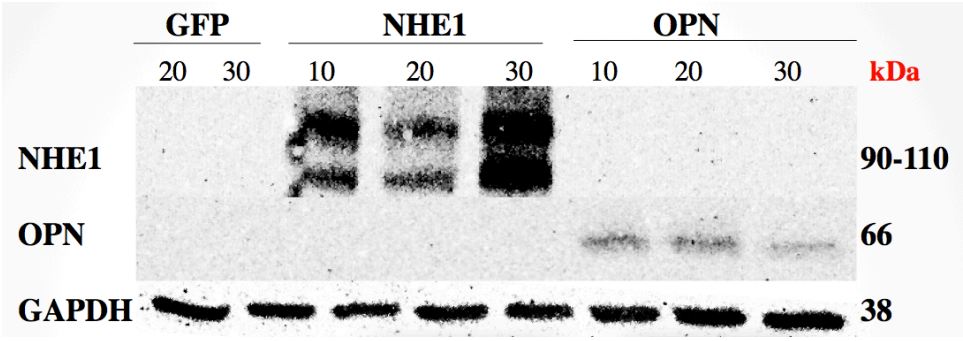

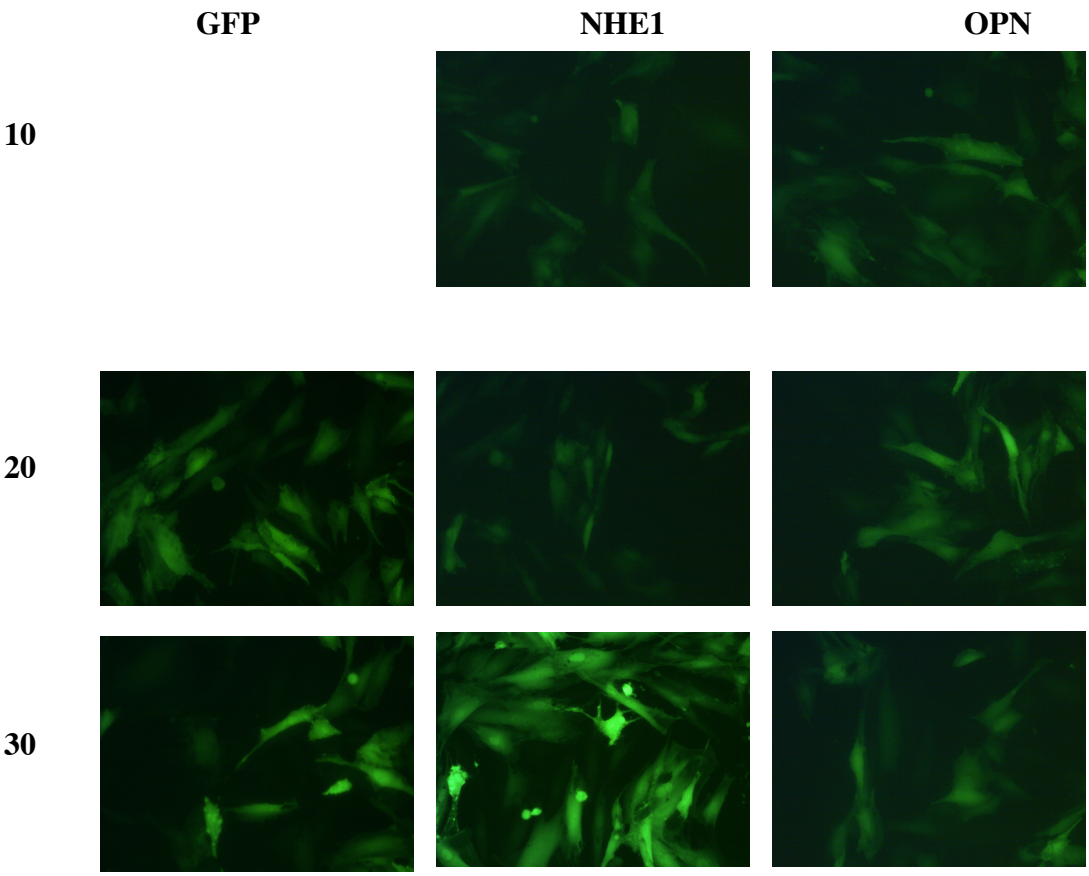

Fig. 4.3: MOI of adenovirus infection and expression levels of *exogenous* NHE1 and OPN proteins in adenovirus infected H9c2 cardiomyocytes. *Upper panel:* Representative western blot of H9c2 cardiomyocytes infected with GFP, active NHE1 or OPN adenovirus 24 hours post infection using an MOI of 10, 20 and 30. Protein expression was determined by immunoblotting against anti-HA and normalization was against GAPDH. Exogenous NHE1 protein was detected between 90-110 kDa, OPN between 66 and GAPDH, as loading control, at 38 kDa. *Lower panel:* Representative images of fluorescence microscopy of H9c2 cardiomyocytes infected with GFP, active NHE1 or wild type OPN adenoviruses using an MOI of 10, 20, or 30 examined 24 hours post infection. n=3/group (representative of 2 experiments).

4.2.2.2 Determination of the Ideal siRNA OPN:Lipofectamine Ratio for Transfection of H9c2 Cardiomyocytes

The use of siRNA as a highly specialized tool to silence specific genes been shown to be effective both *in vitro* and *in vivo* (123, 179, 181, 188). In fact, the siRNA targeting OPN mRNA has been shown to be an efficient tool to downregulate OPN levels *in vitro* (123, 180). In addition, the use of Lipofectamine 2000 (Invitrogen) as a lipid based polymer for transfection of siRNA has previously been proven to be successful (Section 2.2.3.2) (123, 178, 191). In order to determine the optimum *siRNA OPN:Lipofectamine* ratio, we transfected H9c2 cardiomyocytes using siRNA OPN 100nM and Lipofectamine at different ratios including 1:0.6, 0.5:1 and 1:3 (178, 179, 182). We then examined OPN protein expression in the siRNA transfected H9c2 cardiomyocytes using OPN (40 MOI) as a positive control. H9c2 cardiomyocytes were transfected with a scrambled siRNA to confirm that the downregulation of OPN was occurring due to the siRNA and independent of the Lipofectamine used. Our goal was to downregulate OPN protein expression to approximately half amount of basal protein expressed with minimal cell death. OPN protein expression in H9c2 cardiomyocytes transfected with scrambled siRNA appeared to remain unchanged compared to siRNA OPN transfected H9c2 cardiomyocytes. Our results revealed that using a ratio of 1:0.6 and 0.5:1 were not sufficient to downregulate OPN protein expression (Figure 4.4 A). We also analyzed the toxicity of Lipofectamine on cell viability of transfected H9c2 cardiomyocytes using the siRNA OPN:Lipofectamine ratios 1:0.6, 0.5:1 and 1:3. Cell viability assays were preformed using 0.4% Trypan blue solution according to manufacturer's instructions (Section 2.2.3.2) (192). Based on our results, a ratio of 1:3 caused

minimal cell death (Figure 4.4 B). Since our aim was to reduce OPN protein expression by around 50%, we chose an *siRNA OPN:Lipofectamine* ratio of 1:3 for subsequent transfections involving the siRNA OPN.

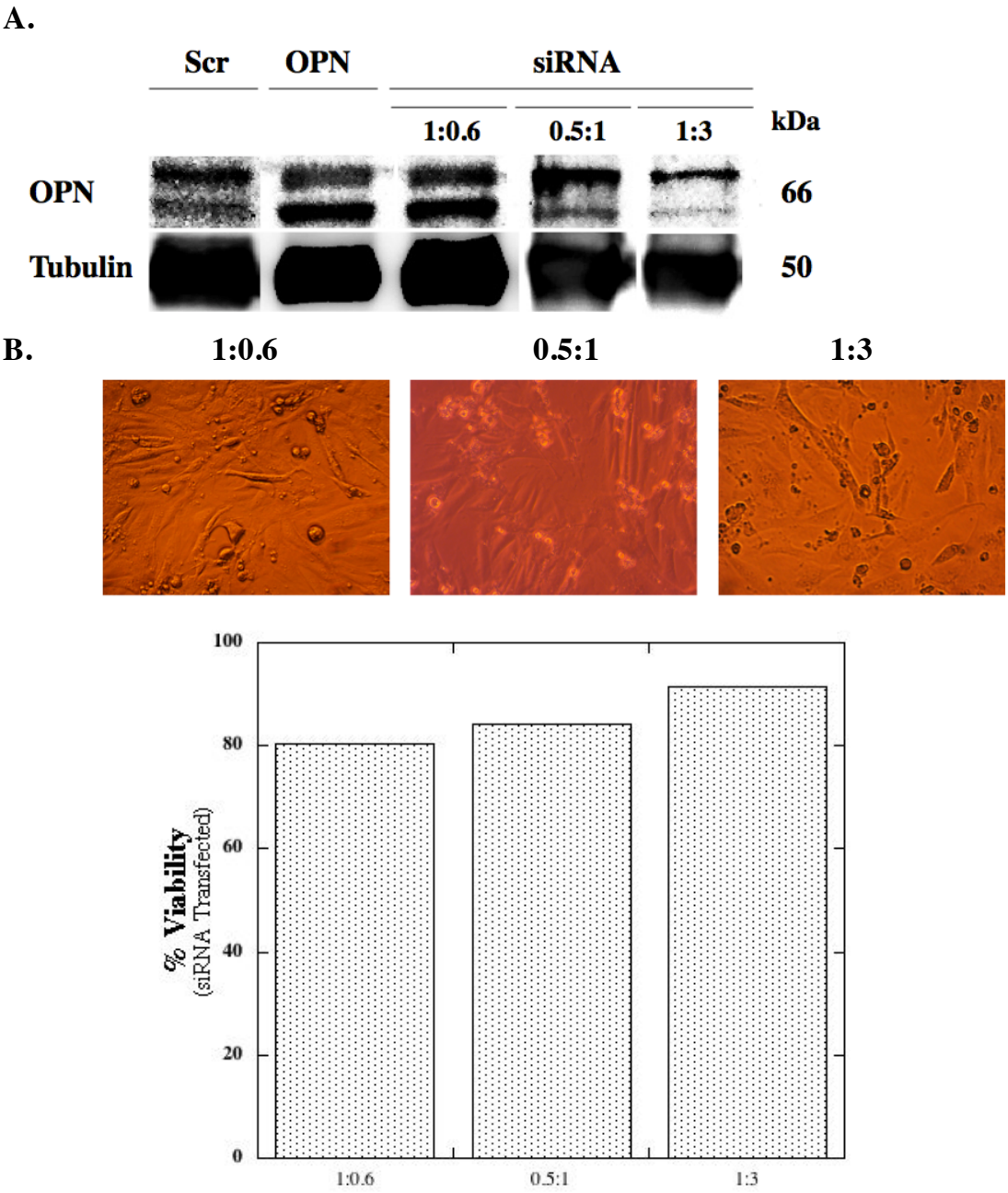

Fig. 4.4: Ratio of siRNA OPN:Lipofectamine for transfection of H9c2 cardiomyocytes. H9c2 cardiomyocytes were transfected with 100nM siRNA OPN:Lipofectamine using a ratio of 1:0.6, 0.5:1 or 1:3. Protein expression and cell viability were examined 24 hours later. **A.** Representative western blot of H9c2 cardiomyocytes transfected with 30nM scrambled siRNA or 100nM siRNA OPN 24 hours post transfection. Protein expression was determined by immunoblotting against anti-OPN and normalization was against α-tubulin. Total OPN protein was detected between 66 and Tubulin, as loading control, at 50 kDa. H9c2 cardiomyocytes infected with OPN adenovirus (40 MOI) were used as a positive control. **B.** Cell viability for the different siRNA OPN:Lipofectamine ratios used. *Upper panel:* Representative bright light microscopy images of siRNA OPN:Lipofectamine ratios. *Lower panel:* Quantitation of cell viability of H9c2 cardiomyocytes transfected with 100nM siRNA OPN 24 hours post transfection (n of 1-2 from 4 experiments).

4.2.2.3 siRNA OPN Concentration and Contact Time

Upon establishing the siRNA OPN:Lipofectamine ratio, a set of experiments were run in order to determine the *optimum concentration* and *contact time* to use for siRNA OPN. Initially we examined the effect of downregulating OPN using 30nM vs. 100nM siRNA OPN for 24 hours. The choice of starting siRNA OPN concentrations of 30 (181) and 100nM (123) was based on previous studies in which both concentrations successfully downregulated OPN expression *in vitro*. H9c2 cardiomyocytes were transfected with a scrambled siRNA to confirm that the downregulation of OPN was occurring due to the siRNA and independent of the Lipofectamine used. We then examined OPN protein expression in the siRNA transfected H9c2 cardiomyocytes using OPN (40 MOI) as a positive control. OPN protein expression in H9c2 cardiomyocytes transfected with scrambled siRNA appeared to remain unchanged compared to siRNA OPN transfected H9c2 cardiomyocytes. Our results indicated that transfection with siRNA OPN using a concentration of 30nM completely abolished OPN protein expression compared to 100nM transfection (Figure 4.5 A *Upper panel*). Interestingly, the siRNA OPN appeared to downregulate GAPDH, however, it had no effect on α-tubulin protein expression (Figure 4.5 A *Lower panel*). A similar set of experiments was preformed using 30nM vs. 100nM siRNA OPN for 48 hours. Figure 4.5 B clearly reflects that transfection of H9c2 cardiomyocytes using 30nM and 100nM siRNA OPN for 48 hours did not adequately downregulate OPN protein expression. As a result, we transfected H9c2 cardiomyocytes using siRNA OPN at a concentration of 100nM for 24 hours and used α-tubulin to normalize protein expression in all subsequent experiments.

A.

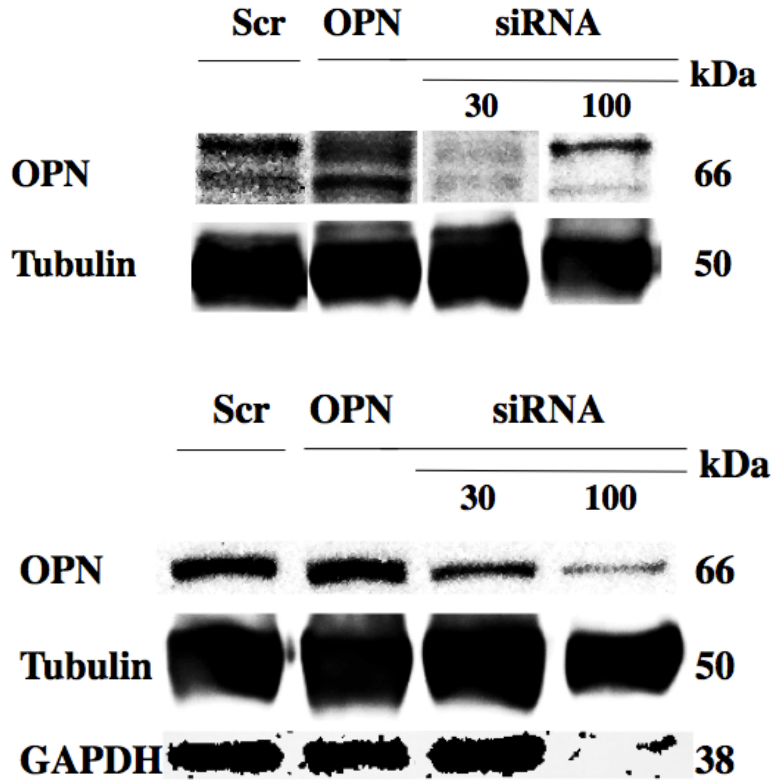

B.

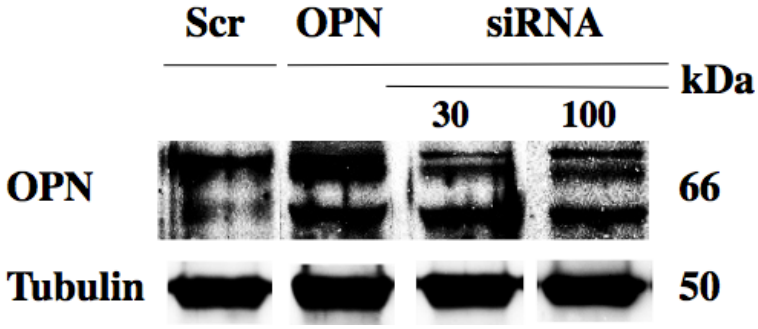

Fig. 4.5: Concentration and duration of siRNA OPN transfection of H9c2 cardiomyocytes. H9c2 cardiomyocytes were transfected with 30nM scrambled siRNA or 30 and 100nM siRNA OPN for 24 and 48 hours. Protein expression was determined by immunoblotting against anti-OPN and normalization was against GAPDH or α-tubulin. Total OPN protein was detected between 66 and Tubulin or GAPDH, as loading control, at 50 and 38 kDa, respectively. H9c2 cardiomyocytes infected with OPN adenovirus (40 MOI) were used as a positive control. **A.** *Upper panel:* Representative western blot of H9c2 cardiomyocytes transfected with 30nM or 100nM siRNA OPN 24 hours post transfection. *Lower panel:* Effect of 30 and 100nM siRNA OPN on downregulating OPN and GAPDH protein expression 24 hours post transfection. **B.** Representative western blot of H9c2 cardiomyocytes transfected with 30nM and 100nM siRNA OPN 48 hours post transfection (n of 1-2 from 2 experiments).

4.2.2.4 NHE1 Adenovirus and siRNA OPN Co-transfection Time

Once we established the siRNA OPN OPN:Lipofectamine ratio and concentration of siRNA OPN, a set of experiments were run to determine the most optimum time frame for co-transfection of H9c2 cardiomyocytes with NHE1 adenovirus and siRNA OPN. Based on our results in Section 4.2.2, an MOI of 30 for the NHE1 adenovirus was most ideal for infection of H9c2 cardiomyocytes (Figure 4.3). In addition, based on the results from Section 4.2.2.3, transfection of H9c2 cardiomyocytes using a concentration of 100nM for the siRNA OPN (Figure 4.5 A) for 24 hours caused the most adequate downregulation of OPN, which represented real-life settings. As described in Section 2.2.3.3 we experimented with different time frames of co-transfection of NHE1 adenovirus (30 MOI) and siRNA OPN 100nM including co-transfection at the same time (0 hours), transfection with NHE1 then siRNA OPN 0.5 hours later (0.5 hours), transfection with NHE1 then siRNA OPN 4 hours later (4 hours) and transfection with NHE1 then siRNA OPN 24 hours later (24 hours). As demonstrated in Figure 4.6 A, transfection with NHE1 (30 MOI) and siRNA OPN (100nM) 4 hours post infection resulted in the most adequate downregulation of OPN protein expression. In addition, fluorescence microscopy images revealed that H9c2 cardiomyocytes appeared most healthy using the 4-hour time frame for co-transfection (Figure 4.6 B). Furthermore, OPN protein expression appeared to be upregulated in the NHE1 adenovirus infected H9c2 cardiomyocytes, which is in agreement with our previous findings with NRVMs (Section 3.2.1.2 Figure 3.3 A). Based on our results, we decided to co-transfect H9c2 cardiomyocytes

using 100nM siRNA OPN 4 hours post infection with NHE1 adenovirus using an MOI of 30.

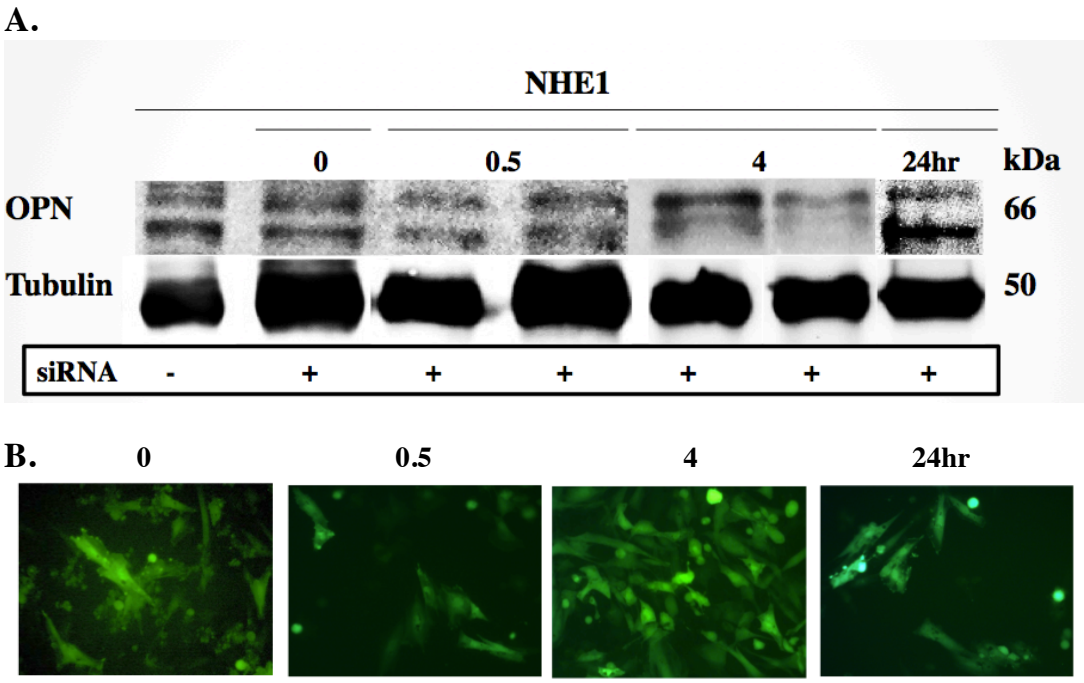

Fig. 4.6: Time frame for co-tranfection of H9c2 cardiomyocytes with NHE1 adenovirus and siRNA OPN. H9c2 cardiomyocytes were infected with NHE1 adenovirus (30 MOI) and transfected with 100nM siRNA OPN at 0, 0.5, 4 and 24-hour time points for 24 hours. **A.** Representative western blot of H9c2 cardiomyocytes co-transfected with NHE1 adenovirus and siRNA OPN at 0, 0.5, 4 and 24-hour time points for 24 hours. Protein expression was determined by immunoblotting against anti-OPN and normalization was against α-tubulin. Total OPN protein was detected between 66 and Tubulin, as loading control, at 50 kDa. H9c2 cardiomyocytes infected with NHE1 adenovirus (30 MOI) was used as a positive control. **B.** Representative fluorescence microscopy images of H9c2 cardiomyocytes co-transfected with NHE1 adenovirus and siRNA OPN, examined 24 hours post-transfection (n of 1-2 from 2 experiments).

4.2.2.5 siRNA OPN Concentration and Duration of Transfection for NHE1 Adenovirus and siRNA OPN Co-transfection

Upon determination of the siRNA OPN:Lipofectamine ratio, concentration of siRNA OPN and time frame for co-transfection of H9c2 cardiomyocytes, a set of experiments were run to determine the most optimum concentration of siRNA OPN and duration of transfection for NHE1 adenovirus and siRNA OPN co-transfection of H9c2 cardiomyocytes. Initially, we examined the efficiency of infecting H9c2 cardiomyocytes using 30 MOI NHE1 adenovirus and 100nM siRNA OPN 4 hours-post infection for 24 hours on OPN protein expression as well as cell health (Figure 4.7A *left panel*). We also compared co-transfecting H9c2 cardiomyocytes using NHE1 adenovirus and 100nM siRNA OPN to co-transfecting with NHE1 adenovirus and 30 or 100nM siRNA OPN for 48 hours (Figure 4.7 A *right panel*). Our results indicated that co-transfection of H9c2 cardiomyocytes using 30 and 100nM of siRNA OPN for 48 hours was not sufficient to downregulate OPN protein expression. In addition, fluorescent microscopy images of co-transfected cardiomyocytes reflected inadequate GFP fluorescence suggesting that transfection for 48 hours could be attenuating the adenovirus. As a result we decided to co-transfect H9c2 cardiomyocytes using 100nM siRNA OPN, 4 hours post-infection with NHE1 adenovirus using an MOI of 30, for 24 hours (Figure 4.7 A *left panel*).

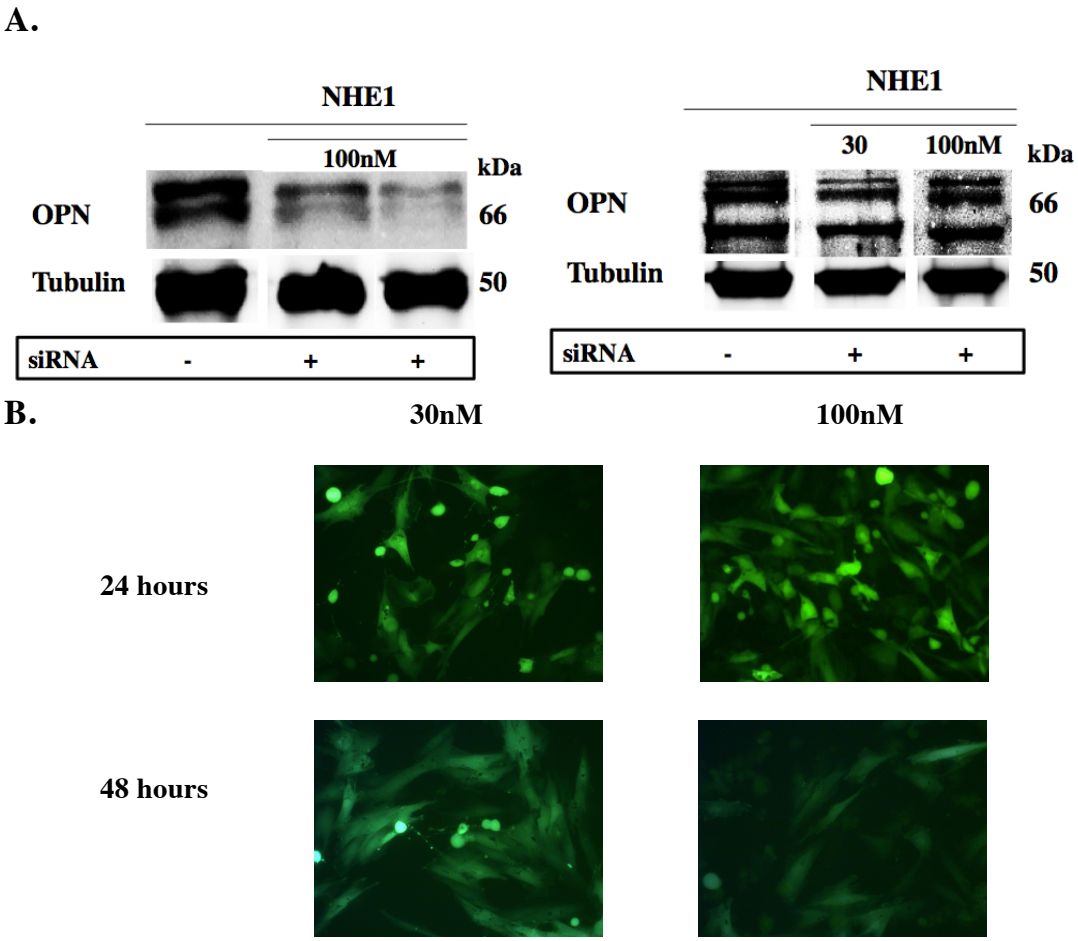

Fig. 4.7: Concentration of siRNA OPN and duration of transfection for co-tranfection of H9c2 cardiomyocytes with NHE1 adenovirus and siRNA OPN. H9c2 cardiomyocytes were infected with NHE1 adenovirus (30 MOI) and transfected with 30 or 100nM siRNA OPN for 24 and 48 hours. Protein expression was determined by immunoblotting against anti-OPN and normalization was against α-tubulin. Total OPN protein was detected between 66 and Tubulin, as loading control, at 50 kDa. H9c2 cardiomyocytes infected with NHE1 adenovirus (30 MOI) were used as a positive control. **A.** *Left panel:* Representative western blot of H9c2 cardiomyocytes co-transfected with NHE1 adenovirus and 100nM siRNA OPN for 24 hours. *Right panel:* Representative western blot of H9c2 cardiomyocytes co-transfected with NHE1 adenovirus and 30 or 100nM siRNA OPN for 48 hours. **B.** Representative fluorescence microscopy images of H9c2 cardiomyocytes co-transfected with NHE1 adenovirus and siRNA OPN examined 24 and 48 hours post infection (n of 1-2 from 2 experiments).

4.2.2.6 NHE1 and OPN Expression in H9c2 Cardiomyocytes Infected with NHE1 and/or Transfected with siRNA OPN

Upon examination of NHE1 protein expression in NHE1 infected H9c2 cardiomyocytes, our results indicated that NHE1 protein expression was significantly increased (30 fold increase±0.12 NHE1 infected of GFP infected H9c2 cardiomyocytes; $P<0.05$) (Figure 4.8 B). This is in agreement with our previous findings with NRVMs infected with NHE1 (Section 3.2.1.2 Figure 3.3 A). In addition, NHE1 expression in OPN infected H9c2 cardiomyocytes showed a trend towards increase compared to GFP infected H9c2 cardiomyocytes. Interestingly, downregulating OPN using siRNA OPN caused a significant reduction in NHE1 protein expression compared to GFP infected H9c2 cardiomyocytes (20.2 fold decrease±0.12 NHE1+siRNA OPN of GFP infected H9c2; $P<0.05$). Our findings, therefore, suggest that NHE1 causes an upregulation of OPN, which in turn may regulate NHE1 protein expression (as demonstrated in Figures 3.2 and 4.8 A-B).

GFP infected H9c2 cardiomyocytes appeared to express basal levels of OPN gene and protein expression (Figure 4.8 A-C). In NHE1 infected H9c2 cardiomyocytes, both OPN gene and protein expression showed a trend towards increase (256.7±70.21% NHE1 infected vs. 100%±61.53 GFP infected H9c2 cardiomyocytes; mRNA expression) and (111.8±9.31% NHE1 infected vs. 100.0% GFP infected H9c2; protein expression). This is to some extent consistent with OPN protein expression in NRVMs infected with NHE1 as shown Section 3.2.1.2 and Figure 3.2 (342.7%±69.22% NHE1 infected NRVMs vs.100.0±33.93% GFP infected NRVMs; $P<0.05$). OPN gene expression was highest in OPN infected H9c2 cardiomyocytes (309±149.62% OPN infected vs. 100%±61.53 GFP infected H9c2

cardiomyocytes). However, OPN protein expression appeared to be higher in NHE1 infected H9c2 cardiomyocytes (106.4±4.29% OPN infected vs. 111.8±9.31% NHE1 infected H9c2 cardiomyocytes). Downregulation of OPN caused a reduction OPN gene expression (213±98.94% NHE1+siRNA OPN transfected vs. 256.7±70.21% NHE1 infected H9c2 cardiomyocytes) and a significant reduction in OPN protein expression compared to NHE1 and OPN infected H9c2 cardiomyocytes (64.9±16.84% NHE1+siRNA OPN vs. 111.8±9.31% NHE1 infected H9c2 cardiomyocytes; $P< 0.05$) (64.9±16.84% NHE1+siRNA OPN vs. 106.4±4.29% OPN infected H9c2 cardiomyocytes; $P< 0.05$) (Figure 4.8 A, B and D), further confirming the effectiveness of the siRNA OPN.

The overexpression of NHE1 and OPN in NRVMs caused an increase in the cleavage of OPN into a 32 kDa fragment (Section 3.2.1.2 Figure 3.2 B). Interestingly, downregulating OPN and the reduction in NHE1 protein expression associated with it caused a significant reduction in OPN cleavage (46.2±9.88% NHE1+siRNA OPN vs. 85.5±13.44% NHE1 infected H9c2 cardiomyocytes; $P< 0.05$) in H9c2 cardiomyocytes (Figure 4.8 E). Our findings indicate that downregulating OPN in cardiomyocytes using siRNA OPN appears to reduce OPN gene expression and significantly reduces expression of the full form of the OPN phosphoprotein as well as the MMP-3/7 cleaved form.

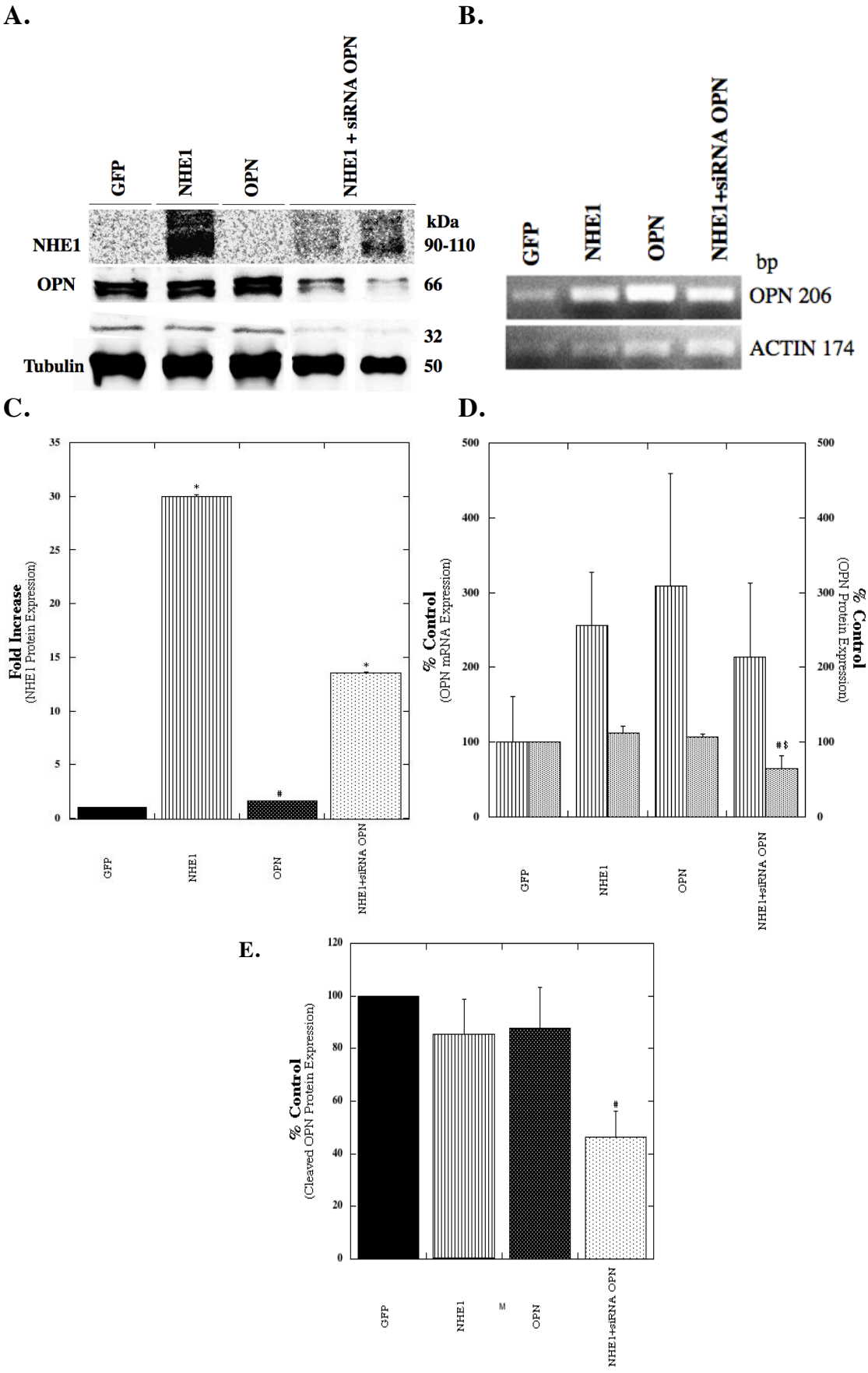
A.
GFP
NHE1
OPN
NHE1 + siRNA OPN
kDa
NHE1
90-110
OPN
66
32
Tubulin
50
B.
GFP
NHE1
OPN
NHE1+siRNA OPN
bp
OPN 206
ACTIN 174
C.
Fold Increase
(NHE1 Protein Expression)
GFP
NHE1
OPN
NHE1+siRNA OPN
D.
% Control
(OPN mRNA Expression)
% Control
(OPN Protein Expression)
GFP
NHE1
OPN
NHE1+siRNA OPN
E.
% Control
(Cleaved OPN Protein Expression)
GFP
NHE1
M
OPN
NHE1+siRNA OPN

Fig. 4.8: Protein expression of *total* NHE1 and OPN gene and protein expression in H9c2 cardiomyocytes transfected with OPN or active NHE1 ± siRNA OPN **A.** Representative western blot of H9c2 cardiomyocytes transfected with GFP, OPN or active NHE1 ± siRNA OPN 100nM 24 hours post transfection. Protein expression was determined by immunoblotting against anti-NHE1 or OPN; normalization was against α-tubulin. NHE1 protein was detected between 90-110 kDa, OPN between 66 kDa and 32 kDa, and Tubulin, as loading control, at 50 kDa. **B.** Representative DNA gel of transfected H9c2 cardiomyocytes. Lane 1-3 represents GFP, NHE1 and OPN infected H9c2 cardiomyocytes and lane 4 represents NHE1 + siRNA OPN. OPN primed products were detected at 207bp and β-actin at 174bp. **C.** Quantification of relative levels of NHE1 protein expression expressed as fold increase ± SEM. **D.** Quantification of relative levels of OPN mRNA expression (*stripped*) and protein expression at 66 kDa (*dotted*). E. Quantification of relative levels of cleaved OPN expression at 32 kDa Results expressed as % of GFP control ± SEM% *** *P* < 0.05** vs. GFP, $^{\#}$ vs. NHE1, $^{\$}$ OPN infected H9c2 cardiomyocytes (n of 6-10 from 4 experiments).

4.2.2.7 NHE1 Activity of NHE1 of H9c2 Cardiomyocytes Infected with NHE1 and/or Transfected with siRNA OPN

In order to confirm the ability of OPN to regulate the activity of NHE1, we examined NHE1 activity of H9c2 cardiomyocytes infected with active NHE1 adenovirus, in the presence and absence of siRNA OPN, as well as H9c2 cardiomyocytes infected with OPN or with an adenovirus containing only GFP (Figure 4.9). NHE1 activity was measured as described in Sections 2.1.3.2.3 and 2.2.3.3.2. Following the induction of an acid load using 50mM NH_4Cl, the rate of cell recovery, inductive of NHE1 activity, was measured (Figure 2.3). Our results revealed that active NHE1 was able to significantly increase NHE1 activity of H9c2 cardiomyocytes (586.5±103.54% NHE1 infected vs. 100.0±38.14% GFP infected H9c2 cardiomyocytes; $P< 0.05$). This is consistent with our previous findings using NHE1-infected NRVMs (Section 3.2.1.3 Figure 3.4). On the other hand, downregulating OPN using siRNA OPN in the presence of the NHE1 adenovirus caused a significant reduction in NHE1 activity compared to NHE1 infected H9c2 cardiomyocytes (235.0±92.14% NHE1+siRNA OPN infected vs. 586.5±103.54% NHE1 infected H9c2 cardiomyocytes; $P< 0.05$) further implicating OPN in regulation of NHE1 activity (Figure 4.9 *Lower panel*). Taken together, our findings strongly suggest that OPN regulates both NHE1 protein expression and activity in cardiomyocytes.

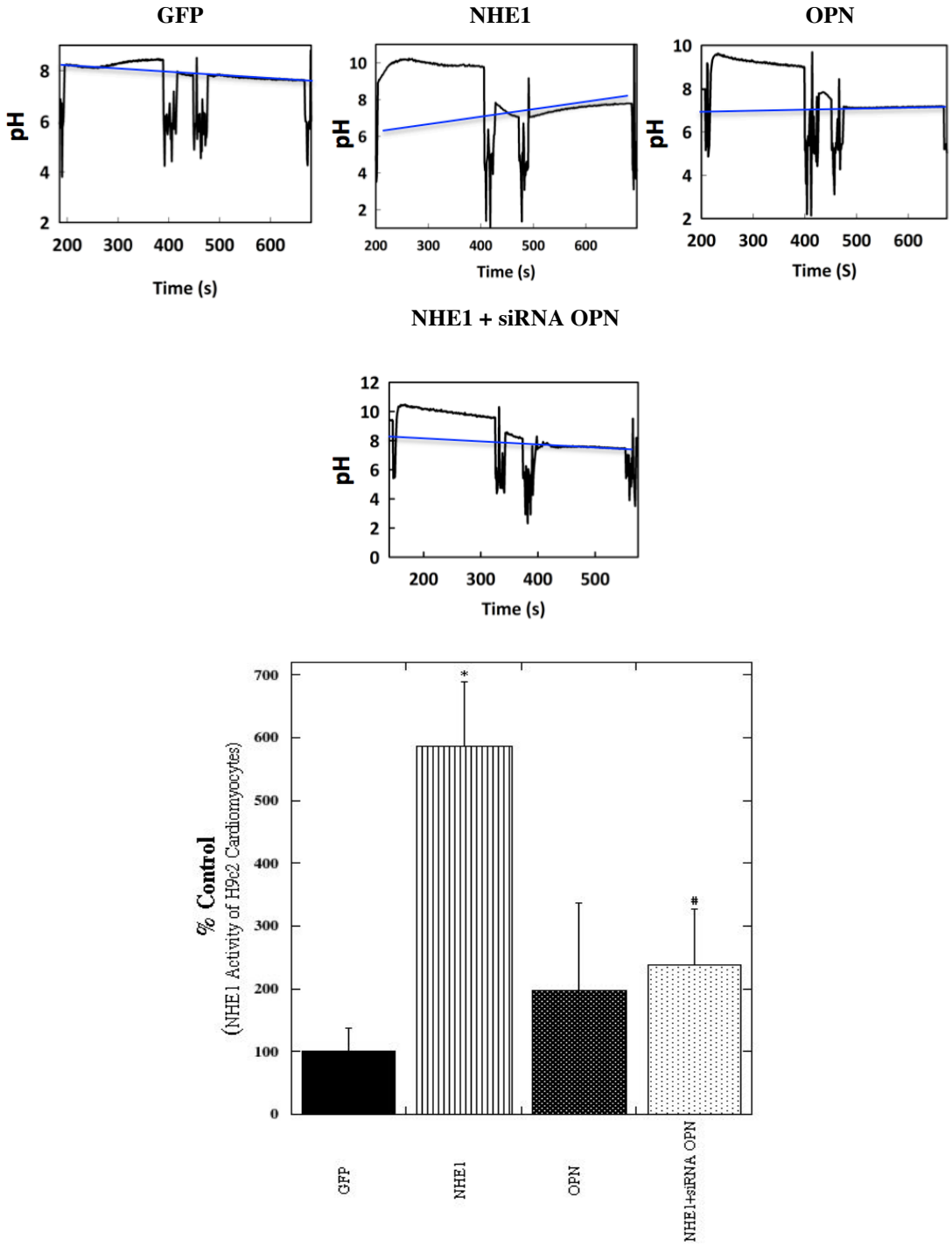

Fig. 4.9: NHE1 activity of H9c2 cardiomyocytes transfected with OPN or active NHE1 ± siRNA OPN 100nM 24 hours post transfection. 2.1.3.3. Cardiomyocytes plated on coverslips were incubated with BCECF-AM as described in Section 2.2.3.2. To induce an acid load, 50mM NH_4Cl was added. Cells were immersed in Na^+ free buffer before the reintroduction of Na^+ (NaCl) and calculation of NHE1 activity. *Upper panel* Representative traces of NHE1 activity assay of transfected H9c2 cardiomyocytes. The true, calculated pH_i trace and rate of recovery slopes are indicated. *Lower panel* Quantification of a series of experiments was conducted, NHE1 activity was expressed as a % of GFP control **±** %SEM. ***** ***P* < 0.05** vs. GFP**,** # vs. NHE1 (representative of 6-10 coverslips, from 3 experiments).

4.2.3 Characterization of Parameters of Cardiac Hypertrophy in H9c2 Cardiomyocytes Infected with NHE1 and/or Transfected with siRNA OPN

4.2.3.1 Cell Area in H9c2 Cardiomyocytes Infected with NHE1 and/or Transfected with siRNA OPN

In order to asses the role of OPN in NHE1-induced CH, we monitored the effects of downregulating OPN on cell area, as a parameter of CH. Following the overexpression of NHE1 in H9c2 cardiomyocytes, cell area appeared to be significantly increased compared to cardiomyocytes infected with the GFP adenovirus (190.9±8.66% NHE1 infected vs. 100.0±23.38% GFP infected H9c2 cardiomyocytes; $P< 0.05$) (Figure 4.10). This is in agreement with our previous findings in which cell area in NRVMs infected with NHE1 was significantly increased (Section 3.2.2.1 Figure 3.6). Similarly, overexpressing OPN in H9c2 cardiomyocytes showed a trend towards increasing (153.2±26.65% OPN infected vs. 100.0±23.38% GFP infected H9c2 cardiomyocytes). On the other hand, downregulating OPN in H9c2 cardiomyocytes caused a significant reduction in cell area compared to NHE1 infected H9c2 cardiomyocytes (68.5±0.24% NHE1+siRNA OPN transfected vs. 190.9±8.66% NHE1 infected H9c2 cardiomyocytes; $P< 0.05$). Our findings thus suggest that OPN may be mediating the hypertrophic effects of NHE1-induced CH by enhancing cell area (Section 3.2.2.1 Figure 3.6) and that downregulating OPN could reduce NHE1-induced CH (Figure 4.10).

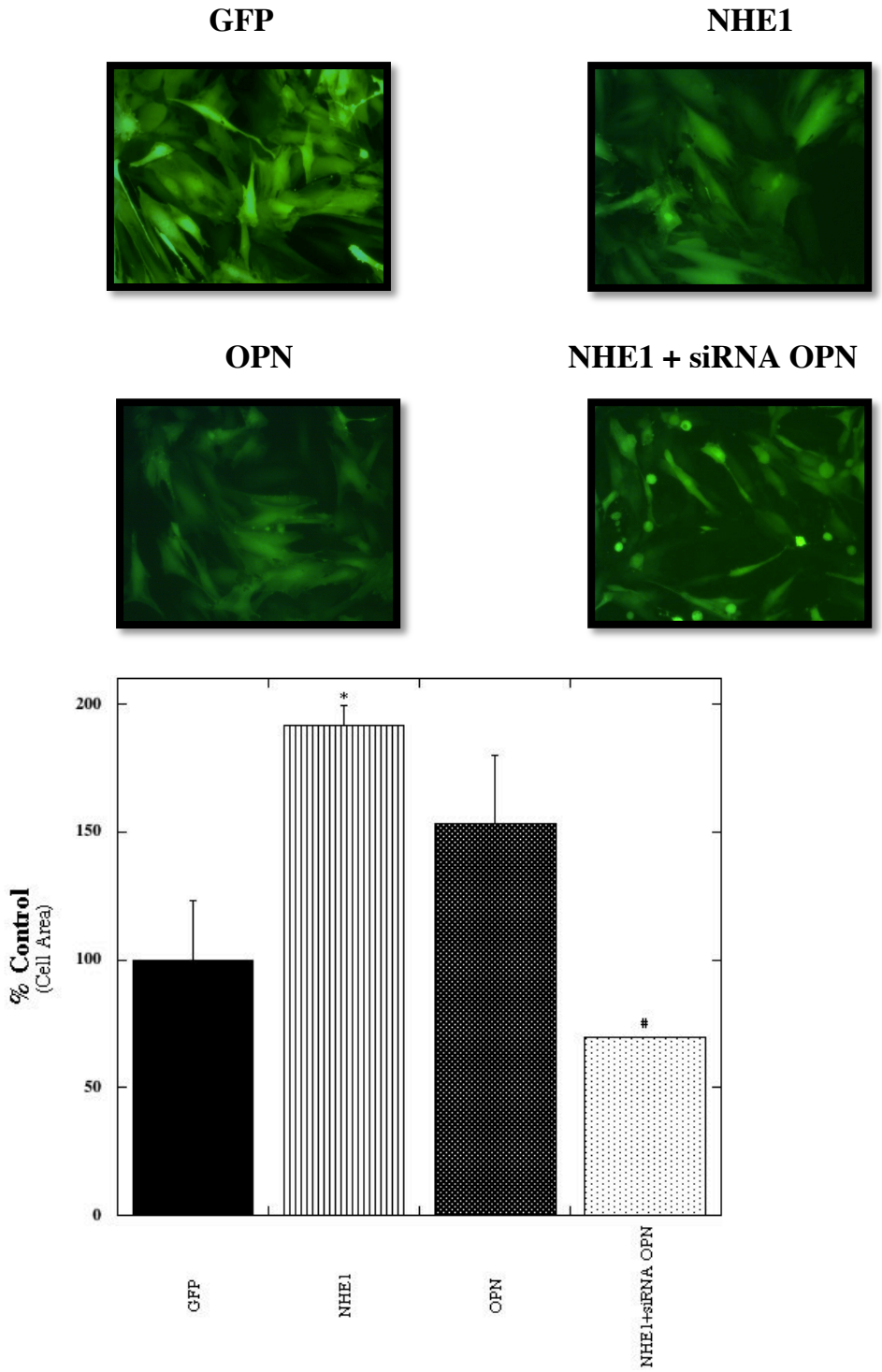

Fig. 4.10: Cell area of H9c2 cardiomyocytes transfected with OPN or active NHE1 ± siRNA OPN 100nM 24 hours post transfection. *Upper panel:* Representative fluorescence microscopy images of GFP, NHE1 or OPN infected and NHE1 and siRNA OPN 100nM transfected cardiomyocytes, 24 hours post-transfection. *Lower panel* Quantification of cell area of GFP, NHE1 or OPN infected and NHE1 and siRNA OPN 100nM transfected cardiomyocytes, 24 hours post-transfection. Results expressed as %GFP ± %SEM. ***** ***P* < 0.05** vs. GFP, # vs. NHE1 (representative of at least 70 cells, measured from 4-6 individual dishes, from 3 experiments).

4.2.3.2 Protein Content H9c2 in Cardiomyocytes Infected with NHE1 and/or Transfected with siRNA OPN

Protein content has been considered another prominent marker of CH in numerous *in vitro* studies (171, 184). Our studies revealed that infection of H9c2 cardiomyocytes with NHE1 caused a significant increase in protein content vs. GFP infected H9c2 (Figure 4.11). This is consistent to the effects of upregulating NHE1 in NRVMs (Section 3.2.2.1 Figure 3.4) and H9c2 cardiomyocytes (Figure 4.10) on cell area, another parameter of CH. Similarly, protein content in H9c2 cardiomyocytes overexpressing OPN showed a trend towards increasing (156.5±19.86% OPN infected vs. 100.0% GFP infected H9c2 cardiomyocytes). This is in agreement with the effects upregulating OPN in H9c2 cardiomyocytes on cell area. Accompanying the reduction in cell area in the presence of siRNA OPN was a significant reduction in protein content compared to NHE1 (87.8±12.58% NHE1+siRNA OPN transfected vs. 136.8±11% NHE1 infected H9c2 cardiomyocytes; $P<0.05$). Thus, our findings strongly suggest that the NHE1-inuced hypertrophic response in cardiomyocytes is mediated through OPN and that downregulating OPN can reverse parameters of CH.

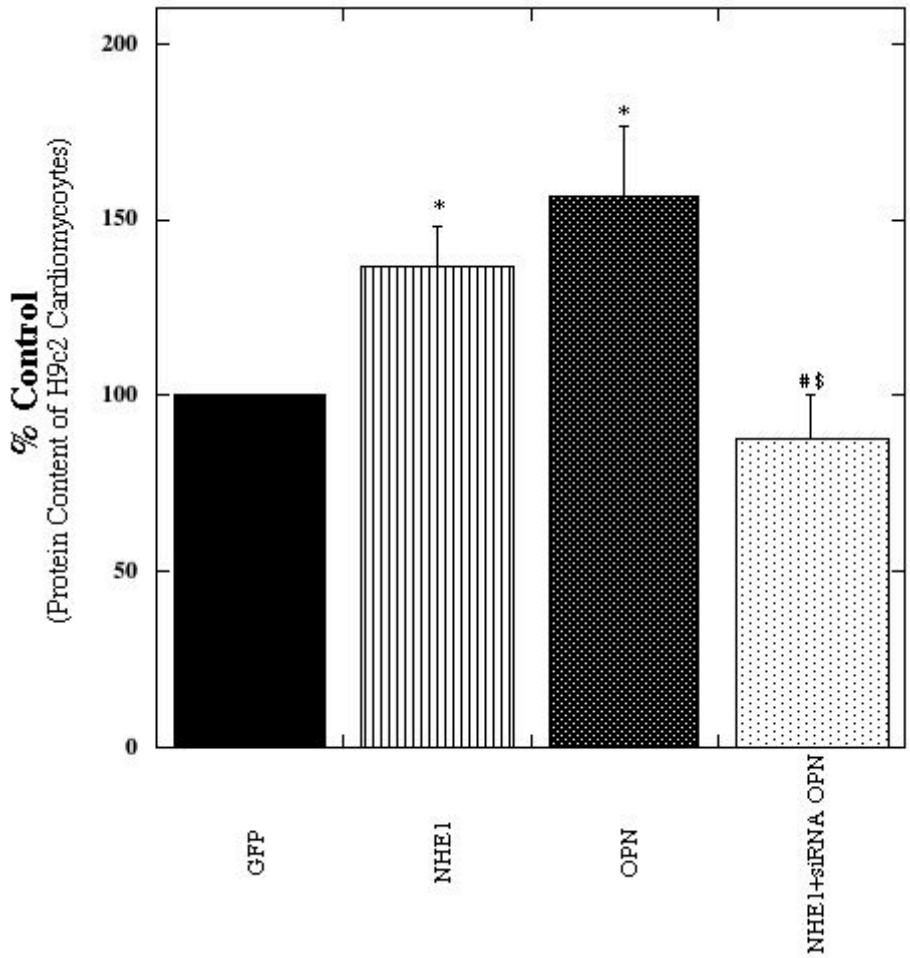

Fig. 4.11: Protein content of H9c2 cardiomyocytes transfected with OPN or active NHE1 ± siRNA OPN 100nM 24 hours post transfection. Protein content of transfected H9c2 cardiomyocytes measured as μg/10 x 10^6 cell. Results expressed as % of GFP control **±** %SEM. * ***P* < 0.05** vs. GFP, # vs. NHE1 (n of 5-7 from 5 experiments).

4.2.3.3 ANP Gene Expression in H9c2 Cardiomyocytes Infected with NHE1 and/or Transfected with siRNA OPN

We also examined another parameter of CH in transfected H9c2 cardiomyocytes, ANP mRNA levels (Figure 4.12). ANP mRNA levels showed a significant increase in NHE1 infected H9c2 cardiomyocytes (247.7±30.81% NHE1 infected vs. 100%±40.83 GFP infected H9c2 cardiomyocytes). A similar effect was seen in OPN infected H9c2 cardiomyocytes (141.5±86.65% OPN infected vs. 100%±40.83 GFP infected H9c2 cardiomyocytes), although it was not significant. Upon downregulation of OPN using siRNA OPN directed at OPN, ANP mRNA levels was significantly decreased (64.6±19.9% NHE1+siRNA OPN transfected vs. 247.7±30.81% NHE1 infected H9c2 cardiomyocytes). Taken together our findings indicate that OPN regulates NHE1 expression and activity during CH. Our findings also confirm that downregulating OPN can attenuate NHE1-induced CH *in vitro* by reversing parameters of CH.

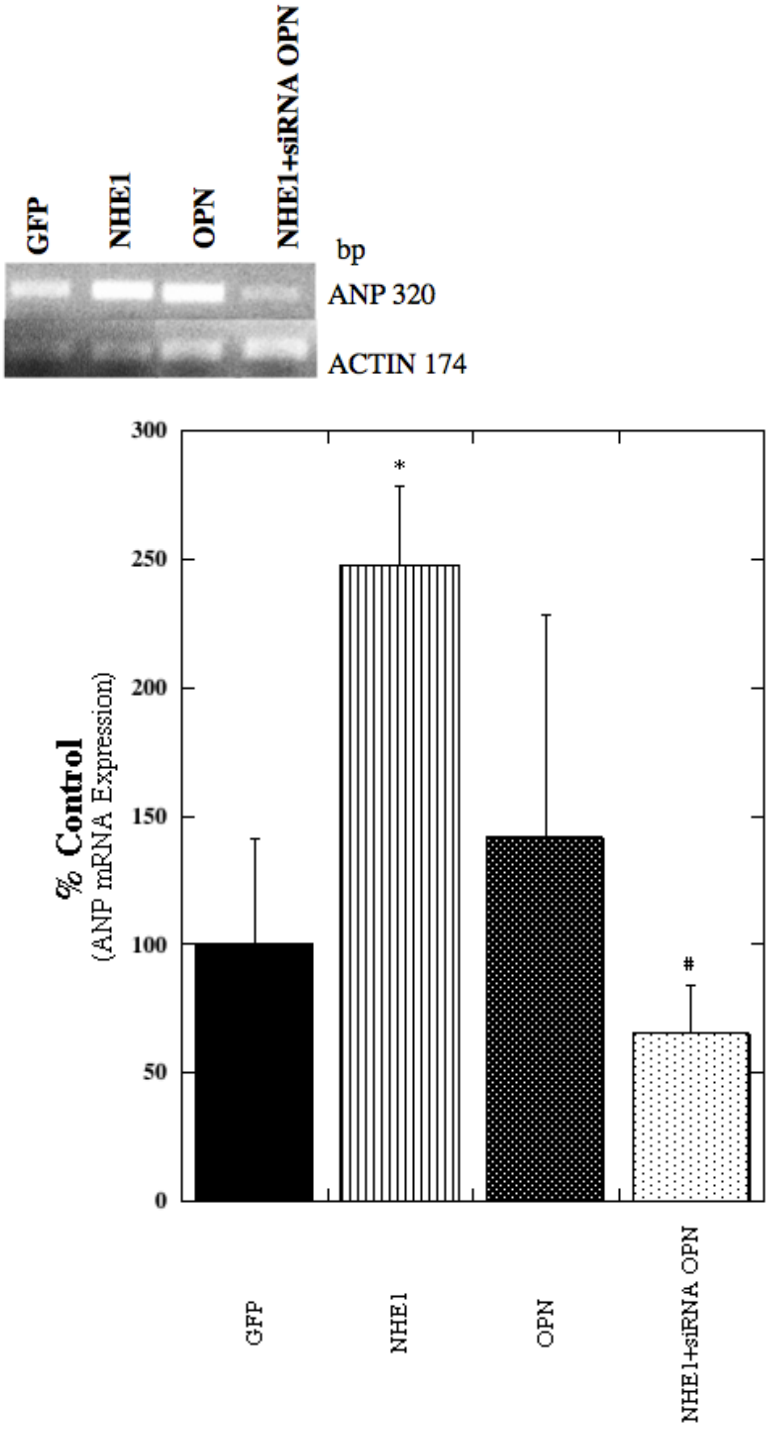

Fig. 4.12: OPN and ANP mRNA in H9c2 cardiomyocytes transfected with OPN or active NHE1 ± siRNA OPN 100nM 24 hours post transfection. *Upper panel:* Representative DNA gel of transfected H9c2 cardiomyocytes. Lane 1-3 represents GFP, NHE1 and OPN infected H9c2 cardiomyocytes and lane 4 represents NHE1 + siRNA OPN. ANP primed products were detected at 320bp and β-actin at 174bp. *Lower panel:* ANP mRNA expression in transfected H9c2 cardiomyocytes were expressed as % of GFP control **±** %SEM. * ***P* < 0.05** vs. GFP, # vs. NHE1 (n of 4-7 from 4-7 experiments).

4.3 Discussion

Previous studies have indicated that elevated NHE1 expression/activity was associated with CH and upregulation of OPN (22, 23). However, neither the cellular interplay between OPN and NHE1 nor the role of OPN in NHE1-induced CH has been identified yet. As such, our first objective aimed to investigate the effects of enhanced NHE1 and OPN expression in an *in vitro* model of cardiomyocytes. In our first objective, we demonstrated for the first time that OPN regulates NHE1 protein expression and activity and appears to contribute to the NHE1-induced hypertrophic response in NRVMs (Section 3.2). We were then intrigued to confirm the ability of OPN to facilitate the NHE1-induced hypertrophic response by analyzing the effect of silencing OPN on the hypertrophic effects of NHE1 in H9c2 cardiomyocytes. Several studies have adopted the approach to use siRNA against OPN to inhibit OPN protein expression (123, 180). Therefore, in this model, an siRNA targeting the OPN mRNA was used to downregulate OPN expression in H9c2 cardiomyocytes. We also used the active NHE1 adenovirus to enhance the expression and activity of the exchanger and simulate the NHE-induced hypertrophic response. In order to confirm the role of OPN in the regulating NHE1 expression and activity, we analyzed changes in OPN and NHE1 expression and activity following the downregulation of OPN. We then studied the effect of downregulating OPN on the NHE1-induced hypertrophic response by examining parameters of CH that included cell area, protein content and ANP mRNA levels.

The role of OPN in CH and remodeling has been well documented since 1997, making it an ideal target to investigate as a mechanism by which NHE1 induces CH (20, 153-155, 162, 163). OPN expression is heightened in the heart in response to

mechanical stress and neurohormonal stimuli, factors which precipitate the progression of heart failure (156). Graf et al. suggested that OPN upregulation in response to ET-1 and NE-induced CH could contribute to the growth and adhesion of cardiac fibroblasts during cardiac remodeling (153). In fact, the cardiac fibrotic and hypertrophic response observed in WT OPN following the administration of Ang II has been attributed to OPN (134, 155). The activity of NHE1 has also been suggested to be stimulated by both Ang II and ET-1 in response to neurohormonal activation during CH (83). Taken together, these findings suggest that the same α1-AR agonists that stimulate OPN and induce CH can mediate NHE1-induced CH, further confirming an association between the 2 proteins during CH. Moreover, the amount of OPN expressed in transgenic mice expressing active NHE1 was much greater than the amount of OPN expressed in NHE1 WT mice (23). These findings clearly indicated an association between NHE1-induced CH and OPN and directed us to examine how OPN may facilitate the NHE1-induced hypertrophic response.

4.3.1 H9c2 Cardiomyocytes as an in vitro Model to Confirm the Role of OPN in NHE1-induced Cardiac Hypertrophy

Cultures of cardiomyocytes including NRVMs and H9c2 myoblasts have been widely used to investigate the cellular and molecular changes that underlie CVDs *in vitro* (14, 15, 90, 175). Due to our inability to import neonatal rat pups into our research facility and the various obstacles we were faced with, we decided to use the H9c2 cell line as our model for NHE1-induced CH for our second objective (175). Since H9c2 cardiomyocytes are isolated from the ventricular tissue of the embryonic BD1X rat heart, they display hypertrophy-associated traits similar to primary cultures

of cardiomyocytes (175, 188) and are considered a valid cell line for the study of CH *in vitro* (90, 184, 187). However, when cultured in 10% FBS *culture media,* H9c2 cells represent an undifferentiated, proliferative myoblastic phenotype and exhibit metabolic parameters that are not consistent with cardiomyocytes including enhanced glycolytic fluxes, increased cytosolic redox state and lower oxygen consumption (187). Ménard et al. were the first to suggest that serum starvation of H9c2 myoblasts induces myogenic differentiation through transdifferentiation rendering the cells skeletal (176). However, treatment of serum starved H9c2 myoblasts with RA enhances cardiac Ca^{2+} channel expression and allows the cells to maintain their cardiac phenotype. In our study, culturing of H9c2 myoblasts, both in the presence of serum starvation and RA, caused differentiation of the cells into H9c2 cardiomyocytes. Through crystal violet staining, we were able to confirm the differentiation of H9c2 myoblasts into elongated, branched and multinucleated cells, which are morphological characteristics of the cardiac phenotype (190). However, it is important to note that crystal violet staining alone is not sufficient to confirm enzyme activity of myokinase and transformation of creatinine kinase from the BB to the MM or the expression of VDCCs and the sarcomeric heavy chain, which are specific to cardiomyocytes (190). Even though in our study we did not detect these changes, the protocol we used to differentiate the H9c2 cells is well cited in the literature (176, 184, 187). Through the use of differentiated H9c2 myoblasts, we were able to further confirm the role of OPN in NHE1-induced CH in H9c2 cardiomyocytes.

4.3.2 NHE1 Protein Expression is Enhanced During Differentiation of H9c2 Cells

Following differentiation of the H9c2 cells, we examined the changes in NHE1 and OPN protein expression. As shown in Figure 4.2, undifferentiated H9c2 cells expressed basal levels of NHE1. This is consistent with previous studies in which NHE1 mRNA and protein expression were detected in H9c2 cells under control conditions (90, 93). NHE1 protein expression appeared to be higher in differentiated H9c2 cardiomyocytes. This is in agreement with a previous report by Carraro-Lacroix et al. which demonstrated that NHE1 protein expression/activity was increased during differentiation of immortalized rat proximal tubule cells (36). In an additional study, Xiuju et al. demonstrated that NHE1 protein expression facilitates cardiomyocyte embryonic stem cell differentiation, which further strengthens our findings (37). Therefore, our results are consistent with previous findings that show that enhanced NHE1 expression is associated with differentiation.

4.3.3 OPN Protein Expression is Enhanced During Differentiation of H9c2 Cells

Basal expression of OPN was detected in undifferentiated H9c2 cells, which may be in part due to the hyperglycemic environment that the cells were cultured in (82, 162). Interestingly, the MMP-3/7 cleaved fragment of OPN appearing at 32 kDa was not detected in neither undifferentiated H9c2 cells nor differentiated H9c2 cardiomyocytes. Our data therefore suggests that a significant upregulation of NHE1 and OPN (Section 3.2.1.2) is necessary for the cleavage of OPN and that under basal conditions; OPN is expressed as the full form protein. OPN protein expression appeared to be increased following differentiation of H9c2 cells. Although no studies have examined OPN expression in differentiated H9c2 cardiomyocytes, a study by

Pereira el al. revealed that OPN was upregulated during differentiation of myoblasts into myotubes (133). This was attributed to OPN's involvement in facilitating myoblast fusion and its role as a key cytokine that regulates tissue repair and inflammation. OPN is also considered to be essential for the differentiation of fibroblasts and the expression of the differentiated myofibroblasts phenotype, which is a necessary response post-MI injury, which further strengthens our findings (122). Our results are therefore consistent with previous findings and confirm that OPN is a key player in inducing the differentiation of myoblasts.

4.3.4 Two-way Crosstalk Between NHE1 and OPN Expression in Cardiac Hypertrophy

In our study, overexpression of NHE1 in H9c2 cardiomyocytes caused a significant increase in both NHE1 expression and activity (Figure 4.8 and 4.9), which is similar to the effects of upregulating NHE1 in NRVMs. This upregulation of NHE1 was associated with enhanced protein and gene expression of OPN (Figure 4.8A-D). This appears to be consistent with our previous findings in which NRVM infection with active NHE1 caused a significant increase in sOPN protein expression. This is also in agreement with previous studies in which upregulation of NHE1 caused enhanced gene expression of OPN (21-23). Interestingly, infection of H9c2 cardiomyocytes with NHE1 in the presence of siRNA OPN caused a significant reduction in both NHE1 and OPN protein expression, and a trend towards reduction in OPN gene expression. In the recent study by Voelkl et al., the authors demonstrated that upon inhibition of SGK1, both NHE1 and OPN gene expression was significantly reduced. This further strengthens our findings and, which suggest that OPN regulates

NHE1 expression. Our findings also revealed that NHE1 activity in NHE1 infected H9c2 cardiomyocytes in the presence of siRNA OPN was significantly reduced (vs. NHE1 infected H9c2 cardiomyocytes). Although the exact mechanism through which OPN is able to regulate NHE1 requires further understanding, SGK1 appears to be a potential mediator (21, 22). OPN has also been shown to induce the activity of CAII, which is known to be a regulator of NHE1 activity (132, 149). However, whether OPN is able to regulate NHE1 activity/expression through SGK1 or CAII is yet to be determined. Taken together, our results are the first to reveal a two-way cross talk between NHE1 and OPN. NHE1 appears to upregulate OPN expression, which in turn increases NHE1 expression and activity.

4.3.5 Downregulating NHE1 and OPN Expression Stabilizes the Full Form Phosphoprotein

Our previous findings have revealed that overexpression of both NHE1 and OPN in NRVMs appeared to enhance the cleavage of OPN (Figure 3.2). Overexpression of NHE1 alone in H9c2 cardiomyocytes had no effect on MMP-3/7 cleavage of OPN. However, in H9c2 cardiomyocytes infected with NHE1 in the presence of siRNA OPN, the detection of the 32 kDa cleaved fragment of OPN was significantly reduced compared to NHE1 infected H9c2 cardiomyocytes. Since both NHE1 and OPN protein expression were significantly reduced in H9c2 cardiomyocytes infected with NHE1 and transfected with siRNA OPN, our findings suggest that NHE1 maybe involved in cleavage of OPN, when sufficient amounts of OPN are present. Although previous studies have indicated that the cleaved fragments of OPN are more biologically active than the full form of the glycoprotein (110, 113,

135), we are yet to establish whether the cleaved form of OPN is responsible for mediating the hypertrophic effects of NHE1. Moreover, whether NHE1 and OPN additively enhance MMP activity and mediate cleavage of the full form of OPN is yet to be determined.

4.3.6 Downregulating OPN Reverses the NHE1-induced Hypertrophic Response

Our findings indicate that upregulation of NHE1 enhances OPN protein expression, which in turn, regulates NHE1 protein expression and activity. In order to determine how this interaction precipitates during NHE1 induced CH, we examined the effects of downregulating OPN on parameters of NHE1-induced CH in H9c2 cardiomyocytes. We demonstrated that infection of cardiomyocytes with active NHE1 significantly increased cell area as well as protein content and ANP gene expression, parameters of CH (Figure 4.10-4.12). This is consistent with several *in vitro* studies in which upregulation of NHE1 significantly enhanced cell area and ANP gene expression (14, 18, 93). In OPN infected H9c2 cardiomyocytes, both cell area and ANP gene expression showed a trend towards increasing, while protein content was significantly increased. Previous studies have indicated that OPN-induced CH causes reactivation of the fetal gene program and ANP gene expression, which is consistent with our findings (153-155). Interestingly, downregulation of OPN in NHE1 infected H9c2 cardiomyocytes significantly reduced cell area, protein content as well as ANP gene expression. Taken together, our findings strongly implicate OPN in contributing to effects of NHE1. Although the exact signaling pathway implicating the upregulation of NHE1 in CH is still under investigation, our findings strongly indicate that OPN regulates the activation of NHE1 and contributes to the NHE1-induced

hypertrophic response in cardiomyocytes.

Chapter 5: Discussion and Conclusions

5.1 Discussion

Enhanced expression/activity of NHE1 has previously been shown to contribute to CH both *in vitro* and *in vivo* (14, 22, 23, 43, 51). Interestingly, enhanced NHE1 activity rather than expression has been suggested to be the culprit inducing the cardiac hypertrophic effects (17, 18, 21, 54, 95). A possible approach to decrease the activity of NHE1 and attenuate the hypertrophic response is through the inhibition of the regulators of NHE1 activity. Alvarez et al. have previously shown that inhibition of CAII, a regulator of NHE1 activity, significantly regressed NHE1 activity and CH in NRVMs and ARVMs (63). Moreover, Voelkl et al. have recently demonstrated that ablation of SGK1, a potential regulator of NHE1 activity, significantly reduced both NHE1 activity and parameters of CH in mice (21). Interestingly, in the WT SGK1 mice, both NHE1 protein expression/activity as well as OPN gene expression were significantly higher than SGK1 KO mice (21, 22). Moreover, Mraiche et al have demonstrated that the upregulation of OPN associated with NHE1-induced CH is much greater than OPN expression transgenic mice expressing WT NHE1 (23). Taken together these findings clearly indicate that enhanced NHE1 activity contributes to the development of CH, which is associated with the upregulation of OPN. However, the importance of OPN in regulating NHE1 expression/activity and the NHE1-induced hypertrophic response remains unknown.

Our project aimed to delineate the ability of OPN to contribute to the hypertrophic effects of NHE1. To investigate the ability of OPN to facilitate the hypertrophic effects of NHE1 during CH; we used both a *gain* and *loss* of function *in*

vitro models. For the *gain* of function model, NHE1 and OPN adenoviruses were used as tools to enhance NHE1 and OPN expression in NRVMs. Changes in the patterns of OPN and NHE1 protein expression as well as activity were analyzed. Cell area, a parameter of CH was measured in order to determine whether OPN facilitates the hypertrophic effects of NHE1 during CH. In the *loss* of function model, the effect of silencing OPN on NHE1 activity and the NHE1-induced hypertrophic response was investigated in H9c2 cardiomyocytes. Initially, we examined the effects of downregulating OPN on NHE1 protein expression as well as activity. We then characterized our infected and transfected H9c2 cardiomyocytes for parameters of CH including cell area, protein content and ANP mRNA levels. Our findings have several implications:

5.1.1 Protein Expression of NHE1 and OPN in Cardiomyocytes

Our results indicated that under control conditions (in the presence of the GFP adenovirus), cardiomyocytes did not express *NHE1* (Figure 3.2 and 4.8). In fact, the NHE1 protein was only detected in cardiomyocytes infected with the NHE1 adenovirus. This is consistent with previous studies that showed that under control conditions, NHE1 was not expressed by cardiomyocytes (15, 32, 57, 90). Our inability to detect NHE1 expression under control conditions in cardiomyocytes may also be attributed to the specificity of the antibody we used.

Basal levels of both *sOPN* and MMP-3/7 *cleaved OPN* appeared to be expressed by our cardiomyocytes under control conditions (Figure 3.2 and 4.8). It is, however, important to note that the *infection media* that was used to culture the cardiomyocytes prior to infection and/or transfection contained 25mM glucose, which

is considered a hyperglycemic environment and has been shown to induce OPN expression (82, 162). Thus, this could justify the increase in basal expression of OPN at 66 kDa in NRVMs under control conditions. The OPN gene was also expressed in basal levels in control H9c2 cardiomyocytes. Although OPN protein expression appeared to be much enhanced in H9c2 cardiomyocytes under control conditions (in the presence of the GFP adenovirus) compared to NRVMs, this may be attributed to the more specific antibody used (ab8448 vs. ab14176) or the upregulation in OPN observed upon differentiation.

5.1.2 Upregulation of NHE1 Enhances OPN Expression in Cardiomyocytes

OPN is differentially expressed as both an intracellular and secreted isoform (118). Our results revealed that protein expression of sOPN at 66 kDa was upregulated in NHE1 infected cardiomyocytes compared to control (Figure 3.2 and 4.8). OPN gene expression also showed a trend towards increasing in NHE1 infected cardiomyocytes (Figure 4.8 B and 4.8 D) compared to control. Mraiche et al. have also demonstrated that transgenic mice expressing cardiac specific active NHE1 were associated with CH and elevated gene expression of OPN, which is consistent with our data (23). Although OPN gene expression was highest in cardiomyocytes infected with OPN (Figure 4.8 B and D), OPN protein expression was higher in NHE1 infected cardiomyocytes and not the OPN infected cardiomyocytes. This suggests that there was a transcriptional increase in OPN expression, however, which was not reflected in terms of translational protein expression. On the other hand, downregulation of OPN in the presence of NHE1 was associated with a significant reduction in both NHE1 and OPN protein expression, to a level much lower than OPN

protein expression under control conditions. This suggests that the reduction in NHE1 expression observed may have contributed to a further reduction in OPN expression in the presence of siRNA OPN (Figure 4.8 C and 4.8 D). Interestingly, OPN gene expression was also reduced in the presence of siRNA OPN and NHE1 adenovirus, although this decrease was not significant compared to neither control nor NHE1 infected cardiomyocytes. This further suggests that the transcriptional and translational regulation of OPN gene and protein expression is easily influenced by external factors and requires a better understanding. Young et al. also previously demonstrated that OPN was reduced following inhibition of NHE1 in deoxycorticosterone acetate treated mice (24), which further strengthens our findings. Our results are therefore consistent with previous findings and further confirm that upregulation of NHE1 enhances OPN expression. The exact mechanism by which NHE1 is able to upregulate OPN quite unknown, however, it may be associated enhancing the interactions between OPN and the protein components of the ECM.

5.1.3 NHE1-inudced Upregulation of OPN Involves $\alpha_v\beta_3$ integrin

In CVDs and cancer, common processes involving stromal remodeling, cell invasion, and angiogenesis can promote progression of the disease. As a result, several similarities exist between the signaling pathways activated during the progression of cancer that can be linked back to CVDs including CH. In tumor cells, the extracellular pH (pH_e) is more acidic than pH_i. In an additional stude, Paradise et al. recently suggested that upregulation of NHE1 mediates acidification of the pH_e, through enhanced H^+ extrusion and activation of the $\alpha_v\beta_3$ integrin (56). As mentioned earlier, the activity of the $\alpha_v\beta_3$ integrin has been shown to be enhanced in several

tumors, thus leading to the activation of OPN (136, 140). Since the changes in the pH documented occurred in the extracellular milleux surrounding the cells, this would suggest that $\alpha_v\beta_3$ integrin-mediated upregulation of OPN would target the secreted form rather than the intracellular OPN form. Therefore, we suggest that the upregulation of sOPN may in part be due enhanced $\alpha_v\beta_3$ integrin binding secondary to the activation of NHE1.

5.1.4 OPN Regulates NHE1 Expression and Activity

Our data suggests for the first time that OPN regulates NHE1 expression and activity in cardiomyocytes (Figure 3.2, 3.3 and 4.8, 4.9). Upregulation of both NHE1 and OPN significantly increased NHE1 protein expression and activity to control as well as cardiomyocytes infected with NHE1 alone. On the other hand, downregulating OPN in cardiomyocytes infected with NHE1 caused a significant reduction in NHE1 protein expression compared to control. The reduction in NHE1 expression was associated with a reduction of more than 50% in NHE1 activity compared to infection with NHE1 alone (Figure 4.9), suggesting that OPN is a key regulator of NHE1 activity. This is further strengthened by previous findings that demonstrated that NHE1 activity was only significantly reduced upon inhibition of the regulators of NHE1 activity including SGK1 (21) and CAII (63). Our study is therefore the first to demonstrate a two-way cross talk between NHE1 and OPN in cardiomyocytes. Our findings indicate that NHE1 upregulates OPN protein and gene expression, which in turn regulates NHE1 protein expression and activity in cardiomyocytes. Whether OPN is able to regulate NHE expression/activity through SGK1, CAII or through other pathways remains to be elucidated.

5.1.5 OPN Regulates NHE1 Expression and Activity Through SGK1

Regulation of NHE1 activity is an intricate process that requires both direct and in direct interaction of proteins and kinases with the C-terminal of the exchanger. Voelkl et al. have previously demonstrated enhanced gene expression of NHE1 and OPN following the activation of SGK1 in HL-1 cardiomyocytes and transgenic mice (21, 22). These findings strongly suggest that enhanced NHE1 gene expression and activity is correlated with the levels of OPN and SGK1, especially since ablation of SGK1 significantly reduced both NHE1 and OPN gene expression (21). SGK1 is thought to be stimulated following activation of the serine threonine kinase phosphatidylinositide 3-kinase (PI_3K), known to be structurally similar to Akt (87). OPN has also been shown to activate the PI_3K-Akt pathway both in tumor cells (137, 154), which further strengthens the notion that OPN is able to regulate NHE1 activity possibly through SGK1. That being said, further studies are necessary in order to confirm the ability of NHE1 to regulate NHE1 expression and activity through SGK1.

5.1.6 OPN Regulates NHE1 Expression and Activity Through CAII

OPN has previously been shown to reduce ectopic calcification in atherosclerotic plaques and calcified aortic valves through the induction of CAII expression (as mentioned in Section 1.4.3.1 and (149)). The Fliegel group were the first to establish that CAII binding to NHE1 significantly enhances the exchanger's activity by up to 2-fold (as mentioned in Section 1.2.2.3.1 and (62)). Enhanced CAII expression, mediated by elevated levels of OPN, may promote acidification of the cytosol, therefore justifying the increase in NHE1 protein expression we observed. Mraiche et al. previously demonstrated that gene expression of proteins involved in

the regulation of pH_i and Na^+, Ca^{2+} homeostasis including $Cl^-/HCO3^-$ exchangers (AEs) NCX and the Na^+ -K^+-ATPase were not altered in transgenic mice expressing cardiac specific active NHE1 (23), however, CAII was not investigated in this study. Therefore, our results reveal, for the first time, that OPN regulates NHE1 protein expression in cardiomyocytes. Whether this occurs through OPN-mediated activation of CAII and independent of pH_i and Na^+ /Ca^{2+} proteins is yet to be determined.

5.1.7 NHE1 and OPN Enhance MMP-3/7 Cleavage of OPN

Studies have reported that the activity of OPN is enhanced following cleavage of the phosphoprotein (113, 121). Cleavage of OPN is crucial as it enhances the exposure of the RGD binding site thus allowing for integrin binding and activation of OPN (113). In our studies, the cleaved form of OPN at 32 kDa showed a trend towards increasing in NHE1 and OPN infected cardiomyocytes. On the other hand, downregulation of OPN in NHE1 infected cardiomyocytes significantly reduced cleavage of OPN compared to NHE1 infected cardiomyocytes. The antibody we used to measure expression of the OPN is only capable of detecting the MMP3/7 C-terminal-cleaved fragment of OPN. Interestingly, OPN has been shown to be a substrate for proteolytic cleavage by MMPs and also appears to regulate the activity of several MMPs (105, 110, 113). As discussed in Section 1.4.1, in several animal models of post-MI injury and CH, MMP-2 and 9 have been shown to be upregulated (Reviewed in (128)). An elevation in MMP3/7-cleaved OPN upon upregulation of NHE1 and OPN suggests enhanced activity of MMP-3 and 7 as well as the phosphoprotein. Whether the upregulation of MMP-3/7 and the subsequent cleavage of OPN mediate the hypertrophic effects of OPN during NHE1-induced CH is yet to

be determined. Therefore, further studies are necessary in order to determine the exact role of cleaved OPN and whether NHE1 and OPN can upregulate MMP-3 and 7 and hence, cleavage of OPN.

5.1.8 OPN Contributes to the NHE1-induced Hypertrophic Response Independent of ERK 1/2, RSK and Akt

Upregulation of NHE1 has been shown to play a role in mediating CH and heart failure in both *in vivo* and *in vitro* animal models (14, 22, 23, 43, 51). Recent reports have demonstrated that active expression of NHE1 produces a more prominent cardiac hypertrophic phenotype compared to expression of wild type NHE1 (17, 18, 21, 54, 95). Although inhibition of NHE1 expression/activity has been shown to attenuate CH *in vivo* (53, 63, 84), NHE1 inhibition in the clinical settings was not successful (97, 99, 101). In our study, we demonstrate that infection of cardiomyocytes with active NHE1 increases cell area significantly compared to control (Figure 3.4). This is consistent with other studies, which have shown that expression of active NHE1 in NRVMs induces an increase in cell surface area (15, 17). Overexpression of NHE1 and OPN in cardiomyocytes also significantly increased cell area. Although the difference between cell area in cardiomyocytes infected with both active NHE1 and OPN was not significantly higher than cardiomyocytes infected with NHE1 alone, this may be justified by the extent of hypertrophy that may be exerted by cardiomyocytes as an *in vitro* model reflecting changes that are visible on a planar level only. Even though the use of adenoviral tools to manipulate gene expression in NRVMs has been shown to be efficient (14, 15, 32), the use of viruses could disrupt the physiology of the cardiomyocyte,

including the extent of sarcomere organization (193). As a result, co-infection of cardiomyocytes with both NHE1 and OPN adenoviruses could also limit the organization of the sarcomere, resulting in an attenuated increase in cell area. Accompanying the increase in cell area in NHE1-infected cardiomyocytes was a significant increase in protein content and ANP gene expression (Figure 4.10-12). Our results are consistent with a previous study by Mraiche et al., which demonstrated a significant elevation in both protein synthesis and ANP mRNA levels in NHE1 infected NRVMs (15). Interestingly, downregulating OPN in the presence of NHE1 caused a significant reduction in cell area, protein content and ANP gene expression compared to NHE1 infected cardiomyocytes. This reduction in protein content was significantly lower compared to OPN infected H9c2 cardiomyocytes, further implicating OPN in facilitating the NHE1-induced hypertrophic response. Taken together, our findings strongly implicate OPN in contributing to the hypertrophic effects of NHE1 during CH. Our findings also demonstrated that hypertrophic effects of NHE1 mediated by OPN occurred independent of ERK 1/2, Akt and RSK (Figure 3.5 and 5.0). This appears to be inconsistent with previous studies that have suggested that the hypertrophic effects of both OPN and NHE1 are in part mediated by the hypertrophic kinases ERK 1/2, RSK and Akt (17, 54, 90, 154, 159). Previous studies have suggested that peak activation of kinases occurs within 5 minutes of stimulation (58, 90), however, in our experiments, cardiomyocytes were infected for a period of 24 hours, which could justify the discrepancies in our findings. Taken together, our findings indicate that OPN contributes to the NHE1-induced hypertrophic response by regulating NHE1 expression and activity as well as parameters of CH.

5.1.9 OPN Activates Pro-hypertrophic Signaling Pathways During NHE1-induced Cardiac Hypertrophy

Studies have suggested hyperactivity of NHE1 during CH leads to Ca^{2+} overload through reverse activation of the NCX (14, 17). This elevation in $Ca^{2+}{}_I$ leads to activation of pro-hypertrophic proteins such as CaMK II and CaN (as discussed in Section 1.3.1 and (13, 14)). CaN is considered a Ca^{2+} dependent pro-hypertrophic molecule that appears to be upregulated in transgenic mice overexpressing active NHE1(17). Interestingly, Hisamitsu et al. recently demonstrated that enhanced activity of NHE1 caused an elevation of pH_i and sensitization of CaN to activation and promotion of both NFATc1 and NFATc4 signaling in NRVMs (14). This upregulation in NHE1 has been suggested to induce CH through activation of CaN/NFAT pathways and reinduction of the fetal gene program (14, 17). In fact PE-induced CH in NRVMs significantly uprgeulated NHE1 and increased $Na^+{}_i$ and $Ca^{2+}{}_i$, CaN activity, nuclear translocation of NFATc4 and GATA-4 activation (93), further emphasizing the role of NHE1 in activating the CaN/NFAT/GATA pathway. The interaction between GATA-4 and NFAT is particularly important since NFAT has been implicated in activating hypertrophic gene expression partly through forming a complex with GATA-4 (4). OPN has been shown to both activate and be activated by NFAT/GATA signaling pathways (155, 164). OPN has been suggested to act upstream of NFATc1 and GATA-3 in OPN transgenic mice (164). Matsui et al. suggested that enhanced activity of OPN may activate the Akt/GSK-3β in mice, thus mediating the NFAT/GATA-4 pathways to hypertrophic gene expression (155). Moreover, in osteoclasts, OPN activated NFATc1 and enhanced osteoclast survival through a CaN/FAT-dependent pathway (141). On the other hand, Nilsson-Berglund

et al. recently identified two NFATc3 responsive sequences in the OPN promoter, suggesting that OPN may be acting downstream of NFAT (82). Although we are yet to determine whether OPN functions through the CaN/NFAT/GATA pathway to mediate NHE1-induced CH, this pathway appears to be common between both NHE1 and OPN signaling and is clearly of high value. OPN has also recently been associated with SGK-induced upregulation of NHE1 as well as CH (21, 22). SGK1 has been suggested to mediate CH (87), however, whether OPN functions through SGK1 to regulate NHE1 activity and mediate the cardiac hypertrophic response remains unknown (Figure 5.0).

5.1.10 Cellular Interplay Between Cardiac Fibroblasts and Myocytes

The crosstalk between fibroblasts and cardiomyocytes during myocardial development and cardiac remolding has attracted much attention recently (194, 195). An important cardiac fibroblast-cardiomyocyte interaction has recently been demonstrated in cardiomyocytes co-cultured with fibroblasts. LaFramboise et al. suggested that through intercellular contact with cardiomyocytes, fibroblasts can induce marked hypertrophy and abolish the contractile capacity of cardiomyocytes while generating a phenotypically different culture of cardiomyocytes characterized by plasticity (195). Our findings have demonstrated that enhanced secretion of OPN from cardiomyocytes contributes to the hypertrophic phenotype of cardiomyocytes expressing active NHE1. However, the extent to which fibroblast-secreted OPN can regulate NHE1 expression/activity and mediate the hypertrophic effects of enhanced NHE1 activity may be different. Therefore the association between NHE1 and OPN

requires further studies in a model investigating the interaction between fibroblasts and cardiomyocytes.

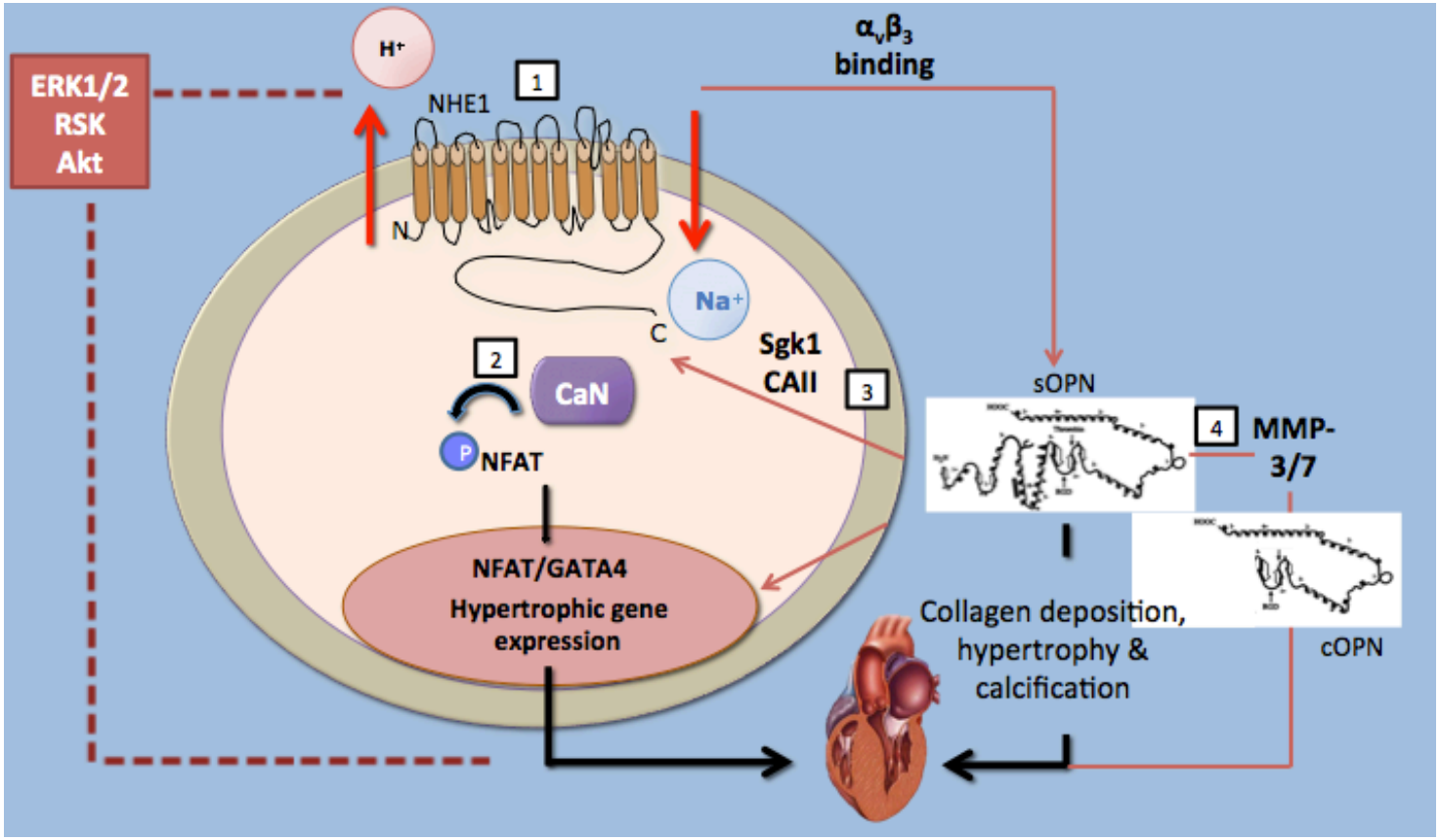

Fig. 5.0 OPN mediates NHE1-induced CH in cardiomyocytes. 1. Overexpression of active NHE1 induces CH associated with the activation of CaN and elevated OPN levels. **2.** Dephosphorylated NFAT translocates into the nucleus and interacts with GATA4 promoting hypertrophic gene expression. **3**. OPN facilitates NHE1-induced CH by enhancing NHE1 activity possibly through SGK1 or CAII activation, which occurs independent of MAPK activation. **4.** OPN enhances activity of MMP-3/7 which cleave the full form of OPN contributing to NHE1-inuced CH. **NHE1**, Na^+/H^+ Exchanger 1; **sOPN**, secreted OPN; **cOPN**, cleaved OPN; **CaN**. Calcineurin; **NFAT**, Nuclear Factor of Activated T-cells; **αvβ3**, integrin; **MMP**, matrix metalloproteinases 3 and 7.

5.2 Conclusions

The pivotal role of NHE1 in CH has been demonstrated in several studies that have indicated that enhanced NHE1 activity, rather than expression, was necessary for the pathological effects of NHE1. In addition, a strong line of evidence has suggested that inhibition of NHE1 would successfully inhibit and even reverse CH in animal models. However, the direct inhibition of NHE1 has proven not to be clinically applicable, stressing the importance of identifying mediators that enhance NHE1 activity as potential therapeutic targets to regress CH.

In our study, we demonstrate that NHE1 regulates OPN gene and protein expression in cardiomyocytes. We also establish for the first time that OPN regulates NHE1 protein expression as well as activity in cardiomyocytes. Moreover, our findings suggest that upregulation of NHE1 and OPN increase the cleavage of secreted form of sOPN. Upon downregulation of OPN, we observe a significant reduction in the C-terminal cleaved fragment of sOPN. Although it is necessary to conduct further studies in order to investigate the effect of C-terminal cleaved fragment of sOPN on NHE1 expression as well as activity, our findings strongly suggest that OPN regulates the expression and activity of NHE1 in cardiomyocytes.

In our study we also establish the importance of OPN's ability to contribute to the NHE1-induced hypertrophic response. We demonstrate that upregulation of NHE1 in cardiomyocytes enhances parameters of CH including cell area, protein content and ANP gene expression. Interestingly, cell area, protein content and ANP gene expression were significantly decreased upon downregulation of OPN. Our results also indicate that OPN facilitates the NHE1-induced hypertrophic response independent of hypertrophic kinases that are also known to regulate NHE1 activity

including ERK 1/2, RSK and Akt. However, further studies are necessary in order to determine the signaling pathways activated by OPN that mediate the hypertrophic effects of NHE1 and to better understand the importance of cleaved OPN during NHE1-induced CH. The interaction between cardiomyocytes and non-cardiomyocytes in the myocardium may also alter the extent to which OPN contributes to the hypertrophic effects of NHE1. As a result, it is important to further examine the cellular interplay between NHE1 and OPN in CH in a setting that would take into consideration the interaction between cardiomyocytes and fibroblasts in the myocardium.

In summary, our study provides novel findings that postulate a better understanding of the mechanistic basis behind NHE1-induced CH *in vitro*. By highlighting OPN as a mediator of NHE1-induced CH, we introduce a potential target, one that may be more effective for inhibition than the ubiquitous, housekeeping protein, NHE1. We also emphasize on the use of siRNA technology as an effective approach to silence OPN gene expression and reverse the hypertrophic response induced by NHE1 during CH. Thus, our study also highlights an effective tool to downregulate specific gene expression, a tool that has numerous applications both *in vivo* and potentially, in clinical settings.

Chapter 6: Future Directions

The findings of our present study demonstrate that OPN contributes to the NHE1-hypertrophic response through enhancing NHE1 activity and parameters of CH in cardiomyocytes. Our study also indicates that NHE1-induced CH was mediated by OPN and independent of hypertrophic kinases ERK 1/2, RSK and Akt. We reveal that upon downregulation of OPN, the NHE1-induced hypertrophic response is reversed as NHE1 activity and parameters of CH are reduced. The assays outlined below will enable me to further examine the signaling pathways through which OPN could be regulating NHE1 activity and how OPN contributes to the NHE1-induced hypertrophic response.

6.1 Determining the Form of OPN Mediating NHE1-induced Cardiac Hypertrophy

Previous studies have shown that due to extensive PTM, OPN exists in different isoforms in addition to the secreted and intracellular forms (109, 113, 118). Our results indicate that the secreted isoform of OPN is responsible for regulating NHE1 activity and mediating NHE1-induced CH *in vitro*. Moreover, studies have suggested that elevated secretion of OPN by fibroblasts induces fibroblast activation, proliferation and ECM deposition (105, 107, 160). However, the role of sOPN in CH has not been completely established. In order to confirm that the secreted form of OPN is the form responsible for regulating NHE1 activity and mediating the hypertrophic effects of NHE1, co-cultures of cardiomyocytes and fibroblasts could be treated with an α1-AR agonist, such as PE or Ang II. Analysis of NHE1

activity/expression and parameters of CH will allow us to conclude if the OPN secreted from the fibroblasts is truly the form responsible for the hypertrophic effects of enhanced NHE1 activity.

Previous studies have indicated that rather than degrading OPN, proteolytic cleavage of OPN enhances the biological activity of OPN (110, 113, 121, 135). In our study, cleaved OPN showed a trend towards increase in cardiomyocytes expressing both NHE1 and OPN, an effect that was significantly reduced upon downregulation of OPN. In order to better the exact role of cleaved OPN in CH, it is important to first confirm whether NHE1 induces MMP-3/7, which are known to cleave OPN. MMP-3/7 activity could be measured on the protein level by immunoblotting against MMP-3/7 antibodies (128) or using zymography. In order to assess the ability of NHE1 to induce MMP-3/7-cleave of OPN and in fact alter the NHE 1 induced hypertrophic response, MMP-3 or MMP-7 enzymes could be downregulated in cardiomyocytes infected with NHE1 and OPN. Parameters of CH including cell area, protein content and ANP mRNA could then be analyzed in the presence and absence of MMP-3 and MMP-7 in order to determine the effects of cleaved OPN on CH.

6.2 The Cellular Interplay Between NHE1 and OPN in Fibroblasts and Cardiomyocytes

The crosstalk between fibroblasts and cardiomyocytes during myocardial development and cardiac remolding has attracted much attention recently (194, 195). The interaction between cardiomyocytes and non-cardiomyocytes in the myocardium may alter the extent to which OPN mediates the hypertrophic effects of NHE1. OPN has also been shown to mainly be expressed by cardiac fibroblasts and expressed to a

much lesser extent by cardiomyocytes only during CH (105, 153-156). As a result, it is important to further examine the ability of OPN to regulate NHE1 expression/activity and contribute to the hypertrophic effects of NHE1 in co-cultures of cardiomyocytes and fibroblasts. LaFramboise et al. have previously established a model in which plated NRVMs were supplemented with fibroblast-conditioned media to create a co-culture of cardiomyocytes and fibroblasts (195). In order to determine the effect of fibroblast-secreted OPN on membrane-bound NHE1 activity and NHE1-induced hypertrophic response, NRVMs may first be plated on coverslips prior to supplementation with fibroblast-conditioned media, as suggested by LaFramboise et al. (195). Co-cultures fibroblasts and NRVMs could then be treated with an α1-AR agonist, such as PE or Ang II, and NHE1 activity may then be measured as described in Sections 2.1.3.3 and 2.2.3.3.2 and compared to NRVMs that have been stimulated with PE or Ang II but not co-cultured with fibroblasts. Moreover, gene and protein expression of both NHE1 and OPN, in addition to parameters of CH could be analyzed. This would enable me to confirm that during hypertrophy, NHE1-induces OPN expression, which in turn regulates NHE1 expression. Moreover, since this setting would take into consideration the interaction between fibroblast-secreted OPN and cardiomyocyte-expressed NHE1, this would provide a better indication of the ability of OPN to contribute to the the hypertrophic effects of NHE1 during CH.

6.3 The Ability of OPN to Contribute to the NHE1-induced Hypertrophic Response In Vitro

In our study, we demonstrated that during CH, NHE1 induces the expression of OPN, which in turn, regulates NHE1 expression/activity using both a *gain* and a

loss of function model. Even though previous studies have demonstrated that elevated OPN gene expression was accompanied by an increase in NHE1 activity, the exact signaling pathway linking OPN and NHE1 has not been yet established (21, 22). Based on the findings of the Voelkl (21, 22) and Fliegel (62, 64) groups, we speculated that OPN may upregulate NHE1 through direct interaction with *SGK1* or *CAII*, respectively. However, this postulation has not yet been confirmed. EMD638683 and 6-ethoxyzolamide (ETZ) are SGK1 and CAII inhibitors that have been previously used *in vitro* to confirm the ability of SGK1 (21) and CAII (63) to regulate NHE1 activity. In order to further understand the roles of SGK1 and CAII in the cellular interplay between NHE1 and OPN in co-culture of fibroblasts and NRVMs, EMD638683 or ETZ could be used. The co-culture could be treated with hypertrophic agents, such as an α1-AR agonists, and the changes in NHE1 expression/activity and OPN expression could be examined. Examining changes in NHE1 expression/activity would allow me to confirm whether OPN regulates NHE1 expression/activity through SGK1 or CAII. SGK1 has been suggested to play a prominent role in the mediation of CH (87). Examining changes in parameters of CH following treatment of the co-culture with EMD638683 could further examine whether SGK1 is a possible mediator of the hypertrophic effects of OPN during NHE1-induced CH. In order to confirm the ability of NHE1 to upregulate OPN, I could also examine changes in OPN expression following the addition of EMD638683 or ETZ.

Another pathway that could potentially allow OPN to contribute to the hypertophic effects of NHE1 is the *CaN/NFAT pathway*. Based on the evidence presented in the literature (14, 82, 141), we speculate that the activation of NHE1

upregulates OPN expression, which in turn activates the CaN/NFAT pathway and promotes hypertrophic gene expression. I propose an experiment in which I use the H9c2 cardiomyocytes transfected with siRNA OPN in the presence of NHE1 adenovirus to determine whether OPN mediates the CaN/NFAT pathway in response to activation of NHE1. Furthermore, investigating the changes in parameters of CH will allow me to confirm that OPN mediates the hypertrophic response of NHE1 in cardiomyocytes following the upregulation of NHE1. The nuclear translocation of NFAT can be determined through western blot analysis of sub-cellular fractionated samples or immunofluorescence. Thus, this will also further confirm whether OPN mediates the CaN/NFAT pathway in response to the upregulation of NHE1 leading to CH *in vitro*.

6.4 OPN Mediates NHE1-induced Cardiac Hypertrophy in vivo

Our results have demonstrated that OPN regulates NHE1 protein expression as well as activity. In a previous study, *OPN KO mice* exhibited a reduced hypertrophic response following AB compared to OPN WT mice (154). Examining NHE1 gene and protein expression in OPN KO mice following AB and comparing the results in WT mice will further confirm the role of OPN in the upregulation of NHE1. Furthermore, I can use the ARVMs isolated from hypertrophic OPN KO mice to measure NHE1 activity and compare to activity of NHE1 in OPN WT mice following AB. These sets of experiments would allow me to establish the ability of OPN to regulate NHE1 expression/activity using an *in vivo* model.

Mraiche et al. have previously demonstrated that the generation of *transgenic mice overexpressing cardiac specific active NHE1* (K-line mice) developed CH

associated with an upregulation of OPN and OPN related molecules (23). In our project, the use of siRNA against OPN proved successful in downregulating OPN expression, which in turn, significantly reduced NHE1 expression. In our study, downregulating OPN was also able to attenuate NHE1-induced CH. It would be interesting to see if downregulation of OPN in the K-line mice would attenuate NHE1-induced CH. Silencing target gene expression *in vitro* seems to be rather simple and effective (180). Although the use of siRNA *in vivo* maybe challenging due to rapid excretion, nonspecific accumulation in tissues and inadequate cellular uptake; several advances have been made in this field in order to overcome these barriers, including chemical modification of siRNA and both viral and non-viral siRNA vectors (180, 191). To date, no studies have examined the potential use of siRNA to inhibit OPN in animal models of CH. Therefore, determining the effects of OPN ablation using siRNA OPN in a model of the K-line mice transgenic mice overexpressing cardiac specific active NHE1 would provide me with further insight into the role of OPN in mediating NHE1-induced CH. Using an animal model would enable me to characterize the cardiac phenotype by analyzing parameters of CH such as heart weight/body weight ratio, myocardial fibrosis as well as cardiac function (18). This would also take into consideration the interaction between cardiomyocytes and fibroblasts.

Funding

This project was made possible by NPRP grant no. 5-330-3-090 from the Qatar National Research Fund *(a member of Qatar Foundation)*. The statements made herein are solely the responsibility of Iman Abdelaziz and Dr. Fatima Mraiche.

References

1. World Health Organization Media Center: World Health Organization; 2013 [cited 2013 March]. Available from: http://www.who.int/mediacentre/factsheets/fs317/en/index.html.
2. Bener A, Zirie MA, Kim EJ, Al Buz R, Zaza M, Al-Nufal M, et al. Measuring burden of diseases in a rapidly developing economy: state of Qatar. Glob J Health Sci. 2013;5(2):134-44.
3. Bradshaw AC, Baker AH. Gene therapy for cardiovascular disease: perspectives and potential. Vascul Pharmacol. 2013;58(3):174-81.
4. Kehat I, Molkentin JD. Molecular pathways underlying cardiac remodeling during pathophysiological stimulation. Circulation. 2010;122(25):2727-35.
5. Mihl C, Dassen WR, Kuipers H. Cardiac remodelling: concentric versus eccentric hypertrophy in strength and endurance athletes. Neth Heart J. 2008;16(4):129-33.
6. Barry SP, Davidson SM, Townsend PA. Molecular regulation of cardiac hypertrophy. Int J Biochem Cell Biol. 2008;40(10):2023-39.
7. Frey N, Olson EN. Cardiac hypertrophy: the good, the bad, and the ugly. Annu Rev Physiol. 2003;65:45-79.
8. Toko H, Shiojima I, Komuro I. The gene expression profiling of concentric and eccentric cardiac hypertrophy. Hypertens Res. 2006;29(12):941-2.
9. Marian AJ, Willerson JT, Wellens HJJ, Cohn JN, Holmes DR. Cardiac Hypertrophy

Cardiovascular Medicine. Springer London; 2007. p. 1177-88.

10. Heineke J, Molkentin JD. Regulation of cardiac hypertrophy by intracellular signalling pathways. Nat Rev Mol Cell Biol. 2006;7(8):589-600.

11. Rohini A, Agrawal N, Koyani CN, Singh R. Molecular targets and regulators of cardiac hypertrophy. Pharmacol Res. 2010;61(4):269-80.

12. Zamilpa R, Lindsey ML. Extracellular matrix turnover and signaling during cardiac remodeling following MI: causes and consequences. J Mol Cell Cardiol. 2010;48(3):558-63.

13. Molkentin JD, Lu JR, Antos CL, Markham B, Richardson J, Robbins J, et al. A calcineurin-dependent transcriptional pathway for cardiac hypertrophy. Cell. 1998;93(2):215-28.

14. Hisamitsu T, Nakamura TY, Wakabayashi S. Na(+)/H(+) exchanger 1 directly binds to calcineurin A and activates downstream NFAT signaling, leading to cardiomyocyte hypertrophy. Mol Cell Biol. 32. United States2012. p. 3265-80.

15. Mraiche F, Fliegel L. Elevated expression of activated Na(+)/H(+) exchanger protein induces hypertrophy in isolated rat neonatal ventricular cardiomyocytes. Mol Cell Biochem. 2011;358(1-2):179-87.

16. Karmazyn M, Kilic A, Javadov S. The role of NHE-1 in myocardial hypertrophy and remodelling. J Mol Cell Cardiol. 2008;44(4):647-53.

17. Nakamura TY, Iwata Y, Arai Y, Komamura K, Wakabayashi S. Activation of Na+/H+ exchanger 1 is sufficient to generate Ca2+ signals that induce cardiac hypertrophy and heart failure. Circ Res. 2008;103(8):891-9.

18. Mraiche F, Oka T, Gan XT, Karmazyn M, Fliegel L. Activated NHE1 is required to induce early cardiac hypertrophy in mice. Basic Res Cardiol. 2011;106(4):603-16.

19. Psarras S, Mavroidis M, Sanoudou D, Davos CH, Xanthou G, Varela AE, et al. Regulation of adverse remodelling by osteopontin in a genetic heart failure model. Eur Heart J. 2012;33(15):1954-63.

20. Renault MA, Robbesyn F, Reant P, Douin V, Daret D, Allieres C, et al. Osteopontin expression in cardiomyocytes induces dilated cardiomyopathy. Circ Heart Fail. 2010;3(3):431-9.

21. Voelkl J, Pasham V, Ahmed MS, Walker B, Szteyn K, Kuhl D, et al. Sgk1-dependent stimulation of cardiac na/h(+) exchanger nhe1 by dexamethasone. Cell Physiol Biochem. 2013;32(1):25-38.

22. Voelkl J, Lin Y, Alesutan I, Ahmed M, Pasham V, Mia S, et al. Sgk1 sensitivity of Na+/H+ exchanger activity and cardiac remodeling following pressure overload. Basic Research in Cardiology C7 - 236. 2012;107(2):1-15.

23. Xue J, Mraiche F, Zhou D, Karmazyn M, Oka T, Fliegel L, et al. Elevated myocardial Na+/H+ exchanger isoform 1 activity elicits gene expression that leads to cardiac hypertrophy. Physiol Genomics. 2010;42(3):374-83.

24. Young M, Funder J. Mineralocorticoid Action and Sodium-Hydrogen Exchange: Studies in Experimental Cardiac Fibrosis. Endocrinology. 2003;144(9):3848-51.

25. Malo ME, Fliegel L. Physiological role and regulation of the Na+/H+ exchanger. Can J Physiol Pharmacol. 2006;84(11):1081-95.

26. Morgan PE, Correa MV, Ennis IE, Diez AA, Perez NG, Cingolani HE. Silencing of sodium/hydrogen exchanger in the heart by direct injection of naked siRNA. J Appl Physiol. 2011;111(2):566-72.

27. Kemp G, Young H, Fliegel L. Structure and function of the human Na+/H+ exchanger isoform 1. Channels (Austin). 2008;2(5):329-36.

28. Putney LK, Denker SP, Barber DL. The changing face of the Na+/H+ exchanger, NHE1: structure, regulation, and cellular actions. Annu Rev Pharmacol Toxicol. 2002;42:527-52.

29. Attaphitaya S, Nehrke K, Melvin JE. Acute inhibition of brain-specific Na(+)/H(+) exchanger isoform 5 by protein kinases A and C and cell shrinkage. Am J Physiol Cell Physiol. 2001;281(4):C1146-57.

30. Fliegel L. Molecular biology of the myocardial Na+/H+ exchanger. J Mol Cell Cardiol. 2008;44(2):228-37.

31. Lee SH, Kim T, Park ES, Yang S, Jeong D, Choi Y, et al. NHE10, an osteoclast-specific member of the Na+/H+ exchanger family, regulates osteoclast differentiation and survival [corrected]. Biochem Biophys Res Commun. 2008;369(2):320-6.

32. Coccaro E, Mraiche F, Malo M, Vandertol-Vanier H, Bullis B, Robertson M, et al. Expression and characterization of the Na+/H+ exchanger in the mammalian myocardium. Mol Cell Biochem. 2007;302(1-2):145-55.

33. Lee BL, Sykes BD, Fliegel L. Structural analysis of the Na+/H+ exchanger isoform 1 (NHE1) using the divide and conquer approach. Biochem Cell Biol. 2011;89(2):189-99.

34. Petrecca K, Atanasiu R, Grinstein S, Orlowski J, Shrier A. Subcellular localization of the Na+/H+ exchanger NHE1 in rat myocardium. Am J Physiol. 1999;276(2 Pt 2):H709-17.

35. Avkiran M, Cook AR, Cuello F. Targeting Na+/H+ exchanger regulation for cardiac protection: a RSKy approach? Curr Opin Pharmacol. 2008;8(2):133-40.

36. Carraro-Lacroix LR, Ramirez MA, Zorn TM, Reboucas NA, Malnic G. Increased NHE1 expression is associated with serum deprivation-induced differentiation in immortalized rat proximal tubule cells. Am J Physiol Renal Physiol. 2006;291(1):F129-39.

37. Li X, Karki P, Lei L, Wang H, Fliegel L. Na+/H+ exchanger isoform 1 facilitates cardiomyocyte embryonic stem cell differentiation. Am J Physiol Heart Circ Physiol. 2009;296(1):H159-70.

38. Lang F, Busch GL, Ritter M, Volkl H, Waldegger S, Gulbins E, et al. Functional significance of cell volume regulatory mechanisms. Physiol Rev. 1998;78(1):247-306.

39. Schelling JR, Abu Jawdeh BG. Regulation of cell survival by Na+/H+ exchanger-1. Am J Physiol Renal Physiol. 2008;295(3):F625-32.

40. Abu Jawdeh BG, Khan S, Deschenes I, Hoshi M, Goel M, Lock JT, et al. Phosphoinositide binding differentially regulates NHE1 Na+/H+ exchanger-dependent proximal tubule cell survival. J Biol Chem. 2011;286(49):42435-45.

41. Manucha W, Carrizo L, Ruete C, Valles PG. Apoptosis induction is associated with decreased NHE1 expression in neonatal unilateral ureteric obstruction. BJU Int. 2007;100(1):191-8.

42. Darmellah A, Rucker-Martin C, Feuvray D. ERM proteins mediate the effects of Na+/H+ exchanger (NHE1) activation in cardiac myocytes. Cardiovasc Res. 2009;81(2):294-300.

43. Karki P, Fliegel L. Overexpression of the NHE1 isoform of the Na(+)/H (+) exchanger causes elevated apoptosis in isolated cardiomyocytes after hypoxia/reoxygenation challenge. Mol Cell Biochem. 2010;338(1-2):47-57.

44. Denker SP, Huang DC, Orlowski J, Furthmayr H, Barber DL. Direct binding of the Na--H exchanger NHE1 to ERM proteins regulates the cortical cytoskeleton and cell shape independently of H(+) translocation. Mol Cell. 2000;6(6):1425-36.

45. Karydis A, Jimenez-Vidal M, Denker SP, Barber DL. Mislocalized scaffolding by the Na-H exchanger NHE1 dominantly inhibits fibronectin production and TGF-beta activation. Mol Biol Cell. 2009;20(8):2327-36.

46. Masereel B, Pochet L, Laeckmann D. An overview of inhibitors of Na(+)/H(+) exchanger. Eur J Med Chem. 2003;38(6):547-54.

47. Avkiran M, Marber MS. Na(+)/H(+) exchange inhibitors for cardioprotective therapy: progress, problems and prospects. J Am Coll Cardiol. 2002;39(5):747-53.

48. Mraiche F. The Role of the Na+/H+ Exchanger isoform 1 in cardiac pathology [Thesis]. Edmonton: University of Alberta; 2010.

49. Wu D, Stassen J, Seidler R, Doods H. Effects of BIIB513 on ischemia-induced arrhythmias and myocardial infarction in anesthetized rats. Basic Res Cardiol. 2000;95(6):449-56.

50. Guzman-Perez A, Wester RT, Allen MC, Brown JA, Buchholz AR, Cook ER, et al. Discovery of zoniporide: a potent and selective sodium-hydrogen exchanger type 1 (NHE-1) inhibitor with high aqueous solubility. Bioorg Med Chem Lett. 2001;11(6):803-7.

51. Huber JD, Bentzien J, Boyer SJ, Burke J, De Lombaert S, Eickmeier C, et al. Identification of a potent Sodium Hydrogen Exchanger isoform 1 (NHE1) inhibitor with a suitable profile for chronic dosing and demonstrated cardioprotective effects in a preclinical model of myocardial infarction in the rat. J Med Chem. 2012.

52. Pedersen SF, King SA, Nygaard EB, Rigor RR, Cala PM. NHE1 inhibition by amiloride- and benzoylguanidine-type compounds. Inhibitor binding loci deduced from chimeras of NHE1 homologues with endogenous differences in inhibitor sensitivity. J Biol Chem. 2007;282(27):19716-27.

53. Chen L, Chen CX, Gan XT, Beier N, Scholz W, Karmazyn M. Inhibition and reversal of myocardial infarction-induced hypertrophy and heart failure by NHE-1 inhibition. Am J Physiol Heart Circ Physiol. 2004;286(1):H381-7.

54. Prasad V, Lorenz JN, Miller ML, Vairamani K, Nieman ML, Wang Y, et al. Loss of NHE1 activity leads to reduced oxidative stress in heart and mitigates high-fat diet-induced myocardial stress. J Mol Cell Cardiol. 2013.

55. Amith S, Fliegel L. Regulation of the Na+/H+ Exchanger (NHE1) in Breast Cancer Metastasis. Cancer Res. 2013;73(4):1259-64.

56. Paradise RK, Lauffenburger DA, Van Vliet KJ. Acidic extracellular pH promotes activation of integrin alpha(v)beta(3). PLoS One. 2011;6(1):e15746.

57. Coccaro E, Karki P, Cojocaru C, Fliegel L. Phenylephrine and sustained acidosis activate the neonatal rat cardiomyocyte Na+/H+ exchanger through phosphorylation of amino acids Ser770 and Ser771. Am J Physiol Heart Circ Physiol. 2009;297(2):H846-58.

58. Karki P, Coccaro E, Fliegel L. Sustained intracellular acidosis activates the myocardial Na(+)/H(+) exchanger independent of amino acid Ser(703) and p90(rsk). Biochim Biophys Acta. 2010;1798(8):1565-76.

59. Misik AJ, Perreault K, Holmes CF, Fliegel L. Protein phosphatase regulation of Na+/H+ exchanger isoform I. Biochemistry. 2005;44(15):5842-52.

60. Wakabayashi S, Ikeda T, Iwamoto T, Pouysségur J, Shigekawa, M. Calmodulin-Binding autoinhibitory domain controls "pH-Sensing" in the Na+/H+ exchanger NHE1 through sequence specific interaction. Biochemistry. 1997;36(42):12854-61.

61. Bertrand B, Wakabayashi S, Ikeda T, Pouyssegur J, Shigekawa M. The Na+/H+ exchanger isoform 1 (NHE1) is a novel member of the calmodulin-binding proteins. Identification and characterization of calmodulin-binding sites. J Biol Chem. 1994;269(18):13703-9.

62. Li X, Liu Y, Alvarez BV, Casey JR, Fliegel L. A novel carbonic anhydrase II binding site regulates NHE1 activity. Biochemistry. 2006;45(7):2414-24.

63. Alvarez BV, Johnson DE, Sowah D, Soliman D, Light PE, Xia Y, et al. Carbonic anhydrase inhibition prevents and reverts cardiomyocyte hypertrophy. J Physiol. 2007;579(Pt 1):127-45.

64. Li X, Alvarez B, Casey JR, Reithmeier RA, Fliegel L. Carbonic anhydrase II binds to and enhances activity of the Na+/H+ exchanger. J Biol Chem. 2002;277(39):36085-91.

65. Yeves AM, Garciarena CD, Nolly MB, Chiappe de Cingolani GE, Cingolani HE, Ennis IL. Decreased activity of the Na+/H+ exchanger by phosphodiesterase 5A inhibition is attributed to an increase in protein phosphatase activity. Hypertension. 2010;56(4):690-5.

66. Bianchini L, Pouyssegus J. Regulation of the Na+/H+ exchanger isoform NHE1: role of phosphorylation. Kidney Int. 1996;49(4):1038-41.

67. Wakabayashi S, Bertrand B, Shigekawa M, Fafournoux P, Pouyssegur J. Growth factor activation and "H(+)-sensing" of the Na+/H+ exchanger isoform 1 (NHE1). Evidence for an additional mechanism not requiring direct phosphorylation. J Biol Chem. 1994;269(8):5583-8.

68. Vila-Petroff M, Mundina-Weilenmann C, Lezcano N, Snabaitis AK, Huergo MA, Valverde CA, et al. Ca(2+)/calmodulin-dependent protein kinase II contributes to intracellular pH recovery from acidosis via Na(+)/H(+) exchanger activation. J Mol Cell Cardiol. 2010;49(1):106-12.

69. Cuello F, Snabaitis AK, Cohen MS, Taunton J, Avkiran M. Evidence for direct regulation of myocardial Na+/H+ exchanger isoform 1 phosphorylation and activity by 90-kDa ribosomal S6 kinase (RSK): effects of the novel and specific RSK inhibitor fmk on responses to alpha1-adrenergic stimulation. Mol Pharmacol. 2007;71(3):799-806.

70. Garnovskaya M. G Protein-Coupled Receptors-Induced Activation of Extracellular Signal-Regulated Protein Kinase (ERK) and Sodium-Proton

Exchanger Type 1 (NHE1). In: Najman S, editor. Current Frontiers and Perspectives in Cell Biology: InTech; 2012. p. 235-58.

71. Snabaitis AK, Yokoyama H, Avkiran M. Roles of mitogen-activated protein kinases and protein kinase C in alpha(1A)-adrenoceptor-mediated stimulation of the sarcolemmal Na(+)-H(+) exchanger. Circ Res. 2000;86(2):214-20.

72. Rockman HA, Koch WJ, Lefkowitz RJ. Seven-transmembrane-spanning receptors and heart function. Nature. 2002;415(6868):206-12.

73. Salazar NC, Chen J, Rockman HA. Cardiac GPCRs: GPCR signaling in healthy and failing hearts. Biochim Biophys Acta. 2007;1768(4):1006-18.

74. Haworth RS, McCann C, Snabaitis AK, Roberts NA, Avkiran M. Stimulation of the plasma membrane Na+/H+ exchanger NHE1 by sustained intracellular acidosis. Evidence for a novel mechanism mediated by the ERK pathway. J Biol Chem. 2003;278(34):31676-84.

75. Maekawa N, Abe J, Shishido T, Itoh S, Ding B, Sharma VK, et al. Inhibiting p90 ribosomal S6 kinase prevents (Na+)-H+ exchanger-mediated cardiac ischemia-reperfusion injury. Circulation. 2006;113(21):2516-23.

76. Muslin AJ. MAPK signalling in cardiovascular health and disease: molecular mechanisms and therapeutic targets. Clin Sci (Lond). 2008;115(7):203-18.

77. Cardone RA, Busco G, Greco MR, Bellizzi A, Accardi R, Cafarelli A, et al. HPV16 E7-dependent transformation activates NHE1 through a PKA-RhoA-induced inhibition of p38alpha. PLoS One. 2008;3(10):e3529.

78. Wakabayashi S, Nakamura TY, Kobayashi S, Hisamitsu T. Novel phorbol ester-binding motif mediates hormonal activation of Na+/H+ exchanger. J Biol Chem. 2010;285(34):26652-61.

79. Meima M, Webb B, Barber D. The Sodium-Hydrogen Exchanger NHE1 Is an Akt Substrate Necessary for Actin Filament Reorganization by Growth Factors. Journal of Biology and Chemistry. 2009.

80. Snabaltis A, Cuello F, Avkiran M. Protein kinase B/Akt phosphorylates and inhibits the cardiac Na+/H+ exchanger NHE1. Circulation Research. 2008.

81. Molkentin JD. Calcineurin–NFAT signaling regulates the cardiac hypertrophic response in coordination with the MAPKs. 2004.

82. Nilsson-Berglund LM, Zetterqvist AV, Nilsson-Ohman J, Sigvardsson M, Gonzalez Bosc LV, Smith ML, et al. Nuclear factor of activated T cells regulates osteopontin expression in arterial smooth muscle in response to diabetes-induced hyperglycemia. Arterioscler Thromb Vasc Biol. 30. United States2010. p. 218-24.

83. Fliegel L. Regulation of the Na(+)/H(+) exchanger in the healthy and diseased myocardium. Expert Opin Ther Targets. 2009;13(1):55-68.

84. Ennis IL, Escudero EM, Console GM, Camihort G, Dumm CG, Seidler RW, et al. Regression of isoproterenol-induced cardiac hypertrophy by Na+/H+ exchanger inhibition. Hypertension. 2003;41(6):1324-9.

85. Karmazyn M. NHE-1: Still a viable therapeutic target. J Mol Cell Cardiol. 2013;61:77-82.

86. Ennis IL, Alvarez BV, Camilion de Hurtado MC, Cingolani HE. Enalapril induces regression of cardiac hypertrophy and normalization of pHi regulatory mechanisms. Hypertension. 1998;31(4):961-7.

87. Das S, Aiba T, Rosenberg M, Hessler K, Xiao C, Quintero PA, et al. Pathological role of serum- and glucocorticoid-regulated kinase 1 in adverse ventricular remodeling. Circulation. 2012;126(18):2208-19.

88. Baczko I, Mraiche F, Light PE, Fliegel L. Diastolic calcium is elevated in metabolic recovery of cardiomyocytes expressing elevated levels of the Na+/H+ exchanger. Can J Physiol Pharmacol. 2008;86(12):850-9.

89. Chahine M, Bkaily G, Nader M, Al-Khoury J, Jacques D, Beier N, et al. NHE-1-dependent intracellular sodium overload in hypertrophic hereditary cardiomyopathy: prevention by NHE-1 inhibitor. J Mol Cell Cardiol. 2005;38(4):571-82.

90. Chen MZ, Bu QT, Pang SC, Li FL, Sun MN, Chu EF, et al. Tetrodotoxin attenuates isoproterenol-induced hypertrophy in H9c2 rat cardiac myocytes. Mol Cell Biochem. 2012;371(1-2):77-88.

91. Amirak E, Fuller SJ, Sugden PH, Clerk A. p90 ribosomal S6 kinases play a significant role in early gene regulation in the cardiomyocyte response to G(q)-protein-coupled receptor stimuli, endothelin-1 and alpha(1)-adrenergic receptor agonists. Biochem J. 2013;450(2):351-63.

92. Kilic A, Velic A, De Windt LJ, Fabritz L, Voss M, Mitko D, et al. Enhanced activity of the myocardial Na+/H+ exchanger NHE-1 contributes to cardiac remodeling in atrial natriuretic peptide receptor-deficient mice. Circulation. 2005;112(15):2307-17.

93. Guo J, Gan XT, Haist JV, Rajapurohitam V, Zeidan A, Faruq NS, et al. Ginseng inhibits cardiomyocyte hypertrophy and heart failure via NHE-1

inhibition and attenuation of calcineurin activation. Circ Heart Fail. 2011;4(1):79-88.

94. Mraiche F, Wagg CS, Lopaschuk GD, Fliegel L. Elevated levels of activated NHE1 protect the myocardium and improve metabolism following ischemia/reperfusion injury. J Mol Cell Cardiol. 2011;50(1):157-64.

95. Doods H, Wu D. Sabiporide reduces ischemia-induced arrhythmias and myocardial infarction and attenuates ERK phosphorylation and iNOS induction in rats. Biomed Res Int. 2013;2013:504320.

96. Cook AR, Bardswell SC, Pretheshan S, Dighe K, Kanaganayagam GS, Jabr RI, et al. Paradoxical resistance to myocardial ischemia and age-related cardiomyopathy in NHE1 transgenic mice: a role for ER stress? J Mol Cell Cardiol. 2009;46(2):225-33.

97. Erhardt LR. GUARD During Ischemia Against Necrosis (GUARDIAN) trial in acute coronary syndromes. Am J Cardiol. 1999;83(10A):23G-5G.

98. Theroux P, Chaitman BR, Danchin N, Erhardt L, Meinertz T, Schroeder JS, et al. Inhibition of the sodium-hydrogen exchanger with cariporide to prevent myocardial infarction in high-risk ischemic situations. Main results of the GUARDIAN trial. Guard during ischemia against necrosis (GUARDIAN) Investigators. Circulation. 2000;102(25):3032-8.

99. Zeymer U, Suryapranata H, Monassier JP, Opolski G, Davies J, Rasmanis G, et al. The Na+/H+ exchange inhibitor eniporide as an adjunct to early reperfusion therapy for acute myocardial infarction: Results of the evaluation of the safety and cardioprotective effects of eniporide in acute myocardial

infarction (ESCAMI) trial. Journal of the American College of Cardiology. 2001;38(6):E1644-E50.

100. Bolli R. The role of sodium-hydrogen ion exchange in patients undergoing coronary artery bypass grafting. J Card Surg. 2003;18 Suppl 1:21-6.

101. Mentzer RM, Jr., Bartels C, Bolli R, Boyce S, Buckberg GD, Chaitman B, et al. Sodium-hydrogen exchange inhibition by cariporide to reduce the risk of ischemic cardiac events in patients undergoing coronary artery bypass grafting: results of the EXPEDITION study. Ann Thorac Surg. 2008;85(4):1261-70.

102. Murphy E, Allen DG. Why did the NHE inhibitor clinical trials fail? J Mol Cell Cardiol. 2009;46(2):137-41.

103. Waller AH, Sanchez-Ross M, Kaluski E, Klapholz M. Osteopontin in cardiovascular disease: a potential therapeutic target. Cardiol Rev. 2010;18(3):125-31.

104. Trueblood NA, Xie Z, Communal C, Sam F, Ngoy S, Liaw L, et al. Exaggerated left ventricular dilation and reduced collagen deposition after myocardial infarction in mice lacking osteopontin. Circ Res. 2001;88(10):1080-7.

105. Singh M, Foster CR, Dalal S, Singh K. Osteopontin: role in extracellular matrix deposition and myocardial remodeling post-MI. J Mol Cell Cardiol. 2010;48(3):538-43.

106. Sodek J, Ganss B, McKee MD. Osteopontin. Crit Rev Oral Biol Med. 2000;11(3):279-303.

107. Okamoto H, Imanaka-Yoshida K. Matricellular Proteins: New Molecular Targets To Prevent Heart Failure. Cardiovasc Ther. 2011.

108. McKee MD, Pedraza CE, Kaartinen MT. Osteopontin and wound healing in bone. Cells Tissues Organs. 2011;194(2-4):313-9.

109. Denhardt DT, Guo X. Osteopontin: a protein with diverse functions. FASEB J. 1993;7(15):1475-82.

110. Gao YA, Agnihotri R, Vary CP, Liaw L. Expression and characterization of recombinant osteopontin peptides representing matrix metalloproteinase proteolytic fragments. Matrix Biol. 2004;23(7):457-66.

111. Rittling SR, Feng F. Detection of mouse osteopontin by western blotting. Biochem Biophys Res Commun. 1998;250(2):287-92.

112. NCBI G-. Spp1 secreted phosphoprotein 1 [Rattus norvegicus (Norway rat)]. 2013.

113. Christensen B, Schack L, Klaning E, Sorensen ES. Osteopontin is cleaved at multiple sites close to its integrin-binding motifs in milk and is a novel substrate for plasmin and cathepsin D. J Biol Chem. 2010;285(11):7929-37.

114. Wang KX, Denhardt DT. Osteopontin: role in immune regulation and stress responses. Cytokine Growth Factor Rev. 2008;19(5-6):333-45.

115. Kazanecki CC, Uzwiak DJ, Denhardt DT. Control of osteopontin signaling and function by post-translational phosphorylation and protein folding. J Cell Biochem. 2007;102(4):912-24.

116. Weber GF, Zawaideh S, Hikita S, Kumar VA, Cantor H, Ashkar S. Phosphorylation-dependent interaction of osteopontin with its receptors

regulates macrophage migration and activation. J Leukoc Biol. 2002;72(4):752-61.

117. Christensen B, Kazanecki CC, Petersen TE, Rittling SR, Denhardt DT, Sorensen ES. Cell type-specific post-translational modifications of mouse osteopontin are associated with different adhesive properties. J Biol Chem. 2007;282(27):19463-72.

118. Singh M, Foster CR, Dalal S, Singh K. Role of osteopontin in heart failure associated with aging. Heart Fail Rev. 2010;15(5):487-94.

119. Zhao W, Wang L, Zhang L, Yuan C, Kuo PC, Gao C. Differential expression of intracellular and secreted osteopontin isoforms by murine macrophages in response to toll-like receptor agonists. J Biol Chem. 2010;285(27):20452-61.

120. Peng L, Guo Y, Zhou Y, Dai J, Wang H. Inhibition of Breast Cancer Metastasis and Angiogenesis by Antiosteopontin Single-Chain Fv-Fc Fusion Protein. Neoplasia. 2009;11(5):p509.

121. Agnihotri R, Crawford HC, Haro H, Matrisian LM, Havrda MC, Liaw L. Osteopontin, a novel substrate for matrix metalloproteinase-3 (stromelysin-1) and matrix metalloproteinase-7 (matrilysin). J Biol Chem. 2001;276(30):28261-7.

122. Lenga Y, Koh A, Perera A, McCulloch C, Sodek J, Zohar R. Osteopontin expression is required for myofibroblast differentiation. Circ Res. 2008;102(3):319-27.

123. Jalvy S, Renault MA, Leen LL, Belloc I, Bonnet J, Gadeau AP, et al. Autocrine expression of osteopontin contributes to PDGF-mediated arterial

smooth muscle cell migration. Cardiovasc Res. 75. Netherlands2007. p. 738-47.

124. Lund SA, Giachelli CM, Scatena M. The role of osteopontin in inflammatory processes. J Cell Commun Signal. 2009;3(3-4):311-22.

125. Frangogiannis NG. Matricellular proteins in cardiac adaptation and disease. Physiol Rev. 2012;92(2):635-88.

126. Bowers SL, Banerjee I, Baudino TA. The extracellular matrix: at the center of it all. J Mol Cell Cardiol. 2010;48(3):474-82.

127. Dobaczewski M, de Haan JJ, Frangogiannis NG. The extracellular matrix modulates fibroblast phenotype and function in the infarcted myocardium. J Cardiovasc Transl Res. 2012;5(6):837-47.

128. Spinale FG. Myocardial matrix remodeling and the matrix metalloproteinases: influence on cardiac form and function. Physiol Rev. 2007;87(4):1285-342.

129. Jourdan-Lesaux C, Zhang J, Lindsey ML. Extracellular matrix roles during cardiac repair. Life Sci. 2010;87(13-14):391-400.

130. Scatena M, Liaw L, Giachelli CM. Osteopontin A Multifunctional Molecule Regulating Chronic Inflammation and Vascular Disease. Arteriosclerosis, Thrombosis, and Vascular Biology. 2008;27(11):2302-9.

131. Narisawa S, Yadav MC, Millan JL. In vivo overexpression of tissue-nonspecific alkaline phosphatase increases skeletal mineralization and affects the phosphorylation status of osteopontin. J Bone Miner Res. 2013;28(7):1587-98.

132. Rajachar RM, Tung E, Truong AQ, Look A, Giachelli CM. Role of carbonic anhydrase II in ectopic calcification. Cardiovasc Pathol. 2009;18(2):77-82.

133. Pereira RO, Universidade do Estado do Rio de Janeiro U, Carvalho SN, Universidade do Estado do Rio de Janeiro U, Stumbo AC, Universidade do Estado do Rio de Janeiro U, et al. Osteopontin expression in coculture of differentiating rat fetal skeletal fibroblasts and myoblasts. In Vitro Cellular & Developmental Biology - Animal. 2005;42(1-2):4-7.

134. Zahradka P. Novel Role for Osteopontin in Cardiac Fibrosis. Circ Res. 208.

135. Wolak T, Sion-Vardi N, Novack V, Greenberg G, Szendro G, Tarnovscki T, et al. N-terminal rather than full-length osteopontin or its C-terminal fragment is associated with carotid-plaque inflammation in hypertensive patients. Am J Hypertens. 2013;26(3):326-33.

136. Behera R, Kumar V, Lohite K, Karnik S, Kundu GC. Activation of JAK2/STAT3 signaling by osteopontin promotes tumor growth in human breast cancer cells. Carcinogenesis. 2010;31(2):192-200.

137. Cao DX, Li ZJ, Jiang XO, Lum YL, Khin E, Lee NP, et al. Osteopontin as potential biomarker and therapeutic target in gastric and liver cancers. World J Gastroenterol. 2012;18(30):3923-30.

138. Rangaswami H, Bulbule A, Kundu GC. Osteopontin: role in cell signaling and cancer progression. Trends Cell Biol. 2006;16(2):79-87.

139. Standal T, Borset M, Sundan A. Role of osteopontin in adhesion, migration, cell survival and bone remodeling. Exp Oncol. 2004;26(3):179-84.

140. Scatena M, Almeida M, Chaisson ML, Fausto N, Nicosia RF, Giachelli CM. NF-kappaB mediates alphavbeta3 integrin-induced endothelial cell survival. J Cell Biol. 1998;141(4):1083-93.

141. Tanabe N, Wheal BD, Kwon J, Chen HH, Shugg RPP, Sims SM, et al. Osteopontin Signals through Calcium and Nuclear Factor of Activated T Cells (NFAT) in Osteoclasts: A NOVEL RGD-DEPENDENT PATHWAY PROMOTING CELL SURVIVAL*. J Biol Chem. 2011;286(46):39871-81.

142. Velupilla iP, Sung C, Tian Y, Dahl J, Carroll J, Bronson R, et al. Polyoma Virus-Induced Osteosarcomas in Inbred Strains of Mice: Host Determinants of Metastasis. PLoS Pathog. 2010;6(1):e1000733.

143. Zhao X, Johnson JN, Singh K, Singh M. Impairment of myocardial angiogenic response in the absence of osteopontin. Microcirculation. 2007;14(3):233-40.

144. Kocher AA, Schuster MD, Szabolcs MJ, Takuma S, Burkhoff D, Wang J, et al. Neovascularization of ischemic myocardium by human bone-marrow-derived angioblasts prevents cardiomyocyte apoptosis, reduces remodeling and improves cardiac function. Nat Med. 2001;7(4):430-6.

145. Wang Y, Chen B, Shen D, Xue S. Osteopontin protects against cardiac ischemia-reperfusion injury through late preconditioning. Heart Vessels. 2009;24(2):116-23.

146. Chen W, Ma Q, Suzuki H, Hartman R, Tang J, Zhang JH. Osteopontin reduced hypoxia-ischemia neonatal brain injury by suppression of apoptosis in a rat pup model. Stroke. 2011;42(3):764-9.

147. Hua Z, Chen J, Sun B, Zhao G, Zhang Y, Fong Y, et al. Specific expression of osteopontin and S100A6 in hepatocellular carcinoma. Surgery. 2011;149(6):783-91.

148. Christensen B, Nielsen MS, Haselmann KF, Petersen TE, Sorensen ES. Post-translationally modified residues of native human osteopontin are located in

clusters: identification of 36 phosphorylation and five O-glycosylation sites and their biological implications. Biochem J. 2005;390(Pt 1):285-92.

149. Steitz SA, Speer MY, McKee MD, Liaw L, Almeida M, Yang H, et al. Osteopontin inhibits mineral deposition and promotes regression of ectopic calcification. Am J Pathol. 2002;161(6):2035-46.

150. Carcaillon L, Alhenc-Gelas M, Bejot Y, Spaft C, Ducimetière P, Ritchie K, et al. Increased Thrombin Generation Is Associated With Acute Ischemic Stroke but Not With Coronary Heart Disease in the Elderly. Arterioscler Thromb Vasc Biol. 2011;31(6):1445-51.

151. Christensen B, Klaning E, Nielsen MS, Andersen MH, Sorensen ES. C-terminal modification of osteopontin inhibits interaction with the alphaVbeta3-integrin. J Biol Chem. 2012;287(6):3788-97.

152. Beausoleil MS, Schulze EB, Goodale D, Postenka CO, Allan AL. Deletion of the thrombin cleavage domain of osteopontin mediates breast cancer cell adhesion, proteolytic activity, tumorgenicity, and metastasis. BMC Cancer. 2011;11:25.

153. Graf K, Do YS, Ashizawa N, Meehan WP, Giachelli CM, Marboe CC, et al. Myocardial osteopontin expression is associated with left ventricular hypertrophy. Circulation. 1997;96(9):3063-71.

154. Xie Z, Singh M, Singh K. Osteopontin modulates myocardial hypertrophy in response to chronic pressure overload in mice. Hypertension. 2004;44(6):826-31.

155. Matsui Y, Jia N, Okamoto H, Kon S, Onozuka H, Akino M, et al. Role of osteopontin in cardiac fibrosis and remodeling in angiotensin II-induced cardiac hypertrophy. Hypertension. 2004;43(6):1195-201.

156. Okamoto H. Osteopontin and cardiovascular system. Mol Cell Biochem. 2007;300(1-2):1-7.

157. Okyay K, Tavil Y, Sahinarslan A, Tacoy G, Turfan M, Sen N, et al. Plasma osteopontin levels in prediction of prognosis in acute myocardial infarction. Acta Cardiol. 2011;66(2):197-202.

158. Suezawa C, Kusachi S, Murakami T, Toeda K, Hirohata S, Nakamura K, et al. Time-dependent changes in plasma osteopontin levels in patients with anterior-wall acute myocardial infarction after successful reperfusion: correlation with left-ventricular volume and function. J Lab Clin Med. 2005;145(1):33-40.

159. Xie Z, Singh M, Singh K. ERK1/2 and JNKs, but not p38 kinase, are involved in reactive oxygen species-mediated induction of osteopontin gene expression by angiotensin II and interleukin-1beta in adult rat cardiac fibroblasts. J Cell Physiol. 2004;198(3):399-407.

160. Zahradka P. Novel Role for Osteopontin in Cardiac Fibrosis. Circ Res. 2008.

161. Ashizawa N, Graf K, Do YS, Nunohiro T, Giachelli CM, Meehan WP, et al. Osteopontin is produced by rat cardiac fibroblasts and mediates A(II)-induced DNA synthesis and collagen gel contraction. J Clin Invest. 1996;98(10):2218-27.

162. Subramanian V, Krishnamurthy P, Singh K, Singh M. Lack of osteopontin improves cardiac function in streptozotocin-induced diabetic mice. Am J Physiol Heart Circ Physiol. 292. United States2007. p. H673-83.

163. Soetikno V, Sari FR, Sukumaran V, Lakshmanan AP, Mito S, Harima M, et al. Curcumin prevents diabetic cardiomyopathy in streptozotocin-induced diabetic rats: possible involvement of PKC-MAPK signaling pathway. Eur J Pharm Sci. 2012;47(3):604-14.

164. Diao H, Iwabuchi K, Li L, Onoe K, Van Kaer L, Kon S, et al. Osteopontin regulates development and function of invariant natural killer T cells. Proc Natl Acad Sci U S A. 2008;105(41):15884-9.

165. Rosenberg M, Meyer FJ, Gruenig E, Lutz M, Lossnitzer D, Wipplinger R, et al. Osteopontin predicts adverse right ventricular remodelling and dysfunction in pulmonary hypertension. Eur J Clin Invest. 2012;42(9):933-42.

166. Lopez B, Gonzalez A, Lindner D, Westermann D, Ravassa S, Beaumont J, et al. Osteopontin-mediated myocardial fibrosis in heart failure: a role for lysyl oxidase? Cardiovasc Res. 2013;99(1):111-20.

167. Hawkins NM, Petrie MC, MacDonald MR, Hogg KJ, McMurray JJ. Selecting patients for cardiac resynchronization therapy: electrical or mechanical dyssynchrony? Eur Heart J. 2006;27(11):1270-81.

168. Francia P, Balla C, Ricotta A, Uccellini A, Frattari A, Modestino A, et al. Plasma osteopontin reveals left ventricular reverse remodelling following cardiac resynchronization therapy in heart failure. International Journal of Cardiology. 2011;153(3):306-10.

169. Mohammed SF, Ohtani T, Korinek J, Lam CS, Larsen K, Simari RD, et al. Mineralocorticoid Accelerates Transition to Heart Failure with Preserved Ejection Fraction Via "Non-Genomic Effects". Circulation. 2010;122(4):370-8.

170. Lang F, Bohmer C, Palmada M, Seebohm G, Strutz-Seebohm N, Vallon V. (Patho)physiological significance of the serum- and glucocorticoid-inducible kinase isoforms. Physiol Rev. 2006;86(4):1151-78.

171. Chan AY, Soltys CL, Young ME, Proud CG, Dyck JR. Activation of AMP-activated protein kinase inhibits protein synthesis associated with hypertrophy in the cardiac myocyte. J Biol Chem. 2004;279(31):32771-9.

172. Ozkan P, Mutharasan R. A rapid method for measuring intracellular pH using BCECF-AM. Biochim Biophys Acta. 2002;1572(1):143-8.

173. Wang Z, Orlowski J, Shull GE. Primary structure and functional expression of a novel gastrointestinal isoform of the rat Na/H exchanger. J Biol Chem. 1993;268(16):11925-8.

174. Chaillet JR, Boron WF. Intracellular calibration of a pH-sensitive dye in isolated, perfused salamander proximal tubules. J Gen Physiol. 1985;86(6):765-94.

175. Watkins SJ, Borthwick GM, Arthur HM. The H9C2 cell line and primary neonatal cardiomyocyte cells show similar hypertrophic responses in vitro. In Vitro Cell Dev Biol Anim. 2011;47(2):125-31.

176. Ménard C, Pupier S, Mornet D, Kitzmann M, Nargeot J, Lory P. Modulation of L-type calcium channel expression during retinoic acid-induced differentiation of H9C2 cardiac cells. J Biol Chem. 1999;274(41):29063-70.

177. Flores-Munoz M, Godinho BM, Almalik A, Nicklin SA. Adenoviral Delivery of Angiotensin-(1-7) or Angiotensin-(1-9) Inhibits Cardiomyocyte Hypertrophy via the Mas or Angiotensin Type 2 Receptor. PLoS One. 2012;7(9):e45564.

178. Dalby B, Cates S, Harris A, Ohki EC, Tilkins ML, Price PJ, et al. Advanced transfection with Lipofectamine 2000 reagent: primary neurons, siRNA, and high-throughput applications. Methods. 33. United States: 2003 Elsevier Inc.; 2004. p. 95-103.

179. Ma Y, Lin H, Qiu C. High-efficiency transfection and siRNA-mediated gene knockdown in human pluripotent stem cells. Curr Protoc Stem Cell Biol. 2012;Chapter 2:Unit 5C.2.

180. Aouadi M, Tencerova M, Vangala P, Yawe JC, Nicoloro SM, Amano SU, et al. Gene silencing in adipose tissue macrophages regulates whole-body metabolism in obese mice. Proc Natl Acad Sci U S A. 2013;110(20):8278-83.

181. Zhang A, Liu Y, Shen Y, Xu Y, Li X. Osteopontin silencing by small interfering RNA induces apoptosis and suppresses invasion in human renal carcinoma Caki-1 cells. Med Oncol. 2010;27(4):1179-84.

182. Chang K, Marran K, Valentine A, Hannon GJ. RNAi in cultured mammalian cells using synthetic siRNAs. Cold Spring Harb Protoc. 2012;2012(9):957-61.

183. Scientific TF. siRNA Transfection Protocol Thermo Scientific DharmaFECT. 1, 2, 3, or 4 H9c2 2008 [cited 2013 July 10]. Available from: http://www.thermo.com/eThermo/CMA/PDFs/Various/File_7303.pdf.

184. Merten KE, Jiang Y, Feng W, Kang YJ. Calcineurin activation is not necessary for Doxorubicin-induced hypertrophy in H9c2 embryonic rat

cardiac cells: involvement of the phosphoinositide 3-kinase-Akt pathway. J Pharmacol Exp Ther. 2006;319(2):934-40.

185. Xia Y, Javadov S, Gan TX, Pang T, Cook MA, Karmazyn M. Distinct KATP channels mediate the antihypertrophic effects of adenosine receptor activation in neonatal rat ventricular myocytes. J Pharmacol Exp Ther. 2007;320(1):14-21.

186. Bhat M, Kalam R, Qadri SS, Madabushi S, Ismail A. Vitamin D Deficiency Induced Muscle Wasting Occurs through the Ubiquitin Proteasome Pathway and Is Partially Corrected by Calcium in Male Rats. 2013.

187. Pereira SL, Ramalho-Santos J, Branco AF, Sardao VA, Oliveira PJ, Carvalho RA. Metabolic remodeling during H9c2 myoblast differentiation: relevance for in vitro toxicity studies. Cardiovasc Toxicol. 2011;11(2):180-90.

188. Ku PM, Chen LJ, Liang JR, Cheng KC, Li YX, Cheng JT. Molecular role of GATA binding protein 4 (GATA-4) in hyperglycemia-induced reduction of cardiac contractility. Cardiovasc Diabetol. 2011;10:57.

189. Kageyama K, Ihara Y, Goto S, Urata Y, Toda G, Yano K, et al. Overexpression of calreticulin modulates protein kinase B/Akt signaling to promote apoptosis during cardiac differentiation of cardiomyoblast H9c2 cells. J Biol Chem. 277. United States2002. p. 19255-64.

190. Sardao VA, Oliveira PJ, Holy J, Oliveira CR, Wallace KB. Morphological alterations induced by doxorubicin on H9c2 myoblasts: nuclear, mitochondrial, and cytoskeletal targets. Cell Biol Toxicol. 2009;25(3):227-43.

191. Shim MS, Kwon YJ. Efficient and targeted delivery of siRNA in vivo. Febs j. 2010;277(23):4814-27.

192. Cell Viability and Proliferation. Sigma Aldrich. St. Louis, MO2011.

193. Louch WE, Sheehan KA, Wolska BM. Methods in cardiomyocyte isolation, culture, and gene transfer. J Mol Cell Cardiol. 2011;51(3):288-98.

194. Takeda N, Manabe I. Cellular Interplay between Cardiomyocytes and Nonmyocytes in Cardiac Remodeling. Int J Inflam. 2011;2011:535241.

195. LaFramboise WA, Scalise D, Stoodley P, Graner SR, Guthrie RD, Magovern JA, et al. Cardiac fibroblasts influence cardiomyocyte phenotype in vitro. Am J Physiol Cell Physiol. 2007;292(5):C1799-808.


جامعة قطر
QATAR UNIVERSITY
Thesis and Dissertation Services
خدمات رسائل الماجستير والدكتوراه